

# **LABORATORY INVESTIGATION OF SCOUR REDUCTION NEAR BRIDGE PIER BY DELTA-WING-LIKE PASSIVE DEVICE**

**A Thesis Submitted  
In Partial Fulfilment of the Requirements  
for the Degree of**

**MASTER OF TECHNOLOGY**

**by  
TRAN DINH NGHIEN**

*to the*

**DEPARTMENT OF CIVIL ENGINEERING**

**INDIAN INSTITUTE OF TECHNOLOGY, KANPUR**

**JANUARY, 1988**

# **LABORATORY INVESTIGATION OF SCOUR REDUCTION NEAR BRIDGE PIER BY DELTA-WING-LIKE PASSIVE DEVICE**

**A Thesis Submitted  
In Partial Fulfilment of the Requirements  
for the Degree of**

**MASTER OF TECHNOLOGY**

**by  
TRAN DINH NGHIEN**

*to the*

**DEPARTMENT OF CIVIL ENGINEERING**

**INDIAN INSTITUTE OF TECHNOLOGY, KANPUR**

**JANUARY, 1988**

CERTIFICATE

13/1/88  
B2

The thesis entitled 'Laboratory Investigation of Scour Reduction near Bridge Pier by Delta-Wing Like Passive Device' by T.D. Nghien (Roll No. 8520315) is hereby approved as a creditable report on research carried out and presented in a manner which warrants its acceptance as a prerequisite for the degree of Master of Technology. The work has been carried out under our supervision and has not been submitted elsewhere for a degree.

*T. Gangadharaiyah*

(Dr. T. Gangadharaiyah)  
Professor  
Department of Civil Engg.  
I.I.T. Kanpur

*A. K. Gupta*

(Dr. A.K. Gupta)  
Professor  
Department of Aero. Engg.  
I.I.T. Kanpur

January, 1988

18 FEB 1988

CENTRAL LIBRARY

I. I. T., Kanpur.

Acc. No. **A** 99710

Thesis  
624.284  
M4906

CE-1988-M-NIG-LAB

## ACKNOWLEDGEMENTS

The author lacks words to express his sincerest gratitude to Dr. T.Gangadharaiah and Dr. A.K. Gupta for their constant help, valuable guidance, inspiration and encouragement during the work.

The author must also thank Dr. V. Lakshminarayana and Dr. K. Subramanya, Dr. S. Ramaseshan Dr. S. Surya Rao, Dr. K.K. Rampal, Dr. C. Venkobachar of the Department of Civil Engineering for useful courses he received from them during the degree programme.

The author is thankful to Mr. Suresh Kumar, Mr. Ram Sanke and other staff members of the Hydraulics Lab. who helped with many of the detail of the experimentation.

Special thanks are extended to Mr. Gautam Roy for his kind help and suggestion in the thesis report writing.

Thanks are due to my friends Mr. T.V. Minh and Mr.N.S.Loc for their constant encouragement and unreserved help.

Thanks are also due to Dr. T.R. Ramachandran former foreign student adviser and Dr. K.V.G.K. Gokhale for their inspiration.

And finally, thanks to Mr. G.S. Trivedi for an excellent job of typing.

TRAN DINH NGHIEN

# CONTENTS

	PAGE
CERTIFICATE	i
ACKNOWLEDGEMENTS	ii
LIST OF TABLES	v
LIST OF FIGURES	vi
NOTATIONS	ix
ABSTRACT	xi
CHAPTER I	INTRODUCTION AND LITERATURE REVIEW
1.1	Introduction 1
1.2	Literature 6
1.2.1	Mechanism of local scour 6
1.2.2	Empirical Method 11
1.2.3	Scour protection 13
1.3	Present Investigation 20
CHAPTER II	EXPERIMENTAL METHOD
2.1	Experimental Set-up 22
2.2	Method of Conducting Experiment 24
2.3	Grain Size Distribution in the Scour Hole 26
2.4	General Flow Parameters 28
CHAPTER III	RESULTS AND DISCUSSION 31
3.1	General 31
3.2	Local Scour Around the Model Pier Without Device Under Different Flow Conditions 33
3.3	Parametric Study with Delta-Wing-Like Passive Device 41

3.3.1	Choice of passive device length in the flow direction	41
3.3.2	Choice of device width	46
3.3.3	Choice of passive device height	46
3.4	Flat Plate	55
3.5	Combination of Delta-Wing-Like Passive Device with Flat Plate	59
3.6	Comparative Tests	64
3.7	Combination of passive devices at Different Height of the Pier under Different Flow Condition	68
3.8	Comparison with Standard Passive Device as Suggested by Gupta (1987)	76
3.9	Flow Visualization by Point Impression	77
CHAPTER IV	CONCLUSIONS AND SUGGESTIONS	
4.1	Conclusions	85
4.2	Recommendation for Further Study	87
REFERENCES		109

## LIST OF TABLES

TABLE NO.	TITLE	PAGE
2.1	Sediment Characteristics Used for this Study	97
3.1	Maximum Scour Depth for Pier Without Protection for Different flow Conditions	100
3.2	Maximum Scour Depth for Different Device Lengths and Other Geometries Fixed	101
3.3	Maximum Scour Depth for Different Device Width and Other Geometries Fixed	102
3.4	Maximum Scour Depth for Different Model Heights and Other Geometries Fixed	103
3.5a,b	Maximum Scour Depth for Different Flat Plate	104
3.6a,b,●	Maximum Scour Depth for Combined Device	105
3.7	Maximum Scour Depth for Different Model Device	107
3.8	Scour Reduction by Combined Device at Different Flow Conditions	108

## LIST OF FIGURES

FIGURE NO.	TITLE	PAGE
2.1	Play Out of Experimental Water Flume	23
2.2	Schematic Pier With Scale and Location of Section LL', AA', BB', CC'	23
2.3	Sediment Size Distribution	27
3.1	Schematic Picture of Flow	32
3.2a	Variation of Scour Depth Against Time for Pier Alone	34
3.2b	Variation of Scour Depth Against Time Under Varied Discharge	35
3.2c	Profile of Scour Hole Around Clean Pier	36
3.2d	Profiles of Scour Hole Around Clean Pier	37
3.2e	Maximum Scour Depth Line Around Clean Pier	38
3.2f	Scour Depth Relative to B Against $R_{ep}$ and $F_r$	40
3.3.1a	Variation of Scour Against Time When Length of Device is Varied	43
3.3.1b	Profiles of Scour Hole Around Pier Fitted with Passive Device	24
3.3a,b,c	Choice of Device Geometry	45
3.3.2	Variation of Scour Against Time When Width of Device is Varied	47
3.3.3a	Variation of Scour Against Time When Height of Device is Varied	48
3.3.3b	Profiles of Scour Hole When Height of Device is Varied as Ratio $h/B$	49
3.3.3c	Location of Maximum Scour Depth Lines when Ratio $h/B$ is Varied	49
3.3 d	Ratio $d_{sm}/d_{smo}$ During Test Time in Section AA', BB', CC'	52

FIGURE NO.	TITLE	PAGE
3.3e	Ratio $d_{sm}/d_{smo}$ in Equilibrium in Section AA', BB', CC'	52
3.4	Ratio $d_{sm}/d_{smo}$ Against $l_1/B$ For Flat Plate	56
3.5a	Ratio $d_{sm}/d_{smo}$ Against $b_b/B$	60
3.5b	Ratio $d_{sm}/d_{smo}$ Against $b_u/b_b$	60
3.5c	Ratio $d_{sm}/d_{smo}$ Against $h/B$	60
3.5d	Variation of Scour Along the Pier Fitted with Combined Device	61
3.5e	Variation of Scour Depth Along the Pier Fitted with Triangular Flat Plate	61
3.6a	Variation of Scour Against Time When Piles, Collar, Caisson and Riprap Mat Used as Protection Device	65
3.6b	Profiles of Scour Hole when Piles, Collar, Caisson and Riprap Used as Protection Device	67
3.7a	Variation of Scour Depth Against Time When Pier Fitted with Combined Device and $F_r = 0.3$	70
3.7b	Profiles of Scour Hole When Pier Fitted with $M_{40}$ and $F_r = 0.3$	71
3.7c	Variation of Scour Against Time with Different Model Under Different $F_r$ Number	73
3.7d	Profiles of Scour Hole With and Without Different Model Devices Under Different $F_r$ Number	73
3.7e,f	Scour Depth Lines Around Pier with and Without Model Devices Under Different $F_r$ Number	74
3.9.1	Paint Impressions of Flow Pattern on the Plate for Pier Alone and Fitted With Device for $F_r = 0.226$	78

FIGURE NO.	TITLE	PAGE
3.9.2	Paint Impressions of Flow Pattern on the Plate for Pier Alone and Fitted With Device for $F_r = 0.555$	79
3.9.3	Paint Impressions of Flow Pattern on the Plate for Pier Alone and Fitted with Device for $F_r = 0.7$	80
3.9.4	Paint Impressions of Flow Pattern on the Surface of Pier	81
3.9.5	The Typical Photo View of Horseshoe Vortex	88
3.9.6	The Typical Photo View of Flow Pattern	89-96

## NOTATIONS

B	-	width of round-nosed pier model
D	-	pier diameter
$\bar{D}$	-	Arithmetic mean size of sediment
$D_{50}, D_{16}, D_{84}$	-	size of sediment such that 50 percent, 16 percent, 84 percent particles are finer than this size
$D_g$	-	geometric mean size of sediment
$F_r = U / \sqrt{gy_0}$	-	flow Froude number
Q	-	discharge of flow
R	-	radius of round-nosed pier
$Re_p$	-	pier Reynolds number
$Re_{Dc}$	-	critical sediment Reynolds number
$Re_{D50} = U_{*b} x D_{50} / \nu$	-	sediment Reynolds number
$S_e$	-	energy slope
T	-	water temperature in °C
U	-	average velocity
$U_0$	-	free stream velocity
$U_c$	-	critical velocity
$U_{*bc}$	-	critical bed shear velocity
$U_{*b} = \sqrt{gr_b S_c}$	-	bed shear velocity
g	-	gravitational acceleration
$r_b$	-	Hydraulic radius for bed
$y_0$	-	flow depth
$\gamma_s$	-	water specific weight
$\gamma_f$	-	sediment specific weight
$\delta$	-	boundary layer thickness

$\sigma$	-	standard deviation of sediment
$\sigma_g$	-	geometric standard deviation of sediment
$\tau_b$	-	bed shear stress
$\tau_{*b}$	-	dimensionless bed shear stress
$\tau_{bc}$	-	critical bed shear stress
$\nu$	-	kinematic viscosity of water
$b$	-	passive device width
$h$	-	passive device height
$l$	-	passive device length in flow direction
$b_u$		width of upper plate of combined device
$b_b$	-	width of bottom plate
$l_u$	-	length of upper plate in flow direction
$l_{1u}$	-	length of upper plate from ahead of the pier in flow direction
$l_b$	-	length of bottom plate in flow direction
$l_{1b}$	-	length of bottom plate ahead of the pier in flow direction
$d_{smo}$	-	maximum scour depth at the pier without any protection device
$d_{sm}$	-	maximum scour depth at the pier with protection device.

## ABSTRACT

A delta-wing-like passive device was suggested by Gupta (1987) to minimize local scour near the base of bridge piers. The present work is a model study to determine the suitability and optimum dimension of such a device for scour minimization.

A round-nosed wooden pier of width 5 cm fitted with a delta-wing-like passive device on its leading nose was placed in a flume 5.0 m long and 0.5 m wide with subcritical flow over a mobile bed. Initially some runs were made without any pier protection device to determine the most detrimental flow condition. Later tests were conducted mostly for this condition ( $F_r = 0.22$ ).

After obtaining the most effective dimensions of both passive device and triangular flat plate, tests were conducted with the passive device plus a flat plate fixed below it as combined device, at the initial bed level. Further model studies were conducted to determine the scour protection ability of some existing scour protection works. The results indicate that the combined device is effective at  $F_r = 0.22$  in controlling scour, and system of combined device placed at and at distance equal to half of pier width under initial bed level is quite effective upto  $F_r = 0.37$ .

Inferences about the flow structure near the pier by paint impression technique used in this study indicates that the passive device modifies the horseshoe vortex structure near the leading nose of pier. It weakens this vortex, thereby reducing scour near the upstream nose, and spreads while strengthening and spreading the counter rotating vortices on either side of the pier. The results of this study are useful in understanding and controlling scour near bridge piers.

## CHAPTER I

### INTRODUCTION AND LITERATURE REVIEW

#### 1.1 Introduction

Scour is a natural phenomenon caused by the erosive action of flowing water on the bed and bank of alluvial channels. At a bridge site, scour introduces the possibilities of reduction in the support given to the bridge foundation or an abutment being undermined. Scour-induced bridge failures occur during flood flows, which are unsteady, and the geometric and dynamic features are complex. The flow interacts with varied mixtures of sediments which may range from alluvial sands to clays and weathered rocks. Frequently, clay banks, rock outcrops, sand, and shingle bars are present in a stretch of river. During a flood the geometry of these features can change drastically. The problem is often further complicated by the large variety of shapes, alignments, and approaches used for piers and abutments. Further large random changes in foundation geometry can be caused by floating debris, e.g. trees, being trapped up stream of bridge piers. These phenomena have drawn the attention of engineers in designing bridges to be built on erodible foundation material. Practically, the only solution to this problem that has had widespread use is to construct the piers and abutment to an elevation low enough, so that their stability will never be endangered [41].

## CHAPTER I

### INTRODUCTION AND LITERATURE REVIEW

#### 1.1 Introduction

Scour is a natural phenomenon caused by the erosive action of flowing water on the bed and bank of alluvial channels. At a bridge site, scour introduces the possibilities of reduction in the support given to the bridge foundation or an abutment being undermined. Scour-induced bridge failures occur during flood flows, which are unsteady, and the geometric and dynamic features are complex. The flow interacts with varied mixtures of sediments which may range from alluvial sands to clays and weathered rocks. Frequently, clay banks, rock outcrops, sand, and shingle bars are present in a stretch of river. During a flood the geometry of these features can change drastically. The problem is often further complicated by the large variety of shapes, alignments, and approaches used for piers and abutments. Further large random changes in foundation geometry can be caused by floating debris, e.g. trees, being trapped up stream of bridge piers. These phenomena have drawn the attention of engineers in designing bridges to be built on erodible foundation material. Practically, the only solution to this problem that has had widespread use is to construct the piers and abutment to an elevation low enough, so that their stability will never be endangered [41].

Unfortunately there is no unifying theory at present which would enable the designer to estimate, with confidence, the scour depth near bridge piers and abutments, although this problem has been investigated since a very long time and quite a lot of laboratory and field data has been collected. This lack of general theory is due to the complexity of the problem of interaction between water and moving sediment at the junctions with piers or abutments.

Therefore, scour depths can be seen to depend upon the properties of flow, the bed material in the stream and at the bridge crossing (grading, layering, particle shape and size, alluvial or cohesive) and the bridge foundation geometry.

The types of scour which may occur at a bridge site could be grouped as follows:

- (i) General scour of the stream which would occur due to changes of the hydraulic or hydrological properties of the water course.
- (ii) Localized scour (or constriction scour) which may occur because of the constriction of the waterway and rechanneling of berm flow by the bridge.
- (iii) Local scour which is caused by the local flow field around the piers and abutment.

Local scour can occur in one of two ways: (a) clear-water scour, and (b) live-bed scour. Local scour can be superimposed on both the general and the localized scour. Local scour can be defined as a decrease in bed elevation in

the vicinity of an abstraction as a consequence of the local flow field around the obstruction. The type of local scour is classified according to the capacity of the flow approaching the bridge to transport bed material. Clear-water scour occurs when the bed material upstream of scour area is at rest. The bed shear stresses away from the scour area are thus equal to or less than the critical or threshold shear stress for the initiation of particle movement. In clear water scour the maximum scour depth is reached when the flow can no longer remove particles from the scour hole.

Live-bed scour, also referred to as scour with sediment transport, occurs when there is general bed load transport by the stream. Equilibrium scour depths are reached when over a period of time the amount of material removed from the scour hole by the flow equals the amount of material supplied to the scour hole from upstream. It is important to distinguish between these two types of scour because both the development of the scour hole with time and the relationship between scour depth and approach flow velocity depend upon the type of scour that is occurring.

Three approaches exist for solving this complex problem (not together with localized scour due to constriction of waterway and rechanneling of berm flow by building bridge simultaneously) as follows:

- (i) Scour relation for predicting maximum local scour depth or equilibrium local scour depth based on variables

characterizing the fluid, the flow, the bed material, and the bridge pier using extensive laboratory data and limited field measurements.

- (ii) Scour depth at local obstruction by analyzing the basic scour mechanism.
- (iii) Using scour protection after making the best choice of the pier shape for minimizing scour to prevent formation of the scour hole. This permits smaller foundation depths and reduces costs.

The extent of the scour area and the equilibrium depth of scour are problems of great importance in the design of hydraulic structures. Knowledge of the magnitude of erosion is very important in safe and economic design of the foundations of these structures.

The number of variables involved in a scouring process is also very large. However, the important variables may be grouped into four main categories: Variables of fluid and flow, characteristics of the bed material and bridge pier. Some of the parameters are too difficult to qualify such as the particles size distribution, the grain form, or the cohesion of the bed materials.

Breusers et al. (1977)[ 7 ] gave influence of parameters on the scour depth in detail such as

- (i)  $\frac{U}{U_c}$  - Approach velocity:
  - a)  $U/U_c \leq 0.5$  , no scour (Hancu,1967),(Nicollet,1971 a,b)

- b)  $0.5 < U/U_c \leq 1.0$ , clear water scour (Chabert and Elgeldinger, 1956, Hancu, 1967, Mata 1968, Chitale 1962, Chien and Melville, 1987)
  - c)  $U/U_c \geq 1.0$ , scour with sediment motion in the form of ripple, dune or transition flat bed known as live-bed condition (Laursen, 1962, Chee 1982, Jain and Fischer 1979).
- (ii)  $D_{50}/B$  - Sediment size (Bonasoundas, 1973).
  - (iii)  $y_o/B$  - Water depth. This factor gives the most conflicting statements [7].
  - (iv) Shape of the pier: Flamant (1900), Rehbock (1921), Shen, Schneilder and Karaki (1969) classified pier shapes into two categories:
    - a) Blunt-nosed pier where a strong horseshoe vortex system and thus the maximum scour depth occurs at the pier nose.
    - b) Sharp-nosed pier, where the horseshoe vortex system is very weak and the maximum scour depth occurs near the downstream end.
  - (v) Angle of attack (Laursen and Toch, 1956).
  - (vi) Spacing of piers.

Depending upon the number of significant hydraulic parameters in each relation the scour relations can be grouped in six categories under two different approaches as 'Regime', and 'Rational' approaches by both Jain (1981) and Modi (1986).

## 1.2 Literature Review

Many investigators in the past have studied the local scour problem around obstructions of various kinds both by conducting experimental work with laboratory models and by collecting field data from alluvial rivers and canals. A brief review of relevant literature is presented in this article.

### 1.2.1 Mechanism of local scour

It appears that the large-scale eddy structure, or the system of vortices developed about the pier is the dominant feature of flow near a pier. The secondary circulation which develops as a result of modified flow pattern in the vicinity of the obstruction is the real cause of the phenomenon. This has been repeatedly observed and independently reported by a large number of investigators from different places at different times.

Keutner (1932) experimentally demonstrated the existence of a lateral water surface slope when an obstruction was placed in a flow field. A secondary flow that was generated due to this slope causing scour of the bed was first suggested by him. A similar view was expressed by Ishihara (1938) that secondary circulation created by obstruction was related to local scour. By defining the intensity of secondary flow in terms of the centrifugal force and lateral water surface slope developed near the obstruction and by accounting for the variation of

7  
point velocities along a vertical, he developed his equation of scour force per unit of stream width at the outer edge of curvature.

Since then a considerable amount of work has been done by Posey (1949), Laursen and Toch (1956), Bata (1960) Neill (1964), Roper, Schneider and Shen (1967), Highway Research Board (1970) , Belik (1973), Melville (1975), Peder Hjorth (1975), Melville and Raudkivi (1977), Rana (1980), Baker (1979, 1980, 1981) , Qadar (1981), Gupta (1984), Gangadhariah and Muzzammil (1985), Gupta (1986). Depending on the type of pier and free stream condition, the eddy structure can be composed of one or more of three basic systems -- the horseshoe vortex system, the wake-vortex system, and/or the trailing vortex system -- as described by Roper (1966). For sufficiently tall piers the horseshoe-vortex system has been recognised as the dominant feature of scour process at the blunt-nose of the pier. The basic cause of 'local scour' is the hydrodynamic flow structure in the form of the horseshoe vortex that is known to develop irrespective of whether the bed is solid like a wind tunnel floor or mobile like an alluvial river bed. Such horseshoe vortex flow structures occur in a variety of other engineering situations as well like the wing-body junction of an aircraft, turbine blade junction with the disc, tall building junction with ground, etc. It is known that a blunt-nosed pier serves as a focusing or concentrating device for the vorticity already present in the

undisturbed stream to form the horseshoe vortex system by means of a three-dimensional separation of the boundary layer due to strong enough pressure field ahead of the pier.

Scour will be initiated where the scouring potential created by this velocity is strong enough to overcome the particles resistance to motion. Sediment particles will be dislodged free along the front portion of the pier and carried out of the scour hole either by the horseshoe vortex system and/or by the wake-vortex system like a vacuum cleaner. Here attempts of various investigators on the formation of vortices and their interpretation of the scouring mechanism are presented.

Hawthorne (1954) used a small perturbation method for computation of energy of the secondary flow around struts and airfoils in shear flow with non uniform distribution of inlet velocity. The method marks only for streamlined shapes, but nevertheless he was able to show that scour depth increases with the energy of secondary flow, and the modification of the primary flow by the secondary flow increases the scouring capacity. Following a somewhat different line of approach Lighthill (1956a, 1957) was able to make an exact computation of the secondary flow.

Taylor (1959), Johnston (1960) and Joubert (1964) tackled the problem as special case of a three dimensional boundary layer. Maskell (1955) and Taylor (1967) have discussed the very complex behaviour of flow separation under

three dimensional conditions. Peake and Galway (1965) tried to determine theoretically the location of the primary line of separation of a three dimensional laminar boundary layer on a flat wall supporting a cylinder.

Belik (1973) made an experimental study of vortex system generated in the region where an incompressible flow with spanwise varying velocity moves about a circular cylinder connected to a flat plate. He discussed the role of horseshoe vortex at the front of the cylinder and derived the dimensionless similarity number which described the flow.

Shen, Karaki, Schneider and Roper (1966) tried to treat the scour mechanism analytically. They used the momentum approach to estimate the strength of the horseshoe vortex and they found that the strength of the vortex should be proportional to the pier Reynolds number  $R_{ep}$ . Their conclusion was that the maximum scour depth should be a function of the pier Reynolds' number,  $R_{ep}$ .

Schneider and Shen (1969) also indicated that the strength of the vortex associated with the redistributed vorticity could be functionally related to a decrease in circulation of the flow caused by presence of the pier.

Baker (1979) proposed a vortex model based on an experimental study. This model assumed that the circulation of vortex remained same throughout the scouring process, only the size of the vortex increased and correspondingly the rotational velocity of the vortex decreased. Based on these

considerations, he found that the non-dimensional scour depth varies with Froude's parameter,  $\bar{U}/\sqrt{gy_0}$ . Qadar measured the rotational velocity and size of the vortex before scour and related these to the approaching flow average velocity and obstruction width respectively. Further these parameters were related to the scour depth at equilibrium condition.

Gangadhariah, Muzzammil and Subramanya (1985) found that horseshoe vortex should be related with wall region flow parameters, along with bulk flow parameters and dimensions of obstruction through  $\frac{U_0 D}{U_* \delta}$  as the strength of initial horseshoe vortex, where  $U_*$  and  $\delta$  represent the friction velocity and boundary layer thickness respectively.

It is clear from the reviews mentioned above that the strength of vortex was estimated in different approaches by different parameters. Further these parameters are related to the scour depth at equilibrium condition. Melville and Raudkivi (1977) pointed out that the vortex strength increased initially as the vortex system sank in the scour hole due to additional fluid having attained downward motion. However Baker (1979) disagreed with Melville's hypothesis. Baker [4] , Gangadhariah, Muzzammil and Subramanya [15], Melville [30] and Qadar [40] observed that with the increase in size of the vortex as it sank in the scour hole, the rotational velocity of the vortex decreased the shear stress beneath the vortex system till the equilibrium condition was reached. Baker [4] , Gangadhariah, Muzzammil and

Subramanya [15] , Gupta [18] , and Qadar [40] showed that the initial vortex strength decreased with increase in pier Reynolds number. Gupta (1986) noted that vorticity decayed very fast with scour development. The horseshoe vortex gradually assumed an elliptical shape as the scour hole developed. He developed a relationship between initial vorticity and equilibrium vorticity in terms of  $R_{ep}$ . Baker's measurements (1979,1981) put the vortex center location at about 0.2-0.3B, and Qadar gave the size of the vortex as about 0.2B while Muzzammil noted it to be about 0.2-0.6B, where B is obstruction width.

#### 1.2.2 Empirical Method

##### a) Regime method

One of the earliest formulae proposed for the estimation of the maximum scour depth is based on Lacey regime flow equation with support of field data taken at Hardinge bridge over the Ganges river and the model experiments of Inglis at Poona Laboratory. The Indian Railways have adopted this formula to estimate the maximum scour depth measured from the free surface water level as twice the Lacey regime depth. It is evident from that formula that parameters like pier geometry and flow depth are unimportant. Regime approach includes formulae given by Sethi (1960), Ahmad (1962), Inglis Lacey, (1949), Arunachalam (1965), Blench (1969), Bridge and Flood Wing of RDSO (1967, 1968). However, it has been generally recognised that the regime approach only tends to concentrate on overall dimensions. The approach does not reveal the internal

mechanism involved in a scouring process. The regime equations, originally derived on straight reaches of channels in equilibrium for parallel flow conditions, are not applicable to flow conditions at bends and obstructions where the flow is mainly characterized by large scale curvature, separation, vortex formation, macroturbulence and energy dissipation.

b) Rational method

The second approach, the tractive force approach, is based on the concept that the tractive force exerted by the flowing water on the bed particles is mainly responsible for the motion of the bed material when its value exceeds the critical limits. Based on this approach, the equilibrium scour depth in long channel constructions has been predicted by some investigators like Straub (1934), Chitale (1962), Knezvic (1960), Bata (1960), Garde (1961), Chabert and Engeldinger (1956), Hancu (1971), Maza (1977), Breusers (1977). Laursen (1960) has proposed design curve and empirical relation for maximum scour depth measured from the bed level which identify the pier geometry, angle of attack and the upstream flow depth as the important variables. Jain (1981), Jain and Modi (1986) had made comparative studies to conclude that the scour depth formula by Laursen and Toch (1956) is the best predictor among those compared in their study, as it envelops all data and overpredicts less than other formulae. However, that formula shows that the scour depth is independent

of sediment size. Effect of sediment size on maximum scour depth was verified by experimental study by Ettema (1976,1980), Hancu (1971), Nicollet (1971), Chee (1982), Melville (1984), Chien and Melville (1987) and Raudkivi and Ettema (1983).

Quite similar to the formula of Laursen and Toch an other formula containing the effect of sediment size on scour depth was proposed by Jain [23]. Really Laursen's assumptions are valid in case of a long channel contraction by making use of continuity equation for sediment and water, and the sediment transport and resistance laws. His solution quite depended upon the equations selected to describe the flow and sediment transport. It seems that the application of results of long channel contraction scour-problems to the bridge pier scour-problem is not reasonable in the latter case, since large scale eddies and vortices developed. On the other hand, some formulae are based on the analysis of the basic mechanism of local scour which has been recognised by many investigators like Tison Bata , Roper et al., [44] , Melville [31] , Qadar [41] and Gangadhariah et al [16] ; Characteristics of mechanism of local scour around bridge pier has been mentioned in Sec. 1.2 a.

### 1.2.3 Scour protection

The effect of local scour is to expose a greater frontal area of the pier to the flow and to reduce the effective pier foundation depth. Both these effects make the pier structurally unsafe. As pointed out by Breusers et al. (1977)

the suitability of a local scour protection arrangement is linked to the cost-safety-benefit criterion. A relatively expensive method is to carry the pier foundation sufficiently deep. This method requires the estimation of maximum likely scour depth during the life time.

The three components of local scour protection problem are: the sediment characteristics in the pier's vicinity, the leading edge geometry of the pier junction, and the flow characteristics in the pier's vicinity. The different methods of local scour protection relate either to any one or a combination of these three components.

a) Riprap mat. Perhaps the earliest, and probably the most effective and extensively employed method of local scour protection is related to the sediment characteristics in the pier's vicinity and is known as the 'riprap mat'. By his model experiments in 1893 Engels recommended excavation of the bed sediment around the pier nose and filling it with riprap flush with the bed. Posey (1974) also experimentally demonstrated the effectiveness of a riprap inverted filter consisting of one or more layers of progressively coarser material. This problem has been examined by many investigators (Shen, 1972, Breusers et al. 1977). Recommendations regarding the choice of materials' size of the boulders for riprap mat extending horizontally upto two times the pier width beyond the pier's exposed surface (with thickness at least three times the diameter of the stone) have been made. Isbash's

formula (1935) covering all data given by Maza and Sanchez (1964), Neill (1973) was an example to determine the diameter of the boulders as a function of critical velocity equal to twice mean-on-vertical value. Recent experimental investigation of Raudkivi and Ettma (1985) has drawn attention to the more complicated nature of local scour around piers in armored river bed.

b) Upstream piles. The flow characteristics upstream of the pier junction were modified by installing smaller diameter piles in different size, numbers and triangular configurations in the experimental works of Tison (1961), Chabert and Engeldinger (1956). Reduction in local scour was observed in several cases as high as 50 percent due to breaking the incident current, weakening the horseshoe vortex that generates erosion by producing wake regions around the leading edge of the pier junction. Similar reduction was obtained by Levi and Luna (1961) for a vertical strip placed at two times pier width upstream of a rectangular pier. However no general law could be found depending on five parameters such as number, diameter, space from each other, sweep angle and distance of the piles away from the pier for these cases. With the same aim of preventing or hindering the development of the horseshoe vortex by placing smaller pier upstream of the main pier some tests have been conducted by Shen, Karaki, Schneider, Roper (1966) giving the finding as of Timonoff (1929).

The pier nose geometry affects the formation of the horseshoe vortex making the vortex weaker as the nose becomes more stream lined and reduces local scour.

c) Foundation Caisson. To contain the horseshoe vortex system inside an enclosure allowing it to escape downstream, reducing dimension of the caisson some experimental works have been made by Shen and Schneider (1970), however, the dimension of the platform and of the vertical lip in relation with the pier and with other parameters (flow sediment) were not known. A horizontal coaxial flat plate of at least three times the diameter of circular pier and embedded slightly below the bed (about 0.3 to 0.4 diameter) has been tested by Chabert and Engeldinger (1956), Tanaka (1969), Thomas (1969). Breusers (1972) has used a flexible skirt around the models of offshore drilling platform pile's junction in his laboratory tests to obtain reduction in local scour. Such devices to modify the pier junction remain effective in reducing local scour upto maximum 50 percent of that reached with the pier alone in laboratory conditions.

d) Flexible Mat. Flexible mats were seemed one of the most effective devices to reduce scour around bridge pier in tests conducted in the Rocky Mountain Hydraulic Laboratory by Posey, Appel and Chamness (1951). From their experiments they found that firstly, the use of any mat having reasonable weight, perviousness and flexibility gave considerable protection from scour, secondly, scour could be completely prevented by

installing a layer of gravel under a heavy pervious, flexible mat and for economical long time use the link-chain and tightjoint block mats have been recommended.

e) Other types. Some other types of model were suggested, for example, Tanaka and Yano (1967) drilled a hole through the pier at bed level to release the pressure created in the vicinity of the front nose of the pier near the bed. This hole was shown to have only a minor influence on the scour depth. They also tested a 'floating pier' and showed that unless the bottom of the pier was very close to the bed, the scour was negligible. Even when the bottom of the pier was at the bed level, the scour was considerably less than for the pier deep into the bottom. They concluded that the vertically downward flow along the surface of the pier seems to be generated secondarily by the vortex motion and does not seem to affect directly the local scour around the pier of small diameter. Shen, like Tanaka and Yano (1964), found that the strength of the secondary flow could not be weakened by a slot in the pier, Roughness elements on the upstream side of the pier, to weaken to vertical downflow, were shown to have no effect.

In summary, no general law as yet enables the dimensions of these protective structures to be determined although valid results can be obtained by means of foundation caissons below the bed level or by means of piles placed upstream of the main pier. Even flexible mat or riprap

protection is considered an effective method but in which the stone dimensions, stone gradation and the location for protection can be evaluated by estimating the river flow velocity.

f) Passive device suggested by A.K. Gupta (1987). Considering the main cause of bed scour to be primary horseshoe vortex it would appear that suppressing or altering the structure of horseshoe vortex can result in significant alleviation of local scour around the vertical pier. Gupta (1987) has recently reported a dye flow visualisation study in which aerodynamic concepts have been employed to invent a delta-wing like plate attached to the leading edge of the pier junction which appears to modify the horseshoe vortex significantly.

Delta-Wing-Like Passive Device. The basic idea of using a triangular plate has its origin in the aerodynamic properties, in particular, the lift of such plates. The circulation theory of lift as proposed and developed by Kutta and Joukowski states that a two-dimensional plate placed at a small angle of attack in uniform flow experiences circulation which results in a lift on the plate given by the product of flow medium's density, free stream velocity and the circulation (Anderson, 1986). The amount of circulation is related to the angle of attack according to the Kutta condition. The directions of lift, circulation and free stream are such that a horizontal flow from left to right with clockwise circulation causes vertically upward lift on the plate. A negative angle

of attack will therefore generate anticlockwise circulation and vertically downward lift. In its simplest form, a potential vortex with its axis perpendicular to the free stream and lift directions can model the generation of circulation.

For a finite span plate, Lanchester and Prandtl discovered the turning of potential vortex axis at the plate tips by 90 degrees towards downstream resulting in two trailing streamwise vortices. The direction of rotation of trailing streamwise vortices is related to the angle of attack of the finite plate, a positive angle of attack resulting in the same sense of rotation as the streamwise trailing arms of the primary horseshoe vortex at the pier junction with ground.

The triangular plates or delta wings in aeronautics with their apex facing the free stream possess distinctly superior aerodynamic characteristics of high lift and low drag in supersonic flows (Kuchemann, 1978). Even at incompressible flow speeds the triangular planform at small angle of attack experiences higher lift due to leading edge separation of flow on the leeward side of the plate. The separated sheets of flow roll into two spiral vortices which trail downstream of the plate as two strong streamwise trailing vortices in much the same manner as for the finite span plate mentioned above.

The basic idea of delta-wing like passive device introduced at a negative angle of attack at junction of the leading nose of model pier by Gupta (1987) was to counter

and modify the sense of rotation of the pier of vortices of the horseshoe vortex. These vortices have sense of rotation opposite to that of the pier of counter-rotating vortices of horseshoe vortex generated without passive device. The change in sense of rotation of vortices tend to pile up the sediment near pier surface, thus tending to alleviate the local scour almost all around the pier. Using this concept Gupta and Gangadhariah conducted a series of experiments for a particular passive device dimension to find the reduction of scour depth. They found the reduction of scour depth in their experiment in an order of 50 percent compared to alone pier under the same flow condition.

### 1.3 Present Investigation

In view of need of scour protection, the aim of present study is as follows:

- (i) Influence of geometry of delta-wing-like passive device suggested by Gupta (1987) of I.I.T. Kanpur on the reduction of maximum local scour depth at bridge pier is first study. This passive device is applied to the leading nose of pier model mounted on mobile bed.
- (ii) The second is to study influence of geometry and shape of flat plate attached to the leading nose of the pier model at mobile bed level on the local scour depth reduction,
- (iii) After obtaining the most effective dimensions both passive device and flat plate, tests will be conducted

with the passive device plus a flat plate fixed below it at the initial bed level to enable optimum dimension of such as device for scour minimization. This combination of passive device with bottom flat plate known as combined device.

- (iv) Some existing protection works are also conducted for comparison.
- (v) An attempt will be made to relate the significant elevation of selected combined device at the pier model with reduction of maximum local scour depth for further high Froude Number. Initially some runs without pier protection device are done to determine the most detrimental flow condition, than most tests will be performed for this flow condition (live-bed condition) as  $F_r = 0.22$ , except some advanced tests for combined device.
- (vi) Paint impression technique will be used in this study to illustrate the effectiveness of passive device in modifying and weakening the original horseshoe vortex structure near leading nose of the pier by streaklines.

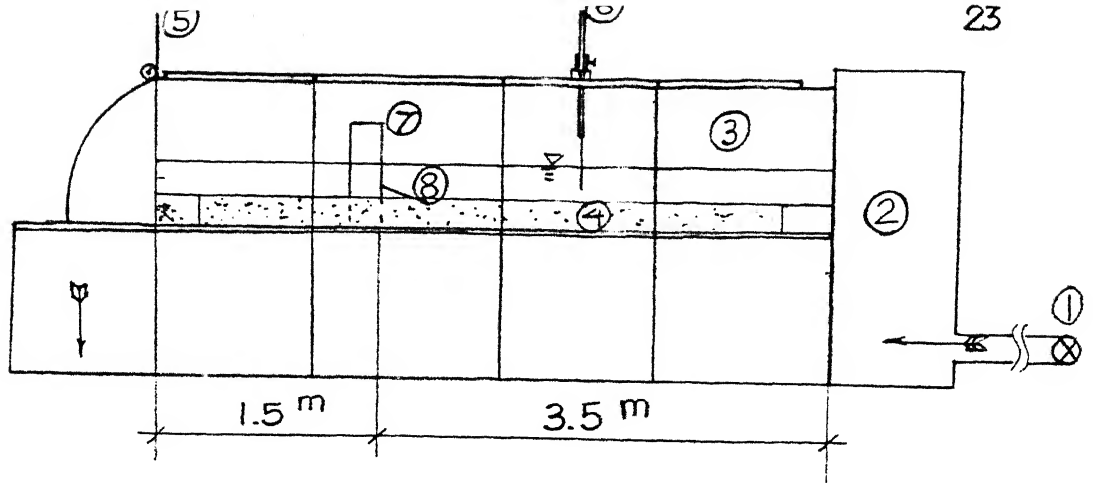
In short the present work is a model study to determine effectiveness of passive device dimensions and combined device dimensions on the reduction of maximum local scour depth for certain flow condition with mobile bed and to study flow pattern over rigid bed to understand original horseshoe vortex to be modified and weakened by passive device fixed at the leading nose of pier.

## CHAPTER II

### EXPERIMENTAL METHOD

#### 2.1 Experimental Set-up

The experiments were conducted in a glass-sided flume 5.00 m long, 0.50 m wide and 0.90 m high. Water supplied to flume is recirculated from a overhead tank by an axial flow pump driven by motor (See Fig. 2.1). A sliding point gauge was used to check the horizontal sand bed surface. The depth of sand bed was 14.00 cm. Discharge passing through the flume was measured by a rectangular weir. The tail gate of flume was adjusted to keep constant flow depth. Constant discharge was maintained by operating a valve over the entrance tank. The test station for all experiments was located at 3.50 m from upstream entrance. Round-nosed wooden pier 5.00 cm wide, 18.00 cm long and 45.00 cm high was employed for all tests. A measuring scale was attached to the pier surface to enable the deepest point of scour hole at any location on the pier at any time to be read visually. A strong light was used to improve visibility especially during experiments with high suspended load. Alluvial sand collected from river Ganges was used as sand bed for all tests. Pier width was 5.00 cm, that is about 10 percent of the flume width, to minimize blockage effects. The mean approach flow depth was kept constant until ripple or dune formed but water surface level still remained



- |                  |                   |
|------------------|-------------------|
| 1. valve         | 5. tail gate      |
| 2. entrance tank | 6. point gauge    |
| 3. water flume   | 7. pier model     |
| 4. sand bed      | 8. passive device |

FIG. 2.1 LAY OUT OF EXPERIMENTAL WATER FLUME

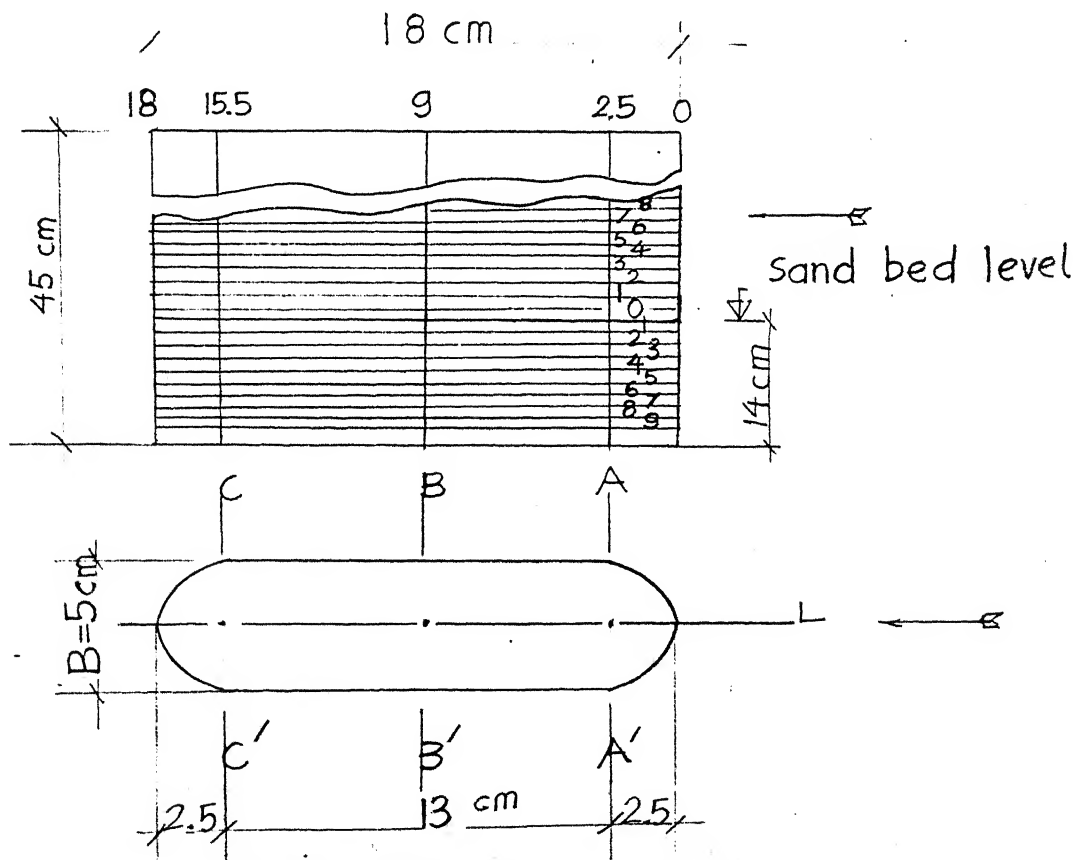


FIG. 2.2 SCHEMATIC PIER WITH SCALE AND LOCATION OF SECTION LL', AA', BB', CC'

near the same during the test.

Tests of pier alone and of some types of scour protection, such as caisson, caisson with vertical lip, collar at different position on the pier, small piles front of the main pier, and riprap, were conducted to be compared under the same flow condition.

Device like delta-wing consists of two flat plates a thin vertical spiral rib on bottom surface of inclined plate along its symmetrical line. The thin vertical spiral rib tapers down to zero height at the delta vertex with its height as the height of device. Devices are made of perspex. The time of test lasts over seven hours.

## 2.2 Method of Conducting Experiment

The procedure for conducting experiment was first to make a flat level sand bed along the flume of 14.00 cm thickness. Then the model-pier was inserted partially at the test station and the bed around the model was levelled flat again as other flat sand bed location and device was attached to the leading nose of the pier with the bottom edge of vertical rib of device touching flat sand bed. The water was allowed to flow by opening the control valve in the supply pipeline over the entrance tank then flow depth and discharge was checked again. The local scour at the pier was read directly on the pier and local scour surrounding the pier was measured with the pointer depth gauge. Recordings of local scour depth were

made at 1 minute interval for first 20 minutes, 5 to 10 minutes interval for rest time upto 60 minutes and then 30 minutes interval upto the end of test. Recordings around the model were made along the directions of LL', AA', BB', CC' (See Fig. 2.2) after one , three, hours and before stopping the test to enable the scourings during the test and average dynamic flow depth for all time of test to be identified. Recording of water surface and bed form along cross-section far from the back nose of the pier 50.00 cm and from the leading nose of the pier, in tern, 25 cm, 50 cm, 100 cm, 150 cm and 200 cm were also made with five points of measuring in each . After seven hours or more of uninterrupted steady water flow the test was terminated upon attainment of equilibrium scour conditions. Water in the flume was allowed to drain and after overnight setting of sand bed, the scour depth recordings around the model were taken in the same directions as mentioned above.

In preparation for the test, sand had washed downstream in the basin nearby back tail-gate from previous test was shoveled toward the head of the flume and then struck off to a constant depth (14.00 cm in all test) as flat as possible by checking of sliding point-gauge, after that device was fixed and test was run as mentioned above.

The mean bed level, the mean water level and discharge were frequently checked during test. Sand was fed in 15 minutes interval after ripple coming to the leading nose

of the pier to ensure that a uniform flow was maintained.

### 2.3 Grain Size Distribution in the Scour Hole

The properties of the alluvial sediment grains selected from the deep portion of the scour hole surrounding the pier and device for all tests were given in Table. 2.1. Sieve analysis has been carried out for these sediment samples and their data have been plotted as shown in Fig. 2.3. The median particles of size of a sediment,  $D_{50}$ , was taken as the representative particle size of the sediment. The degree of uniform of the particle size distribution of a sediment is defined by the value of its geometric standard deviation,  $\sigma_g$ , which was evaluated by using

$$\sigma_g = \sqrt{\frac{D_{84}}{D_{16}}}$$

Geometric mean size

$$D_g = \sqrt{D_{84} \times D_{16}}$$

In general for all tests the following properties of fine bed sediment can be acceptable as follows:

Arithmetic mean size  $\bar{D} = 0.152$  mm

Median size  $D_{50} = 0.155$  mm

Geometric mean size  $D_g = 0.162$  mm

Standard deviation  $\sigma = 0.05$

Geometric standard deviation  $\sigma_g = 1.22$ .

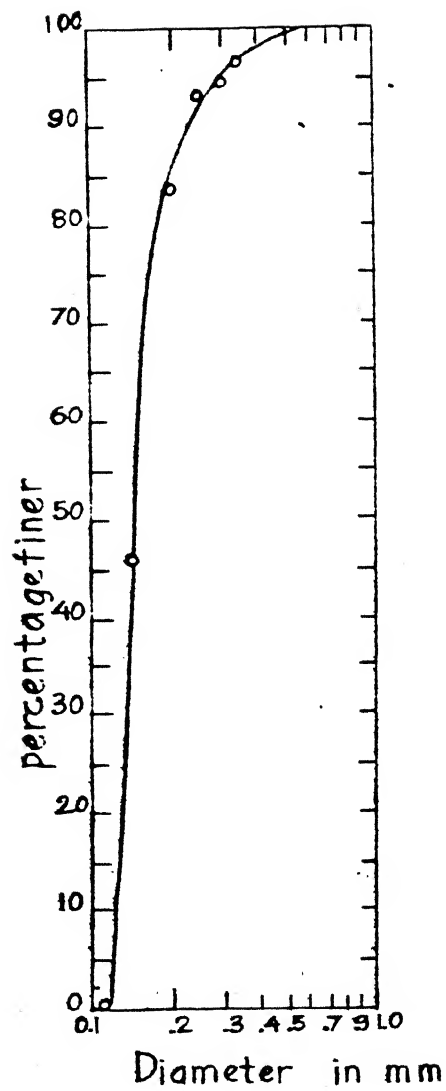


FIG.23.SEDIMENT SIZE DISTRIBUTION

## 2.4 General Flow Parameters

In this investigation temperature varied 20 °C to 34 °C from each to other experiment , average temperature is taken as 27°C then  $\frac{\tau_{obc}}{(\gamma_s - \gamma_f) D_{50}} = 0.06$ . Refering to the Shield's criterion and Table 3.2 , page 57 of the R.J.GARDE and K.G. RANGA RAJU, 1977. We get,

$$U_{*bc} = 1.227 \text{ cm/sec.}$$

$$\tau_{bc} = 1.50534 \times 10^{-3} \frac{\text{kg}}{\text{cm x sec.}^2}$$

$$ReDc = \frac{U_{*bc} D_{50}}{\nu} = 2.237$$

as written in this investigation discharge was kept then other flow parameters were not varied in a large range for the first phase. General flow parameter also seen in Table 2.2 and Table 2.3.

To calculate shear velocity, shear stress, sediment grain Reynolds Number and  $\tau_{*b}$  for the bed, side-wall correction procedure has been used (Journal of Hydraulic Division, January 1971, ASCE) here,

$$U_{*b} = \sqrt{g r_b S_e} \quad (\text{m x sec.}^{-1})$$

$$\tau_b = \rho_f U_{*b}^2 \quad (\text{kg x cm}^{-1} \text{ x sec.}^{-2})$$

$$\tau_{*b} = \frac{\tau_b}{\rho_f g (1.65) D_{50}}$$

$$ReD_{50} = \frac{U_{*b} \times D_{50}}{\nu}$$

where,

$g$  - gravitational acceleration =  $981 \text{ cmx sec}^{-2}$

$r_b$  - bed hydraulic radius (cm)

$S_e$  - Energy slope

$$\frac{\rho_s}{\rho_f} = 1.65$$

$\rho_s$  - specific gravity of sand grain

$\rho_f$  - water specific gravity

$\nu$  - kinematic viscosity of water given by

$$\nu = \frac{0.0179}{1 + 0.0337 \times T + 0.000221 \times T^2} (\text{cm}^2 \times \text{sec}^{-1})$$

has been calculated for present investigation,

$T$  - water temperature

$D_{50}$  - median size of sand grain = 0.155 mm.

TABLE 2.2 : GENERAL FLOW PARAMETER FOR FIRST PHASE OF TEST

$Q$ (l/sec.)	$y_o$ (cm)	$U$ (cm/sec)	$Fr$	$U_{*b}$	$\tau_b$
10.724	9.2-10	20.84 -22.1	.21-.22	4.61-5.4	21.28-29.2
$ReD_{50}$	$t^{\circ}C$				
7.5-10.8	$20^{\circ}-34^{\circ}$				

TABLE 2.3 : GENERAL FLOW PARAMETERS FOR DIFFERENT FLOW CONDITIONS

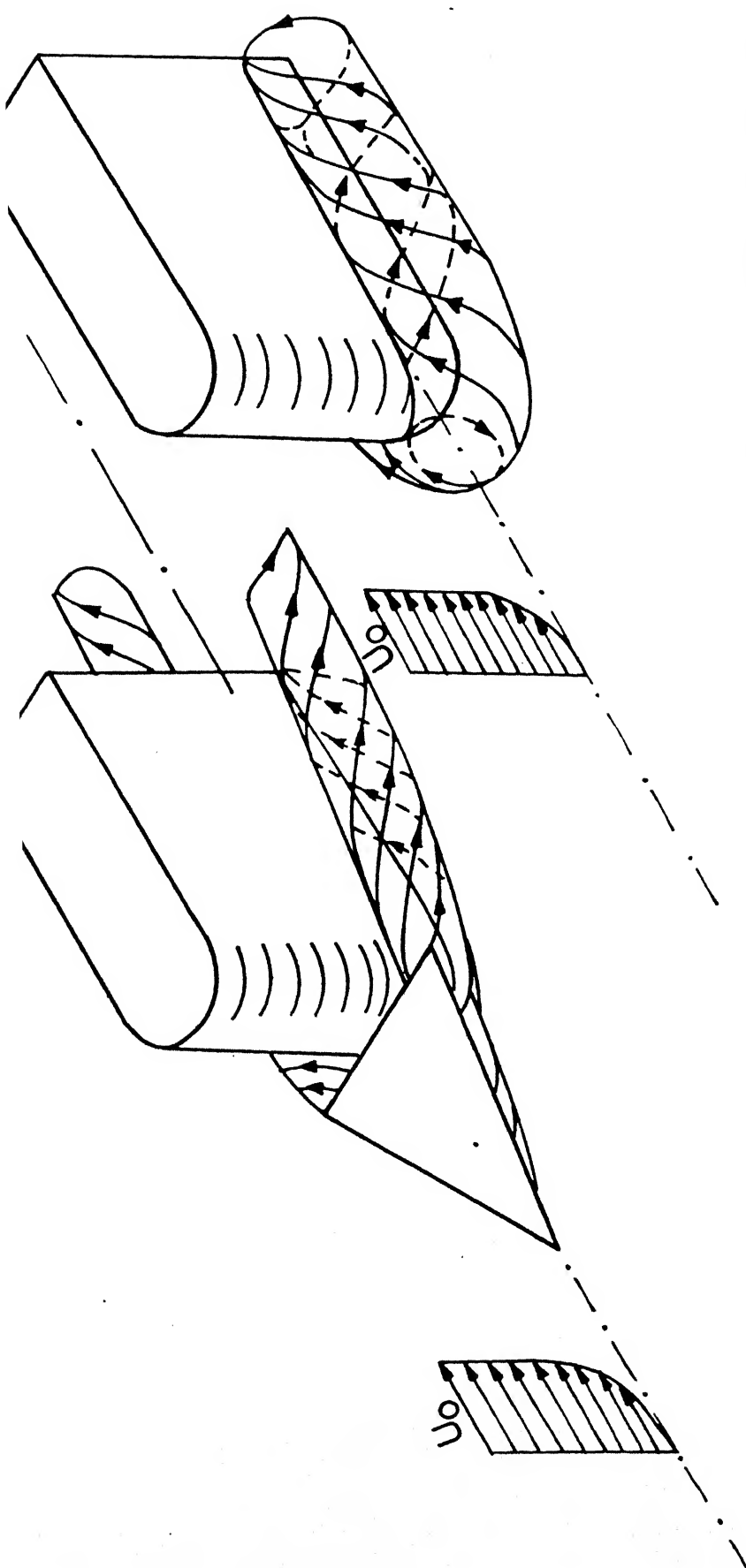
Discharge $Q$ (l/sec)	Average Velocity $U$ (cm/sec)	Energy Slope $S_e \times 10^{-3}$	Bed Friction Factor $f_b \times 10^{-3}$	Bed Hydraulic Radius $r_b$	Bed Shear Velocity $U_b$ (cm/sec)	Bed Shear Stress $\tau_b \times 10^{-3}$ (kg.cm <sup>-1</sup> sec. <sup>-2</sup> )	$R_{eD50}$	$\tau_{*b}$	Dynamic Average Flow Depth $y_o$ (cm)
10.72	21.93	2.77	432.96	9.58	5.10	26.03	8.75	1.04	9.78
18.70	37.40	1.03	49.59	8.58	2.94	8.67	4.67	0.35	10.00
18.75	35.98	1.77	102.13	9.52	4.07	16.53	6.45	0.66	10.42
15.70	32.66	2.33	154.87	9.03	4.54	20.64	7.21	0.82	9.61
14.25	29.91	2.49	198.42	9.09	4.71	22.19	9.59	0.88	9.55
18.72	36.46	1.08	157.23	9.98	3.08	9.51	6.16	0.38	10.27
14.25	29.58	1.64	132.75	9.03	3.81	14.52	7.76	0.58	9.65
14.25	29.96	1.89	147.69	8.94	4.07	16.57	8.29	0.66	9.51
15.74	33.63	1.67	99.97	8.63	3.76	14.14	7.66	0.56	9.36
15.74	32.72	1.95	128.43	8.98	4.15	17.18	8.53	0.69	9.62
15.74	31.89	2.42	174.41	9.40	4.72	22.37	9.78	0.89	9.87
18.66	37.18	2.30	122.00	9.34	4.59	21.07	9.51	0.84	10.04

## CHAPTER III

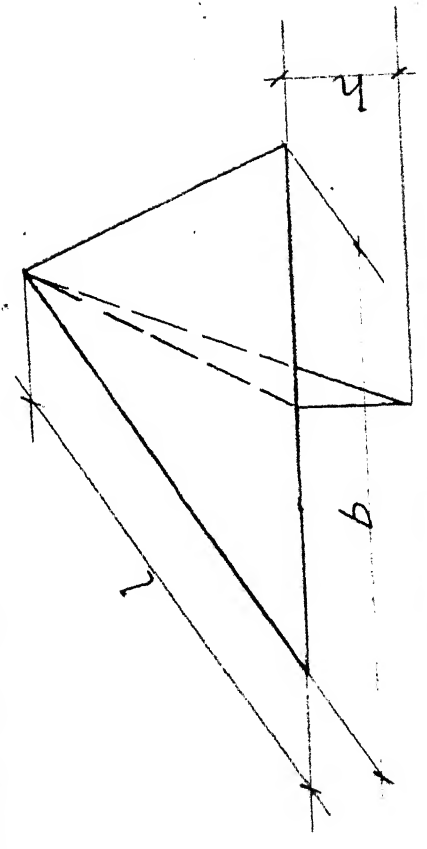
### RESULTS AND DISCUSSION

#### 3.1 General

In attempting to study protection against local scour around bridge piers during floods the flow past a pier has been modelled in the laboratory flume. In this investigation a delta shaped passive device was attached to the leading nose of the model pier for local scour protection (see Fig.3.1a, b and c). The only shape of model pier tested was the semi-circular shape which is a common shape in use. Furthermore, it is reasonable to believe that if this device provides satisfactory protection for the round-nosed pier, it would not be too difficult to find the requirement for piers of other shapes. For similar reasons, the investigation was limited to the case of cohesionless bed material, since non-cohesive bed materials are by far the most common at the site of permanent-type bridges. Before and during tests with device some tests without device were conducted to enable comparison and to understand the effects of devices of different dimensions. Based on satisfactory results of one type of device, some combinations of devices were made and tested under different discharge conditions. The maximum local scour depth for each case was measured and analysed for each purpose such as choice of the dimension of device, comparison with some previous protection works, and to test



(a) Without passive device



(b) With passive device

(c) Schematic passive device

the combinations of devices for scour prevention.

3.2 Local Scour Around the Model Pier without Device under Different Flow Conditions

Maximum scour depth in the scour hole around model pier at different time under different flow conditions were measured as  $d_{smo}$  given in Table 3.1 and Fig. 3.2a and 3.2 b. The maximum local scour depth data after stopping the flow and draining water overnight are plotted in Fig. 3.2c and 3.2d to present the profiles of scour hole along the longitudinal section passing through the pier centre-line with flow direction from left (L) to right (L') , and also along cross-sections passing across 2.5 cm, 9.0 cm and 15.5 cm from the leading nose of the model pier denoted as AA', BB' and CC', respectively (see Fig. 3.2c,d).

Defining the locus of all points where scour depths is maximum on sections normal to the flow as the maximum scour depth line, this line is plotted for  $F_r = 0.198$  and  $0.224$  in Fig. 3.2e. From Figs. 3.2a , 3.2b it may be observed that the data appear to plot on three curved segments on semi-logarithmic graph. The first steep segment is associated with rapid scouring by the down flow. The down flow digged sediment around the front nose of the model pier by forming different grooves. The second slightly steep segment shows the development of the scour-hole as the horseshoe vortex moves away from the cylinder and grows in strength. The last segment describes the equilibrium local scour depth due to dunes or

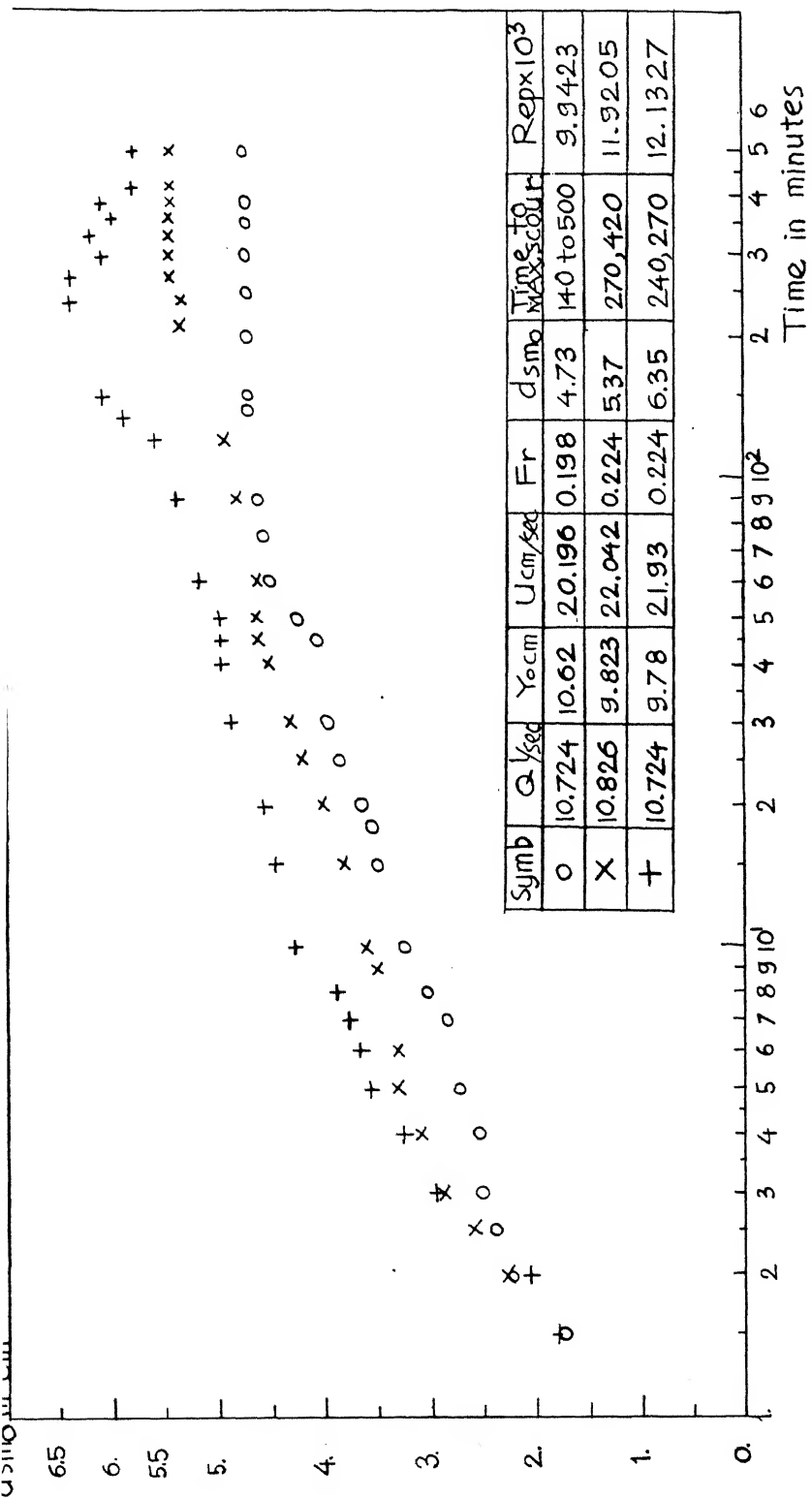


FIG.3.2 a. VARIATION OF SCOUR DEPTH VS TIME FOR PIER ALONE

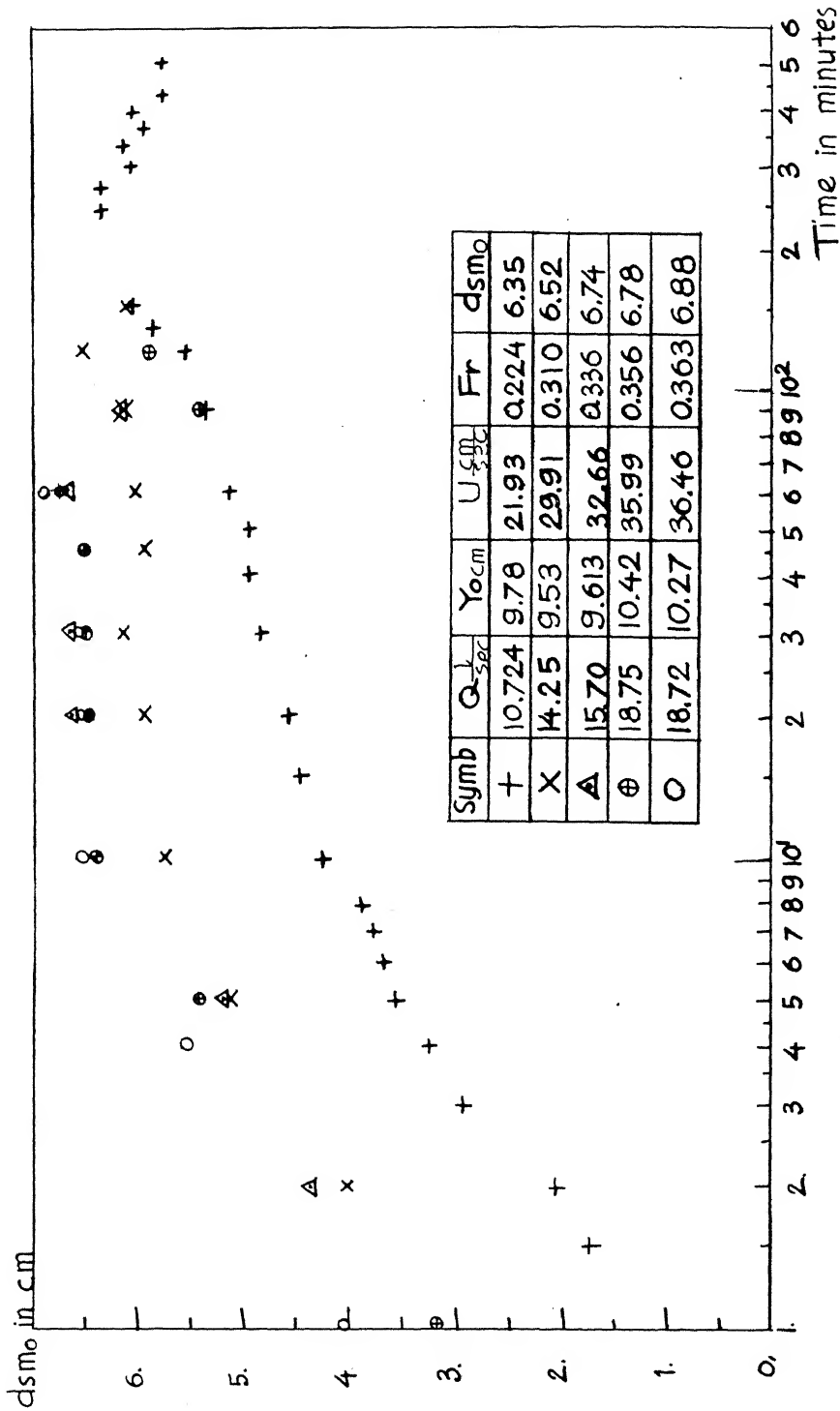


FIG.3.2.b. VARIATION OF SCOUR DEPTH VS TIME  
UNDER VARIED DISCHARGE FOR CLEAN PIER,  $B=5$  cm.

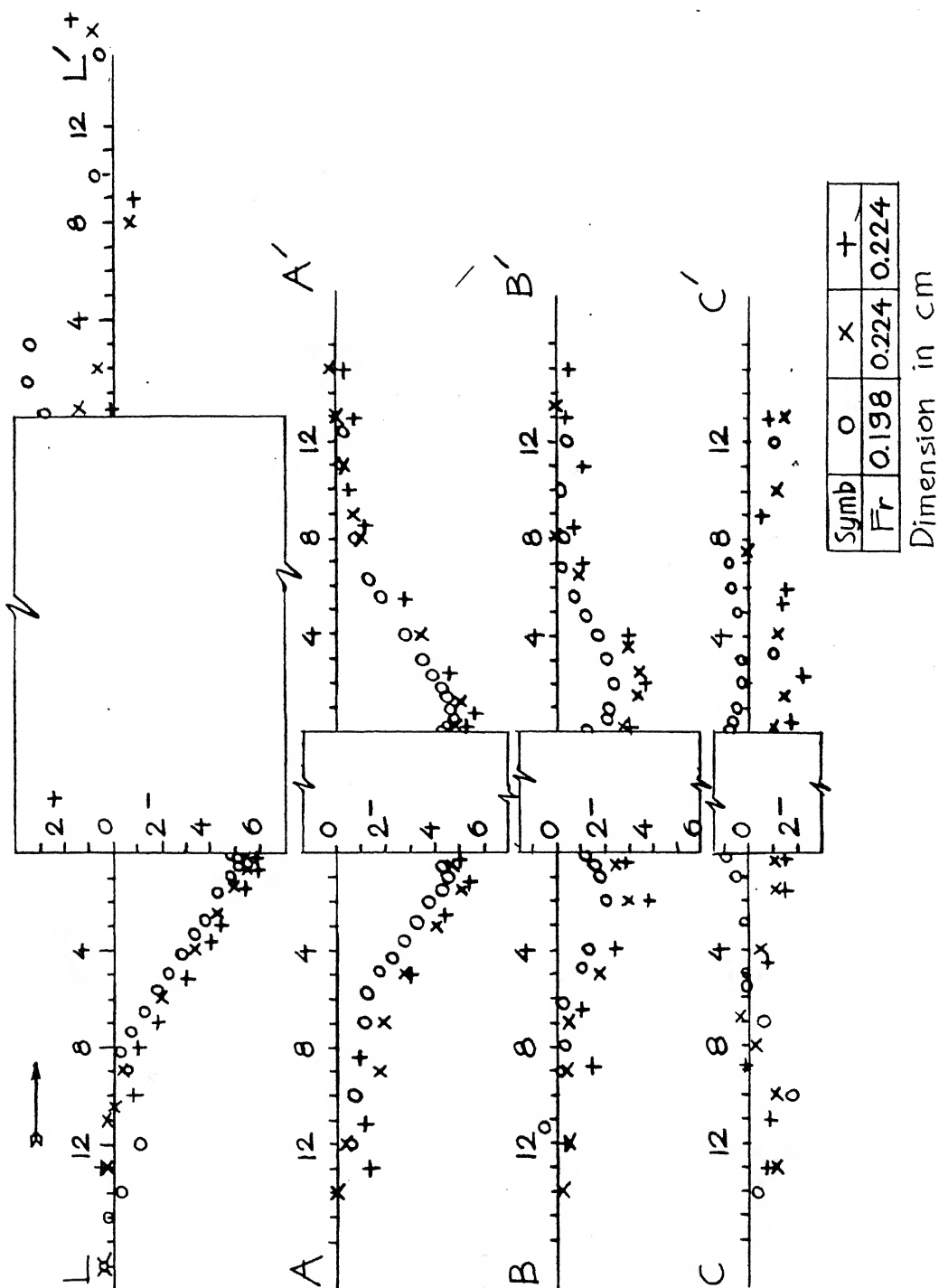


FIG.3.2.C. PROFILES OF SCOUR HOLE FOR CLEAN PIER,  $B=5$  cm

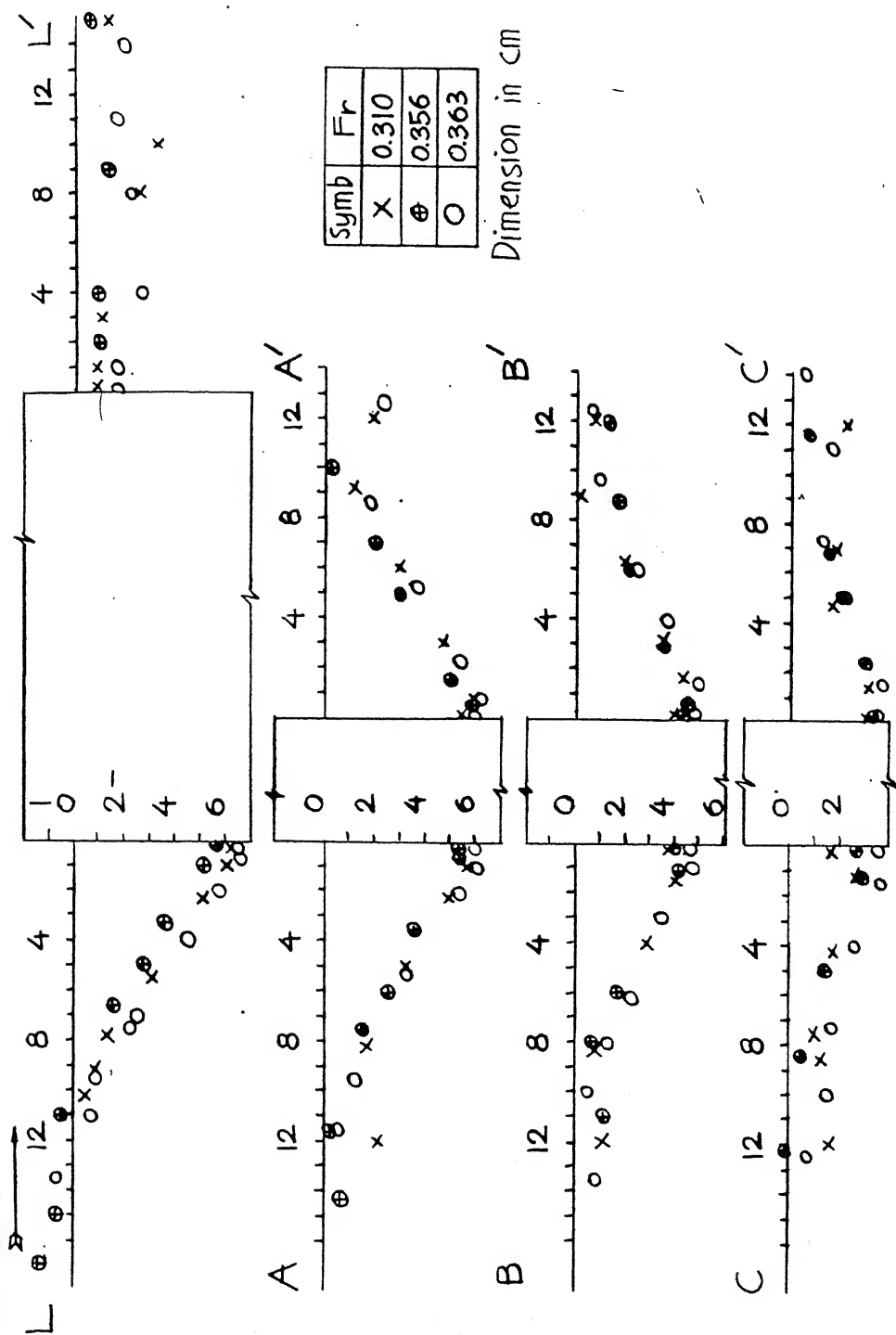


FIG.32.d. PROFILES OF SCOUR HOLE AROUND CLEAN PIER,  $B=5\text{cm}$

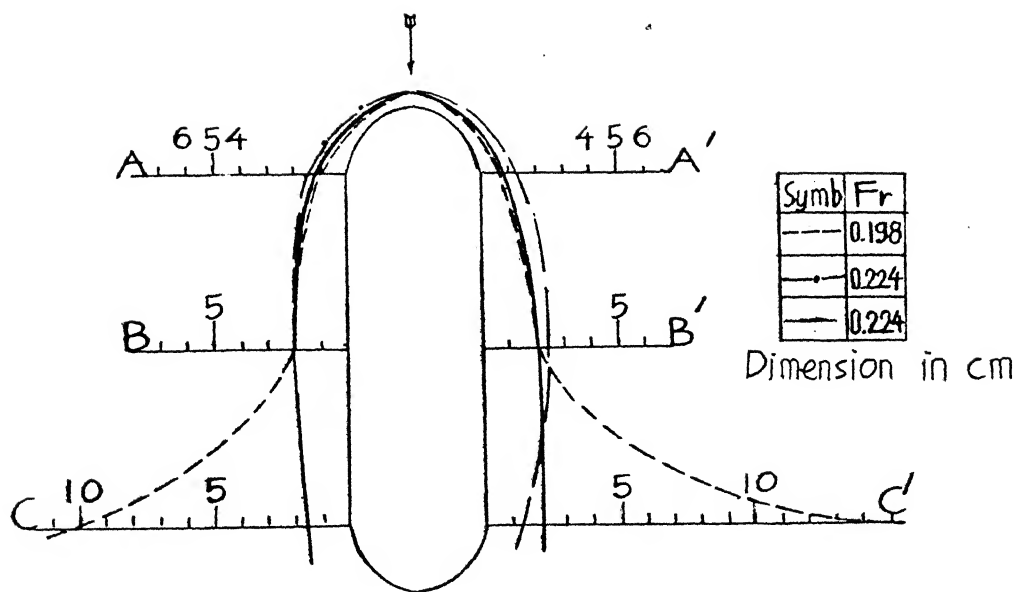
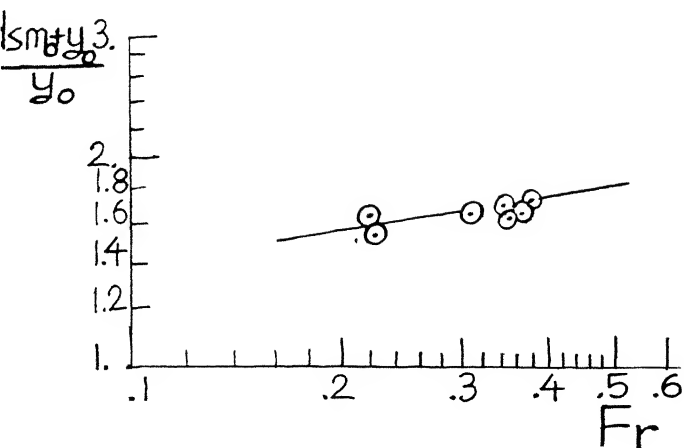


FIG. 3.2.e. MAXIMUM SCOUR DEPTH LINE  
AROUND CLEAN PIER,  $B = 5$  cm

ripples formed on the bed by interaction between flow and sediment. In general local scour depth varies with the passing of a dune or ripple. The scour value is often less than maximum just before ripples or dunes reach the pier. The data indicate that the higher the froude number the higher maximum local scour depth at the leading node of model pier, but the difference is not much under the flow conditions tested.

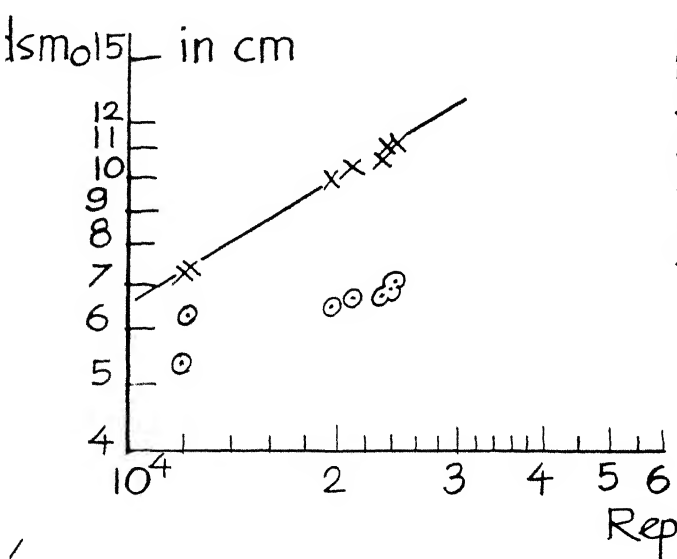
From Fig. 3.2a it appears that maximum local scour depth as function of time and maximum value is higher when ripples form and approach the pier assymmetrically. It also appears that the higher the second curve segment the deeper the scour depth around the leading nose of the model pier, and if the flow conditions are nearly the same the maximum scour depth appears approximately at the same time (see tests 30, 31 in Table 3.1 ). From the point of view of maximum scour depth accuring in test 31 ( $d_{smo} = 6.35$  cm), it was taken for comparison with other tests in which device was applied.

Figures 3.2c, d,e show that scour depth line for same flow conditions, in the down stream direction is quite near the pier and is egg-shaped in plan, with its value reducing from the leading nose to the rear of the pier. The higher the Froude number the larger the scour hole extent in plan and the deeper the local scour value in all sections, and there is no deposit behind the model pier along section LL' when  $F_r \geq 0.31$ , but scour only.

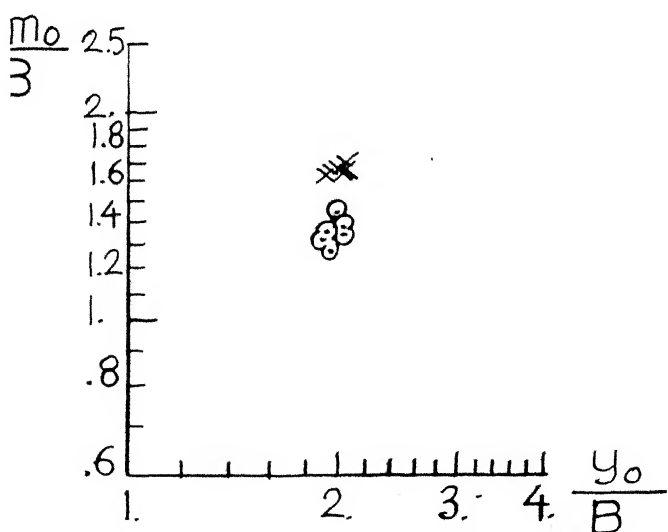


$\frac{d_{smo} + y_0}{y_0}$	Fr
1.65	.22
1.70	.34
1.68	.31
1.67	.36
1.65	.35
1.72	.38
1.55	.22

Rep EXP. RESULTS 0.00022 Rep<sup>.619</sup>



12132.7	6.35	7.42
11920.5	5.37	7.34
24077.0	7.17	11.34
23168.0	6.78	11.07
21025.6	6.74	10.43
19656.8	6.52	10.00
23472.0	6.88	11.60
	(O)	(X)



Rep	$\frac{y_0}{B}$	$\frac{d_{smo}}{B}$	$1.35 \left( \frac{y_0}{B} \right)^3$
	1.96	1.27	1.65
	1.92	1.34	1.64
	1.91	1.31	1.64
	2.05	1.38	1.67
	2.08	1.36	1.68
	2.0	1.43	1.66
		(O)	(X)

FIG. 3.2.f

i, RATIO  $d_{smo} + y_0 / y_0$  AGAINST Fr  
 ii, SCOUR DEPTH  $d_{smo}$  AGAINST Rep  
 iii, SCOUR DEPTH RELATIVE TO B VS  $y_0 / B$

Taking  $B$  as pier width and  $d_{smo}$  as maximum scour depth the maximum scour depth relative to  $B$  (i.e.  $d_{smo}/B$ ) as a function of pier Reynolds number ( $R_{ep}$ ) and of flow Froude number ( $F_r$ ) have been plotted in Fig. 3.2f for  $R_{ep}$  in the range  $11.92 \times 10^3$  to  $24.08 \times 10^3$  and for  $F_r$  from 0.22 to 0.37, respectively. Scour data are also plotted against the scour profiles of Laursen and Toch and of Shen as shown in Fig. 3.5f. From these Figures one can say that maximum local scour depth at the leading nose of the pier depends upon both  $R_{ep}$  and  $F_r$  under flow conditions tested for a given pier shape and size.

### 3.3 Parametric Study with Delta-Wing-Like Passive Device

The passive device used is a thin delta-wing-like plate. On its bottom flat side is attached a thin vertical spinal rib along the line of symmetry of the delta wing. The thin vertical spinal rib tapers down to zero height at the delta vertex as shown in Fig. 3.1b.

#### 3.3.1 Choice of passive device length in the flow direction

The choice of device length was based on effective hydraulic reason namely maximum local scour depth, extent of scour hole and location of maximum local scour depth in plan. Five model devices designated as  $M_1, M_2, M_3, M_4$  and  $M_5$  were fabricated and tested, in which only the length of the passive device in the flow direction has been varied while other dimensions were kept constant as  $h = 0.5B$  and  $b = 1.5 B$ . The results for comparison are recorded in Table 3.2. Scour depth as function

of time is plotted in Fig. 3.3.1a for different tests.

Profiles and extents of scour hole around model pier for the five model devices are drawn in Fig. 3.3.1b. Relative scour depth as ratio  $d_{sm}/d_{smo}$  against relative length of device as  $l/B$  has been plotted in Fig. 3.3a. Here  $d_{sm}$  is maximum scour depth at the leading nose of the pier when model device is attached to the leading nose of the pier,  $l$  is the length of model device along the flow direction. From the above figures some significant remarks can be made:

- a) Maximum scour depth as function of time increases with time for both pier without and with device attached. The difference in value of local scour depth in the case of pier with device is less than that in case of pier alone. The maximum reduction achieved in case of pier attached with device is 36.4 percent for model  $M_2$  with  $l/B = 2.5$ .
- b) Deposition occurs in the Section CC' and behind the pier along section LL' (see Fig. 3.3.1b) .
- c) Scour depth in the maximum scour depth line is less and its location is far away from the pier surface compared to that in case of pier without device.
- d) Effect of the length of the passive device on the scour depth is not very significant as the data plots nearly parallel to the abscissa. However,  $M_2$  gives slightly better choice with a length 12.5 cm and maximum reduction of scour depth is 36.4 percent. Thus the length of model

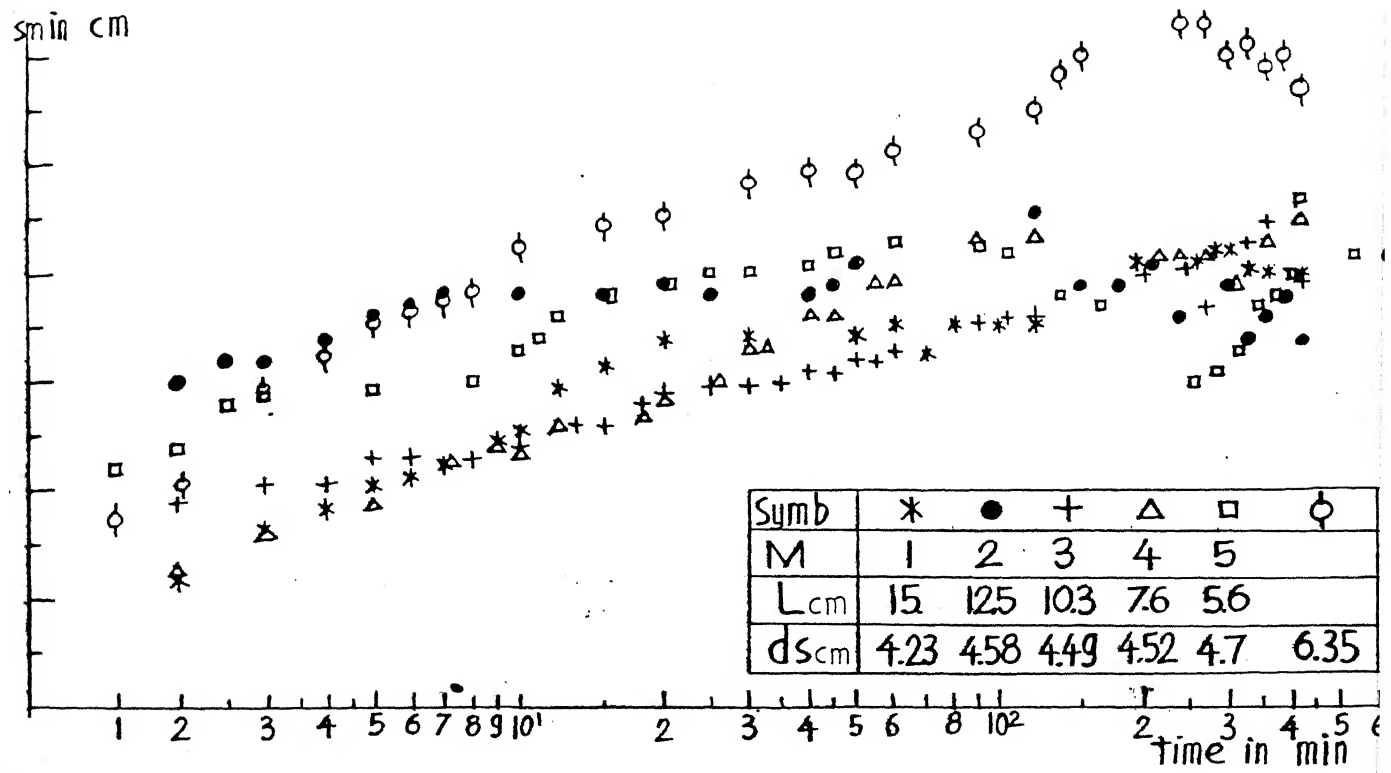


FIG.3.3.1.a. VARIATION OF SCOUR VS TIME WHEN THE LENGTH OF DEVICE IS VARIED

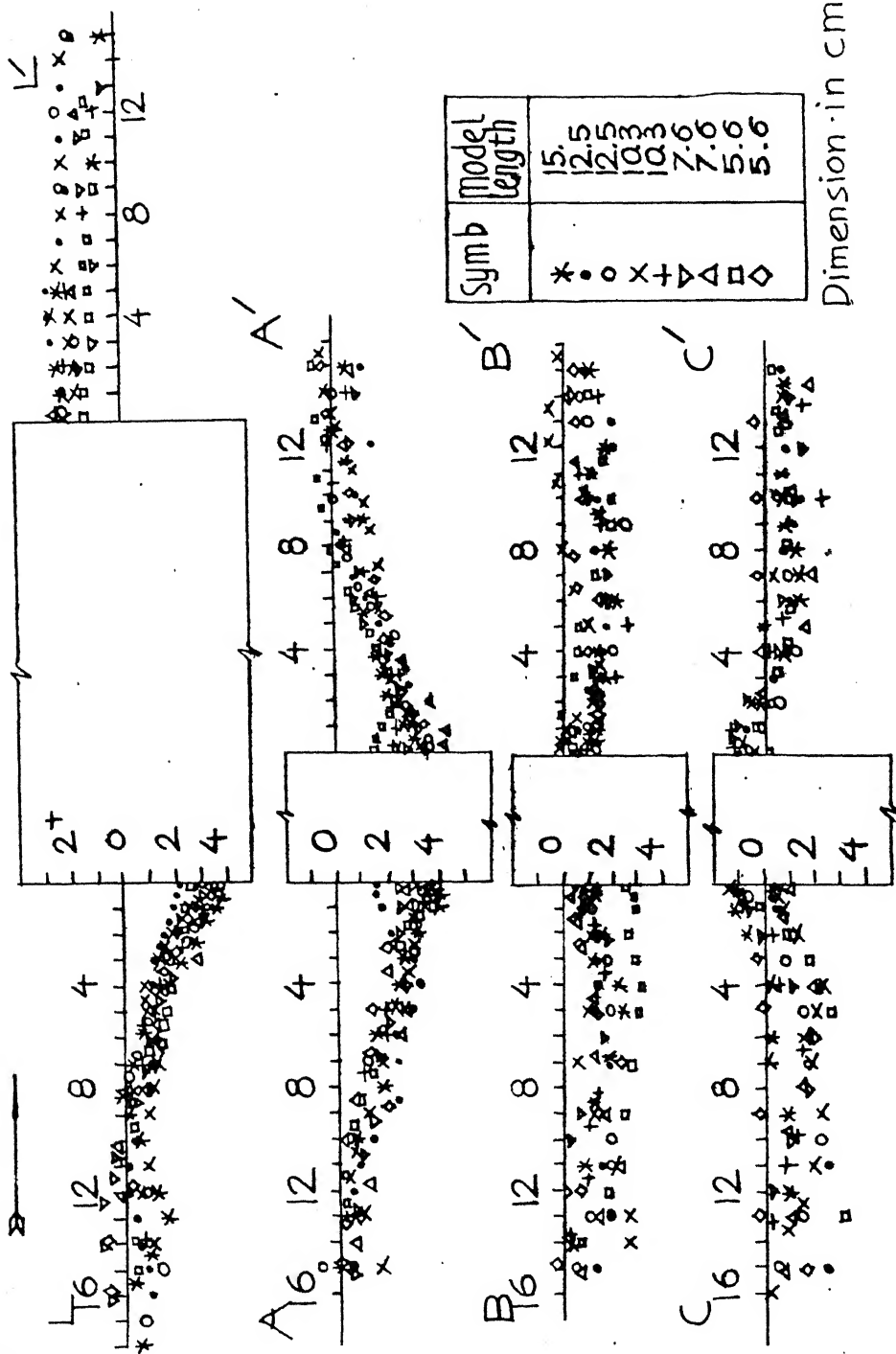


FIG.3.3.1.b. PROFILES OF SCOUR HOLE AROUND PIER  
FITTED WITH THE PASSIVE DEVICE

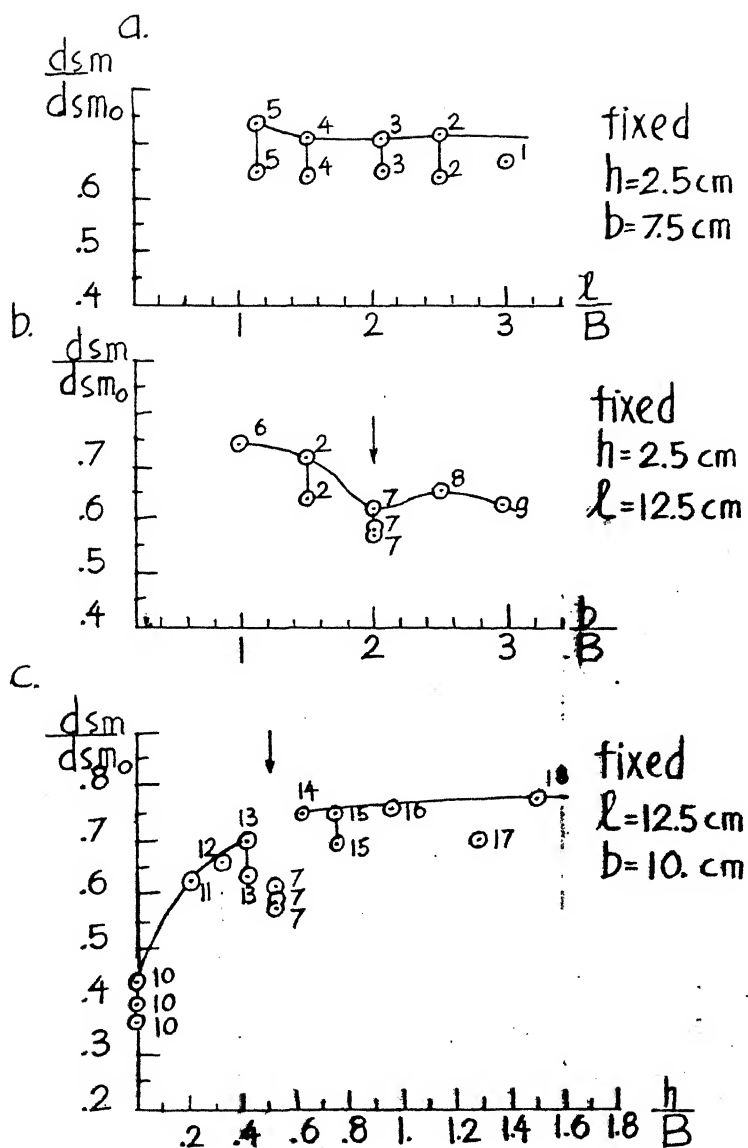


FIG. 33.a. RATIO  $d_{sm}/d_{sm0}$  vs  $l/B$

b. RATIO  $d_{sm}/d_{sm0}$  vs  $b/B$

c. RATIO  $d_{sm}/d_{sm0}$  vs  $h/B$

FOR CHOICE OF DEVICE GEOMETRY

device equal to 12.5 cm or 2.5 B was selected for further study.

### 3.3.2 Choice of device width

In order to choose the width of the passive device four model devices denoted as  $M_6$ ,  $M_7$ ,  $M_8$  and  $M_9$  were made and tested after the length of the model device was chosen as mentioned in Section 3.3.1. The resulting maximum scour depth data are given in Table 3.3. Maximum scour depth as function of time in plotted in Fig. 3.3.2, and ratio  $d_{sm}/d_{smo}$  against  $b/B$  is drawn in Fig. 3.3b. In these tests model  $M_7$  with its width equal to 2B appears to effect a remarkable reduction in scour depth (38.6 percent). This enables model width as 2B to be chosen for further tests to determine optimum model height.

### 3.3.3 Choice of passive device height

For this last choice of dimension of model device nine devices of different height designated  $M_{10}$ ,  $M_{11}$ ,  $M_{12}$ ,  $M_{13}$ ,  $M_{14}$ ,  $M_{15}$ ,  $M_{16}$ ,  $M_{17}$  and  $M_{18}$  were made and tested after the length and the width of the model device were selected as  $l = 2.5B$  and  $b = 2B$ . Table 3.4 presents the results of these tests. Maximum scour depth as function of time for different heights of the passive device has been plotted in Fig. 3.3.3a. Profiles of scour hole and location of maximum scour depth with varied model device height, or ratio  $h/B$ , has been plotted in Figs. 3.3.3c,d. The ratio of  $d_{sm}/d_{smo}$  against ratio  $h/B$  as given in Fig. 3.3c shows a tendency of reduction of maximum

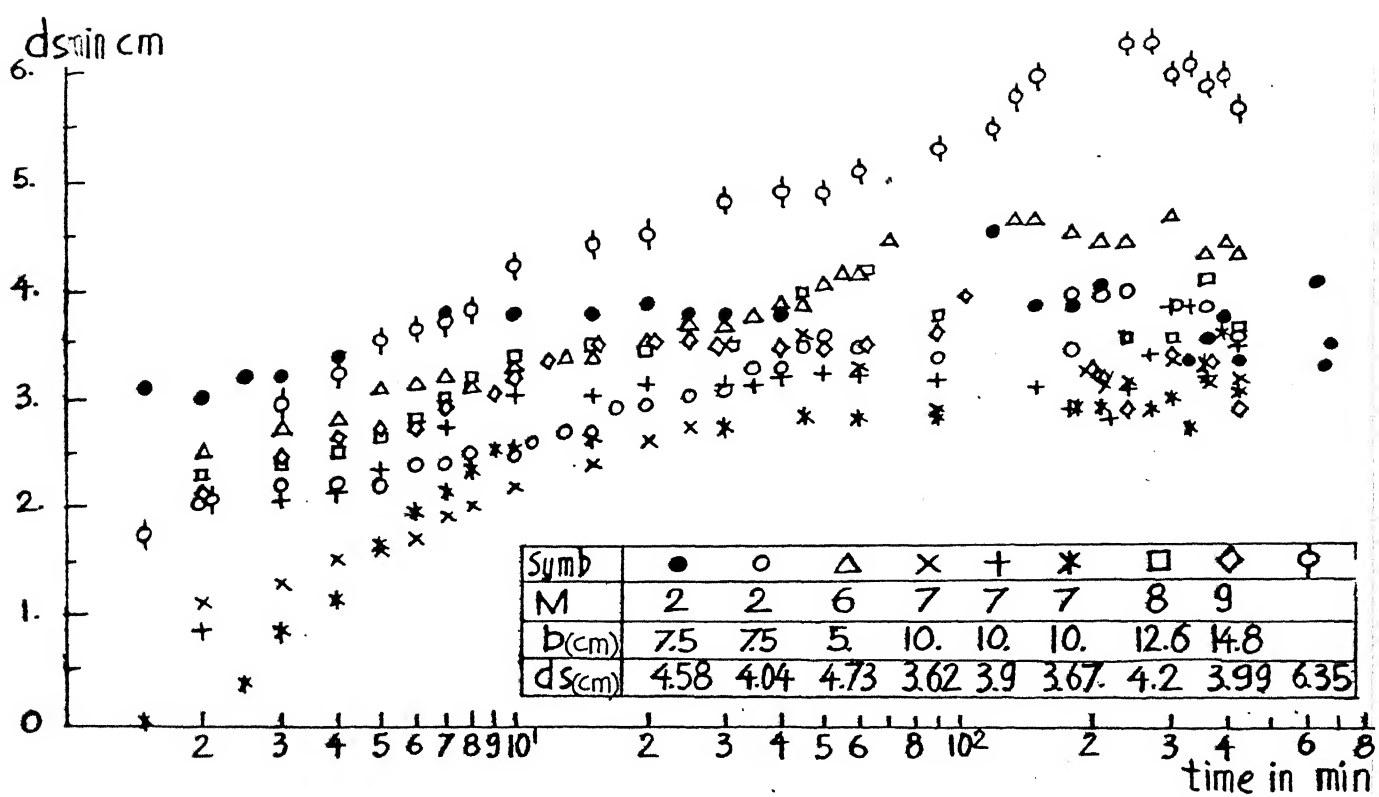


FIG. 3.3.2. VARIATION OF SCOUR VS TIME WHEN THE WIDTH OF DEVICE IS VARIED

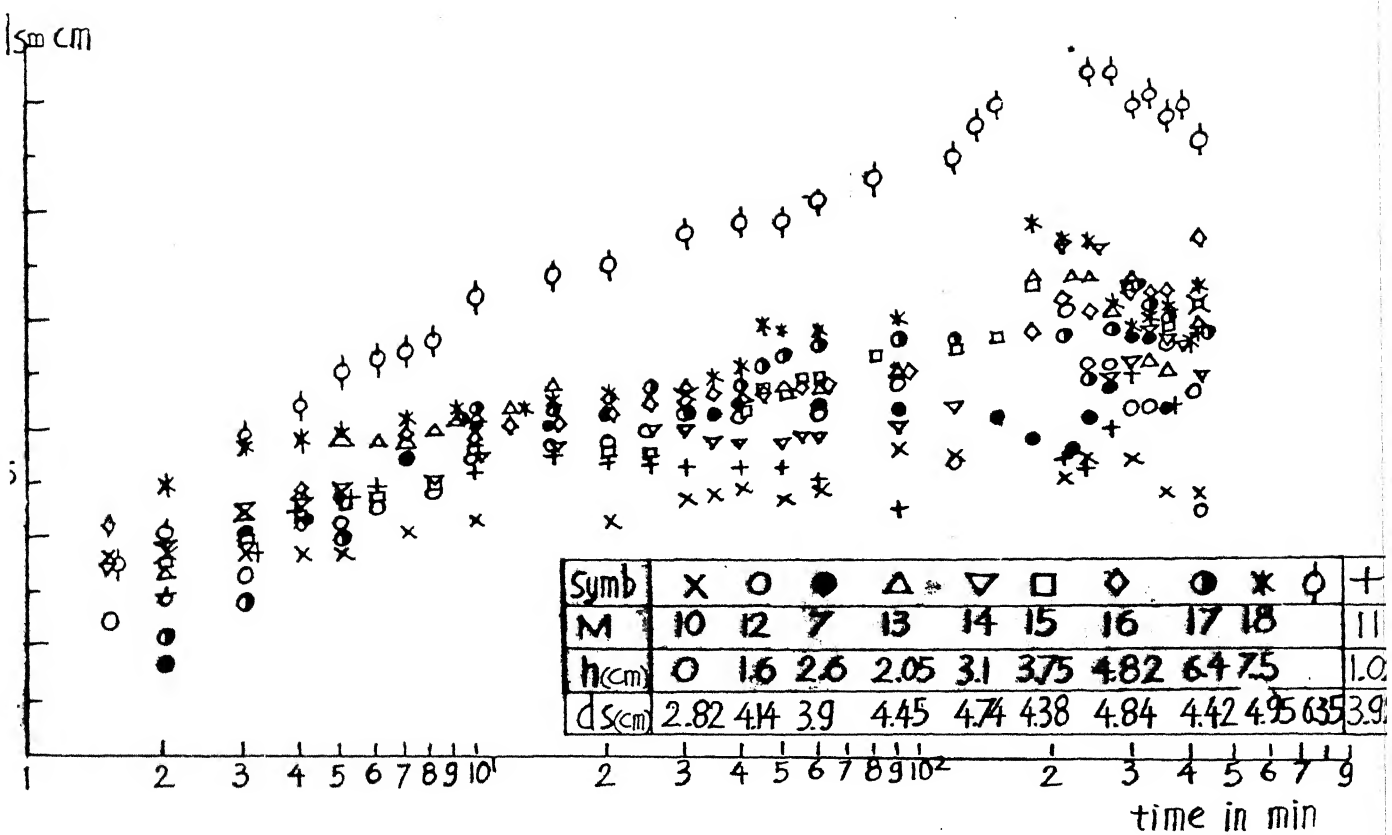


FIG.3.3.3.a VARIATION OF SCOUR VS TIME WHEN HEIGHT OF DEVICE IS VARIED

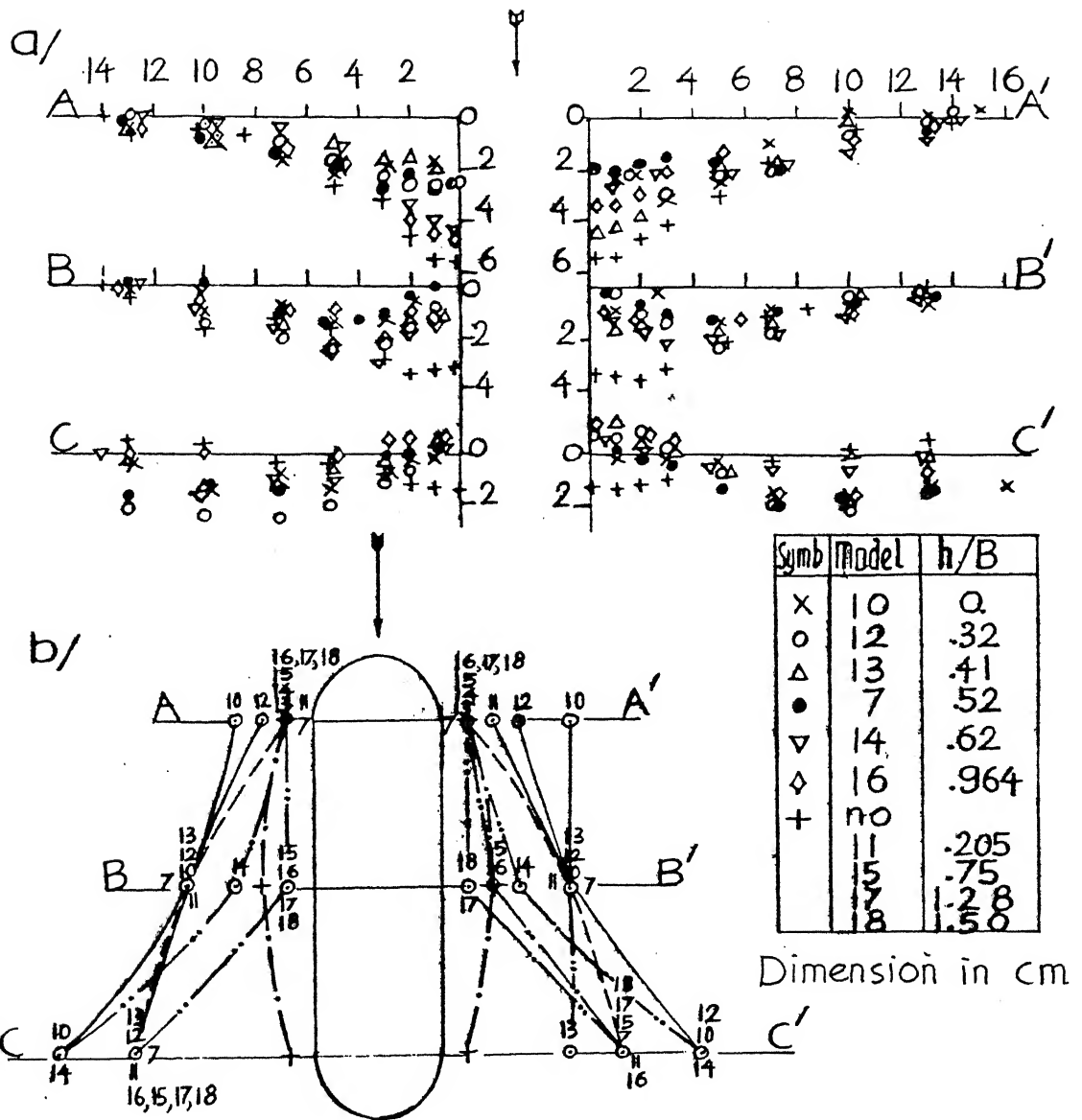


FIG.3.3.3 b. PROFILES OF SCOUR HOLE WHEN  
HEIGHT OF DEVICE VARIED AS RATIO  $h/B$   
c. LOCATION OF MAX. SCOUR DEPTH LINES  
WHEN RATIO  $h/B$  VARIED

scour depth as the model height reduced.

Some significant observations on influence of model height on maximum scour depth are:

- (a) Model  $M_{10}$  with its height equal to zero produces the highest reduction of maximum scour depth (as 63.8 percent). While maximum scour depth as function time goes lower compare to data of all model device tested.
- (b) The maximum local scour depth, and the location of scour depth lines in section BB' , CC' are affected by model device height significantly as can be observed in Figs. 3.3.3b,c . In section BB' that location is away from the pier surface about  $0.75B$  to  $1B$  but in CC' it is about  $1.5 B$  away. Reduction in scour depth is also observed at section BB'. Near the pier surface scour depth is quite less compared to pier without device, but in CC' deposition near the pier surface is seen.
- (c) It seems that location of maximum scour depth line in section BB' is closer to pier surface when ratio  $h/B \geq 0.62$ . When ratio  $h/B$  increases from 0 to  $0.5 B$  and higher location of maximum scour depth line in section AA' is coming closer to pier surface as in the case of pier without device and stops there. However in cross-section CC' that location is far away from pier surface, a considerable distance of about  $1B$  to  $2B$ , but concentrates at a point  $1.4B$  away from the pier surface

with its maximum scour depth value similar to the case of pier without device. Influence of model height on the maximum scour depth along the pier in cross-section AA', BB' and CC' during the run and in equilibrium condition is illustrated in Figs. 3.3d and 3.3e respectively. It may be observed that the scour in cross-section CC' scatters. Visually it is observed that an action similar to vacuum cleaning process is taking in the section CC' during scouring process before equilibrium reaches. In some cases scour in cross-section CC' is higher than that in cross-section AA' and BB'. Model  $M_{18}$ , appears maximum scour not only in cross-section AA' but in section CC' as well. Scour depth value in section AA', BB' and CC' are higher compared to all other models. Model  $M_7$ , leaving  $M_{10}$  seems to give better reduction of scour depth in all sections during the run. In equilibrium condition model  $M_7$  appears better than all other models. This effect is seen in the variation of  $b/B$  also near  $b/B = 2$ .

- (d) The probable enveloping curves for the data are drawn in Fig. 3.3c. This enveloping curve appears to consist of two segments. The first curve segment associates with the model height ratio  $h/B$  from zero to 0.4 and second part from ratio 0.6 to 1.5. In the second segment, when  $h/B > 0.6$ ,  $d_{sm}/d_{smo} = 0.76$  remained constant, is indicating the ineffectiveness of height-variation on

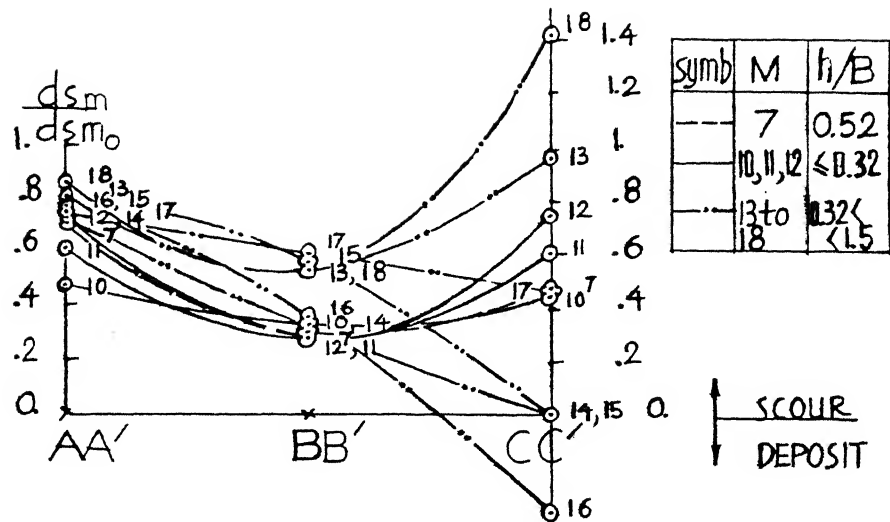


FIG. 3.3.d. RATIO  $\frac{d_{sm}}{d_{sm0}}$  DURING TEST TIME IN SECTION AA', BB', CC'

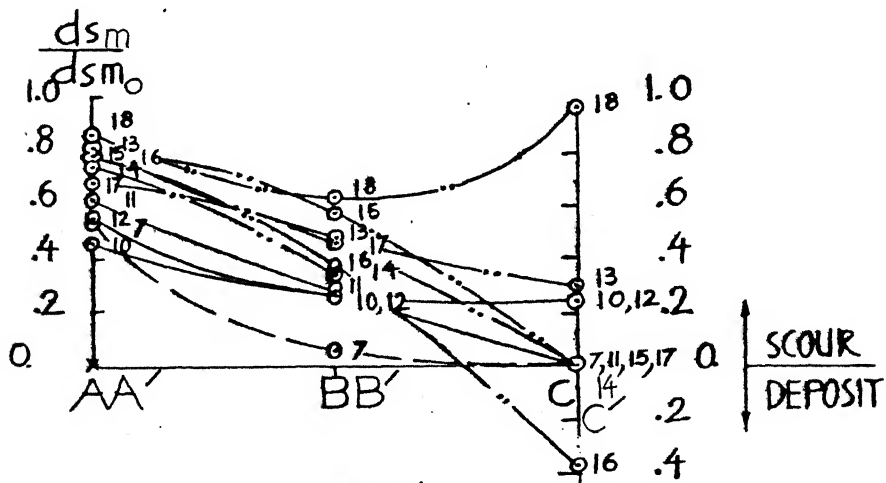


FIG. 3.3.e. RATIO  $\frac{d_{sm}}{d_{sm0}}$  IN EQUILIBRIUM IN SECTION AA', BB', CC'

scour reduction.

When model height equal to zero reduction is in a range of 55.6 percent to 63.8 percent. Reduction is about 38.6 percent to 43 percent at model height ratio  $h/B = 0.5$ .

Some statements of parameteric study of passive device effect can be made as follows:

- (a) Reduction of maximum scour depth fluctuates in a range 22 percent ( $M_{18}$ ) to 43 percent ( $M_7$ ) for model height larger than zero.
- (b) Profiles of scour hole appear better in a hydraulic sense, illustrated by reduction of maximum scour depth, location of maximum scour depth line diverged far from the pier surface in section (BB') and the appearance of deposition in section (CC') and behind the model pier in section (LL').
- (c) Model  $M_7$  seems to give better reduction of maximum scour depth when model height is larger than zero. It may be selected as protection passive device for comparison with previous protection works and for further study.
- (d) When model height equal zero it may considered as a part of collar used for protection of pier against scour. Under tests flow condition model  $M_{10}$  with its height equal to zero gives maximum reduction of maximum scour depth in a range 55.6 percent to 63.8 percent compared to model pier alone (without device).

- (e) This better hydraulic performance of model  $M_{10}$  and  $M_7$  enables us to couple flat plate and passive device as a combined device that will be tested.

It can be stated that, except for model height equal to zero, the horseshoe vortex formation at the pier junction with 'mobile bed' is deflected and modified to form counter-rotating vortex on either side of the pier from the vertex of the passive device. As an explanation to this effect, the schematic line diagram of the vortex with and without passive device are shown in Fig. 3.9.1, and Fig. 3.9.2 and Fig. 3.2.3. They appear as two streamwise streaks to wrap around the leading edge of the passive device and become stronger as they move beneath the wing or either side of the vertical spiral rib and push sediment towards the pier. Also along all other verticals within the fluid affected by passive device, there would be a vertical pressure gradient. These pressure gradients give rise to vertical secondary flows. On the upstream side along the edges of delta-wing these secondary flows are downward at least within the layers of fluid affected by model device height. This leads to an increase of the fluid velocity of counter rotating vortex in the vicinity of device junctioned with pier. Thus, sediment is no longer far away from the pier but is pushed towards the pier. However the residual original horseshoe vortex also exists beneath the passive device near the leading nose of the model pier but its strength is reduced considerably. That is why scour exists

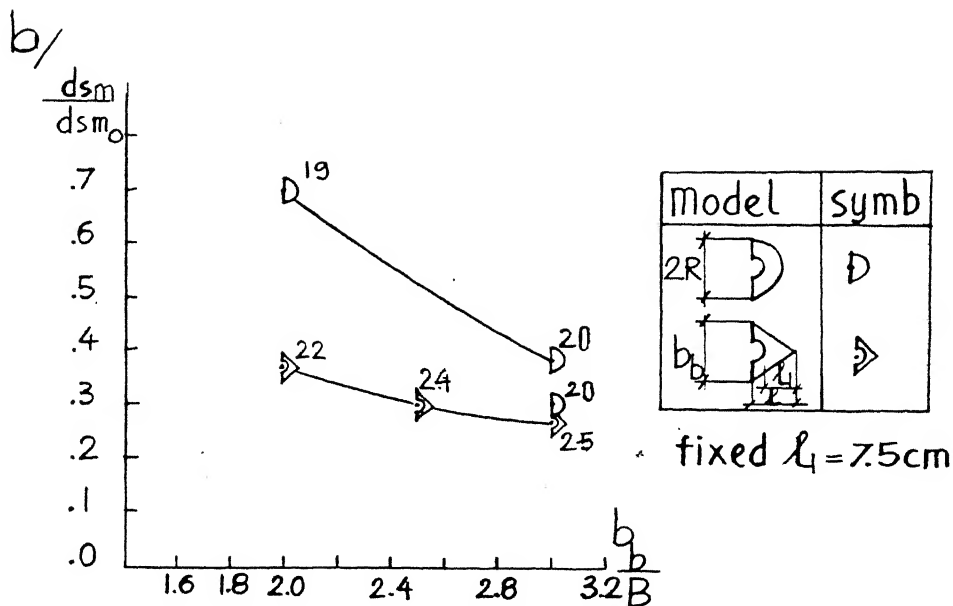
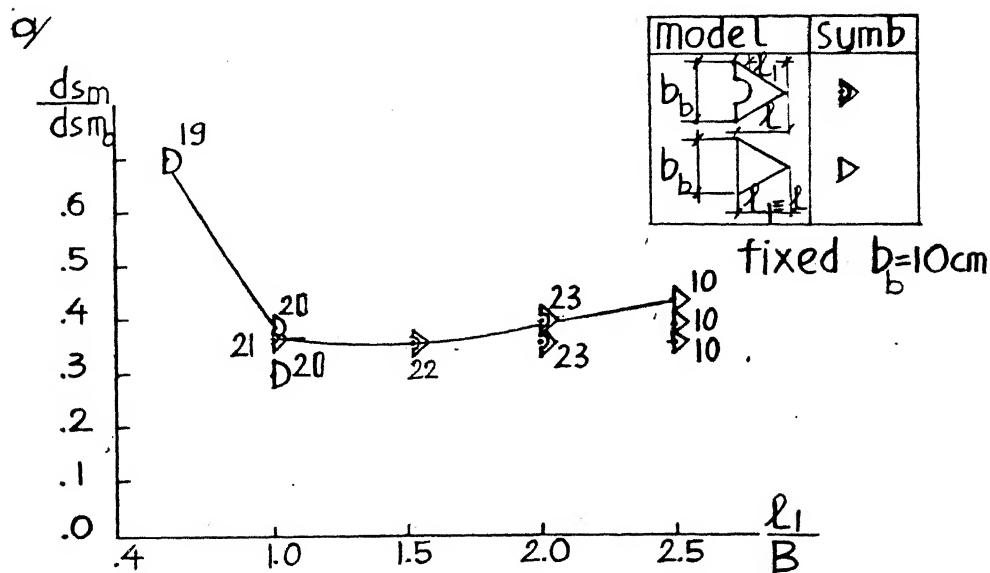
beneath the passive device. The reduction of maximum scour depth is not only due to weakening of the original horseshoe vortex but strengthening of the counter-rotating vortex as well.

Scour first occurs at the leading nose about  $\pm 45^\circ$  to  $\pm 75^\circ$  on both sides of the pier, then reaches to the spinal rib of the passive device along the centre-line of the pier. After some time scour extends to the vertex of passive device. The scour depth at this location more or less depends on the passive device length, but is always less than that at the pier nose. Scour at the pier nose deepens as the scour hole widens on both sides of the pier and along the spinal rib under passive device, until ripple or a dune reaches the pier.

Furthermore, due to the arresting of scour development at the pier nose the strengthened counter-rotating vortices dig scour holes on both sides of the downstream half of the pier and slightly far from it about pier width. These scour holes are large in plan and low in depth, and they move down stream diagonally towards the rear of the pier.

### 3.4 Flat Plate

To study the influence of shape and dimension of flat plate on maximum scour depth, three types of flat plate (see Fig. 3.4) were tested. The flat plate was situated at undisturbed bed level, symmetrically fixed to the leading nose

FIG.34. RATIO  $ds/dsm$  VS  $b/B$  FOR FLAT PLATEFIG.34.a RATIO  $ds/dsm$  VS  $l_1/B$  FOR FLAT PLATE

of the model pier along its centre-line.

- (a) Semicircular plate with inner diameter  $B$  enveloping the leading nose of the pier.
- (b) Triangular plate touching leading nose of the pier.
- (c) Triangular plate with a semicircular cutout having radius equal to half pier width,  $B/2$ , for enveloping the leading nose of the pier.

The experimental results given in Table 3.5a,b are plotted in Figs. 3.4a,b. Lengths  $l$  and  $l_1$  are defined for the plate as shown in the index of Fig. 3.4a and b. The effect of variation of  $l_1/B$  on the scour reduction ratio  $d_{sm}/d_{smo}$  is shown in the Fig. 3.4a. In all the triangular plates used, the width of the plate is fixed as  $b_p/B = 2.0$ . From Fig. 3.4a the maximum value of  $d_{sm}/d_{smo}$  occurs for model  $M_{19}$ . All other model the scour depth more or less remains same. However, the minimum value occurs at  $l_1/B = 1.5$ . Fig. 3.4a clearly indicates the invariant effect of  $l_1/B$  on the ratio  $d_{sm}/d_{smo}$ . For the study on width variation  $l_1/B = 1.5$  or  $l/b = 2.0$  is chosen. As can be seen in Fig. 3.4b, the effect of increase in width of the plate, type (a) has a greater influence in the reduction of scour depth. Type (c) plate is more effective than type (a) at  $b_p/B = 2$  and further increase of  $b_p/B$  ratio causes minimal further reduction in  $d_{sm}/d_{smo}$  in which  $b_p$  is defined as the width of flat plate. The effective width ratio will be  $b_p/B = 3$  as seen in Fig. 3.4b.

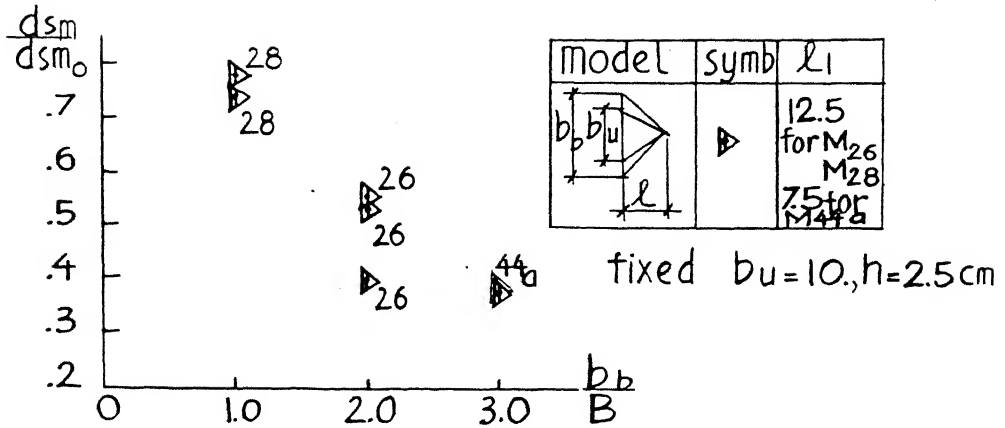
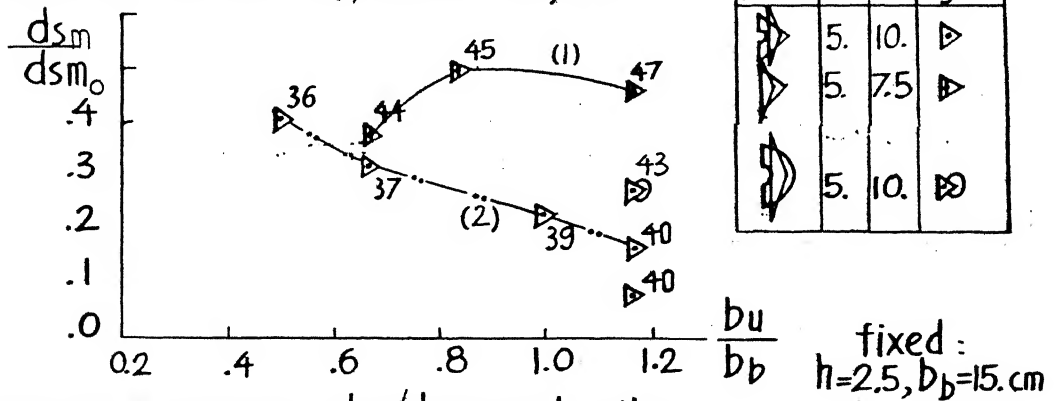
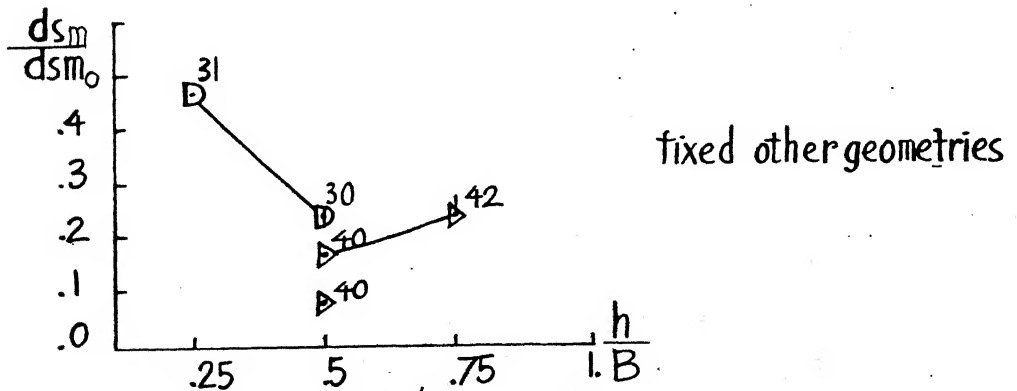
At  $b_p/B = 2$ , the size of the vortex may be more than the plate size, hence it results in more scour. As the plate width increases, the vortex is contained on the plate itself. This may results in less scour as observed in Fig. 3.4b. Plate type(c) appear to perform better than type(a). Hence this is used for further investigation.

When flat plate is fixed to the leading nose of the pier with its width and length large enough to control horse-shoe vortex<sup>not</sup> to penetrate into mobile bed or weaken its capacity of digging mobile bed, scour depth occurred at the leading part on both side of the pier and under the plate is quite less but higher in either rear, even at the back nose of the pier. This phenomenon of scour around the pier has been recognized long time due to wake vortex acting as vacuum cleaner. In this case flat plate acts somewhat as rigid bed preventing downflow which could erode bed material. The scour first occurs in the corner formed between the leading nose of the pier and device on either side. After some time scour forms at the vertex of the triangular plate or at the edge of the semicircular plate along the centre-line of the pier, then this process continues to dig bed material to form scour hole beneath the plate. Depending upon shape, geometry of flat plate and extent of leading part of the pier enveloped by flat plate. The horizontal extent and depth of scour will be more or less (see Fig. 3.5e). In the case of flat plate it seems some layers of downflow go along the edge of triangular flat plate or along the edge of semicircular

flat plate upto location of the second half of the pier in downstream far away from pier surface about pier width to form vortex and scour hole. This scour hole runs towards the pier rear as it shifts downstream. Under this flow condition better shape of flat plate is triangular with its width equal to  $3B$  and its length along the flow direction equal to or larger than  $15B$  because model  $M_{25}$  enveloped leading part of the pier having its width equal to  $3B$  and its length equal to  $1.5 B$  gives maximum scour depth reduction upto 73.23 percent compared to pier alone.

### 3.5 Combination of Delta-Wing-Like Passive Device with Flat Plate

Passive device with dimensions  $b_u/B = 2$ ,  $h/B = 0.5$  and  $l/B = 1.5$  and  $2.5$  is attached with bottom triangular flat plate below the rib of the device. The flat plate edge is tangential to the front nose of the pier and on the same vertical plane of the upper plate edge. Models 26, 28, 44a for different  $b_b/B$  ratio were tested. The ratio of maximum relative scour depth is plotted against bottom width ratio  $b_b/B$  is shown in Fig. 3.5a. It may be observed that as  $b_b/B$  increase from 1 to 3, the relative scour depths  $d_{sm}/d_{smo}$  reduces from 0.78 to 0.4. For each model experiments are conducted twice at more so that mean value of the relative scour may be used. It is logical to think that as the width of bottom plate increases, the possibility of containing the vortex developed beneath the passive device in front nose of pier increases. This leads to reduction in relative scour

FIG.3.5.a. RATIO  $d_{sm}/d_{sm_0}$  VS  $b_b/B$ FIG.3.5.b. RATIO  $d_{sm}/d_{sm_0}$  VS  $b_u/b_b$ FIG.3.5.c. RATIO  $d_{sm}/d_{sm_0}$  VS  $h/B$

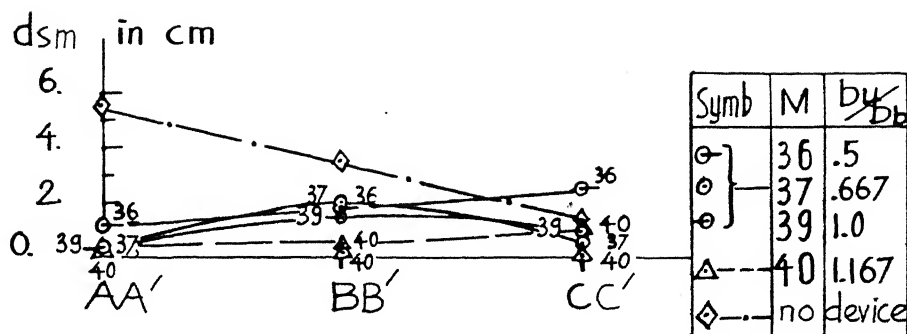


FIG.3.5.d. . VARIATION OF SCOUR ALONG THE PIER FITTED WITH COMBINED DEVICE

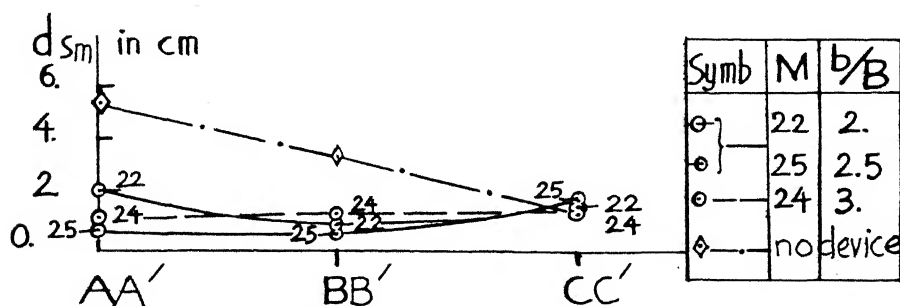


FIG. 3.5.e . VARIATION OF SCOUR DEPTH ALONG THE PIER FITTED WITH TRIANGULAR FLAT PLATE

depth. Experimental results show effective hydraulic reason for model 44a as reduction of maximum scour depth about 62 percent. So that model 44a with  $b_b/B = 3$  and  $l_1 b/B = 1.5$  is chosen for next study.

The second phase of experiments on the combination of passive device with flat plate is aimed to study the variation in width of the passive device (upper plate width) with respect to constant flat plate width  $b_b/B = 3$  and  $l_1 b/B = 1.5$  or  $l_b/B = 2$ . The dimensions of passive device fixed as  $h/B = 0.5$ ,  $l_u/B = 1$  and passive device width varied is  $b_u/b_b = 0.5$  to  $1.166$  or  $b_u/B = 1.5$  to  $3.5$ . This phase consists of two case. In the first case bottom plate is fixed tangential to the front nose of the pier. The model No. 44, 45, 47 made with  $b_u/b_b = 0.666$  to  $1.166$  or  $b_u/B = 2$  to  $3.5$  for this case. The relative scour depth  $d_{sm}/d_{smo}$  is plotted against  $b_u/b_b$  in Fig. 3.5b. It is observed that increase in  $b_u/b_b$  results in increase of  $d_{sm}/d_{smo}$  (see curve No. 1 in Fig. 3.5b).

In the next case the triangular bottom plate with inner diameter  $B$  is cut and fixed to front nose of the pier. The model No. 36, 37, 39 and 40 with  $b_u/b_b$  varied  $0.5$  to  $1.166$  or  $b_u/B$  varied  $1.5$  to  $3.5$  were tested. The plot of  $d_{sm}/d_{smo}$  with  $b_u/b_b$  shown in Fig. 3.5b as curve (2) represents their results. It may be observed that the relative scour depth  $d_{sm}/d_{smo}$  reduces considerably with increase in  $b_u/b_b$  ratio.

The reason for this conflicting trend in the two case may be as follows. On the front face of pier, below near the passive device horseshoe vortex of certain reduced strength will be developed. This horseshoe vortex is not controlled by the bottom plate when it is intangential to the front nose of the pier. In the second case, this horseshoe vortex is fully contained on the bottom plate and it is channelized along the pier surface downstream. Thus the scour due to the horseshoe vortex much reduced in the second combination of plate and passive device.

In the third phase all the other dimensions are fixed and only height is varied. The dimensions fixed are  $b_u/B=3.5$ ,  $h/B = 0.5$ ,  $l_u/B = 1$ ,  $b_b/B = 3$ ,  $l_b/B = 2$  and only model height varied 0.5 to 0.75B for triangular combined device as model No. 40, 42. For case of model No. 30,31 bottom plate with inner diameter B is semicircular having it diameter equal to 3B fixed. Dimensions of upper plate fixed are  $b_u/B = 3$ ,  $l_1/B = 1$  only model height varied 0.25 B to 0.5B. The resulting maximum scour depth in relation to  $d_{smo}$  of model No. 30,31, 40, 42 is plotted against  $h/B$  in Fig.3.5c. It is observed that  $h/B = 0.5$  gives the reduced value of  $d_{sm}/d_{smo}$  and for either increase or decrease in  $h/B$   $d_{sm}/d_{smo}$  increases.

Another model denoted as model No. 43 having the same upper plate dimension and its height as model No. 40 but bottom plate is elliptic shape with minor axis equal to

3B and major axis equal to 4B in the flow direction. This bottom plate is cut with a semicircular hole of diameter B and fixed to front nose of the pier. This model as shown in Fig. 3.5b in the second phase gives  $d_{sm}/d_{smo}$  ratio higher than that of model No. 40. From Figs. 3.5a, b and c one can say that model No. 40 give highest reduction of scour depth about 83.7 percent to 92.1 percent. This model will be used for further study.

Figures 3.5d and 3.5e show the magnitude of  $d_{sm}$  at lateral locations AA', BB', CC' respectively for combined device and for triangular plate. The magnitude of maximum scour depths at AA', BB', CC' for pier without device is also incorporated for comparison. It is observed that in both case the magnitude of scour by model No. 40 give the minimum possible scour depth.

### 3.6 Cooperative Tests

Several types of local scour protection work are in vogue since a long time. In this investigation four such types have been studied under the selected flow condition. The experimental results are recorded in Table 3.7, and relevant parameters are plotted in Figs. 3.6a and 3.6b for comparison with the delta-wing-like device.

Type 1 caisson with vertical lip was studied. The vertical lip effect on local scour depth is not clear under this flow condition because time for scour reaching collar

Symb	type of protection	dsm (cm)
○	collar $\equiv$ bed level	0
⊕	collar under bed level $B/2$	2.5
+	collar over bed level $B/2$	4.3
◇	caisson under bed level $B/2$	2.7
□	caisson with v. lip under b. level $B/2$	2.9
△	c. with v. lip unde b. level $B$	5.2
▽	piles having diameter $= B/5$	4.98
⊖	riprap mat	0

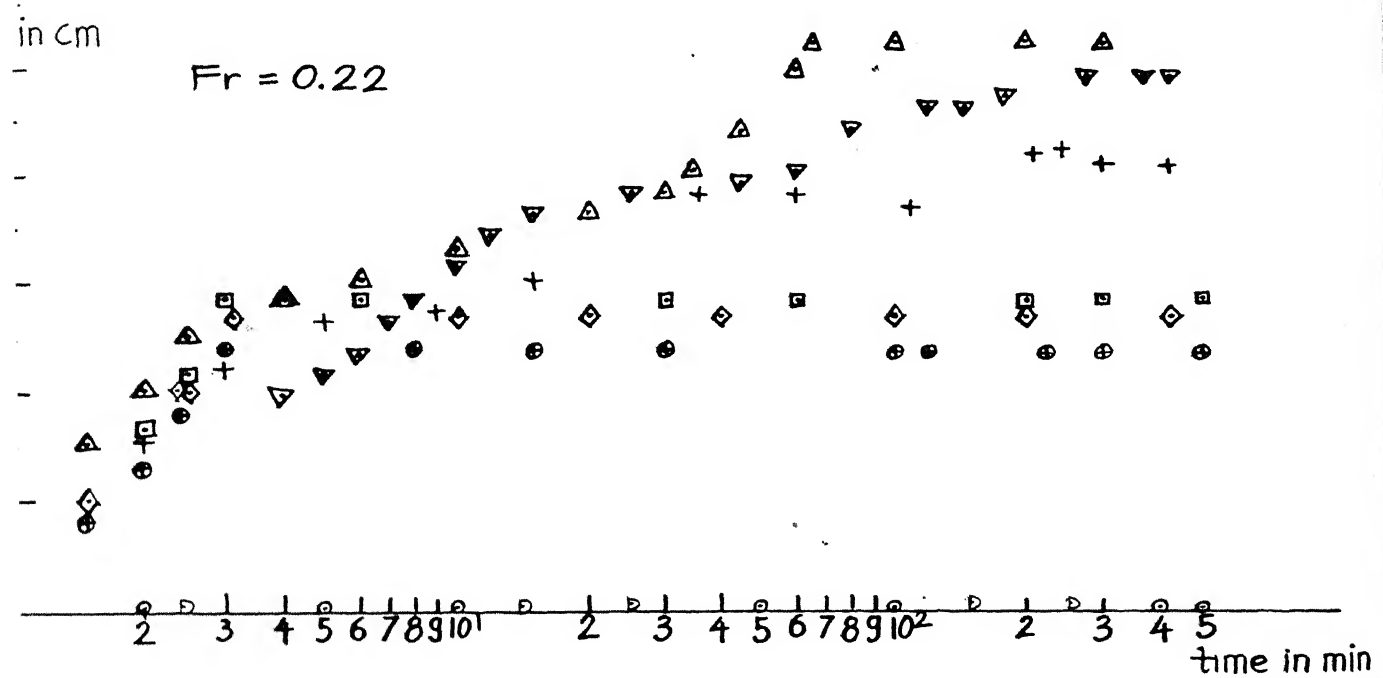


FIG. 3.6. a. VARIATION OF SCOUR VS TIME WHEN PILES, COLLAR, CAISSON AND RIPRAP MAT USED AS PROTECTION DEVICE

surface when collar, caisson without vertical lip and with vertical lip placed below bed level  $B/2$  is the same. Scour steps on the surface of caisson because that surface is practically rigid at bridge site.

Type 2 axial circular collar width different positions on the pier was tested as shown in Table 3.7 and plotted in Fig. 3.6. It is evident that the circular collar placed on the sand bed level prevented scour completely under this flow condition. When it is inserted a depth  $B/2$  below flat bed level the scour stopped on its surface after three minutes, when fixed distance  $B/2$  over bed level it gives maximum scour depth of 4.29 cm, that is a reduction of 32.44 percent. For the latter case local scour occurs as if no collar existed and the confinement of horseshoe vortex and of secondary flow is less effective compared to the case of collar placed on bed level. This shows the extreme importance of the vertical position of the collar.

Type 3: 'Riprap mat' with diameter of boulders about 1.2 cm to 1.45 cm was placed around pier with its thickness equal to three times its diameter. No scour occurs for this test. This diameter of boulders is selected following formular of Isbash (1935).

Type 4- Smallpiles. Experiment with five small piles of diameter equal to 1 cm ( $= B/5$ ) ahead of main model pier as indicated in Table 3.7 was conducted. The maximum scour

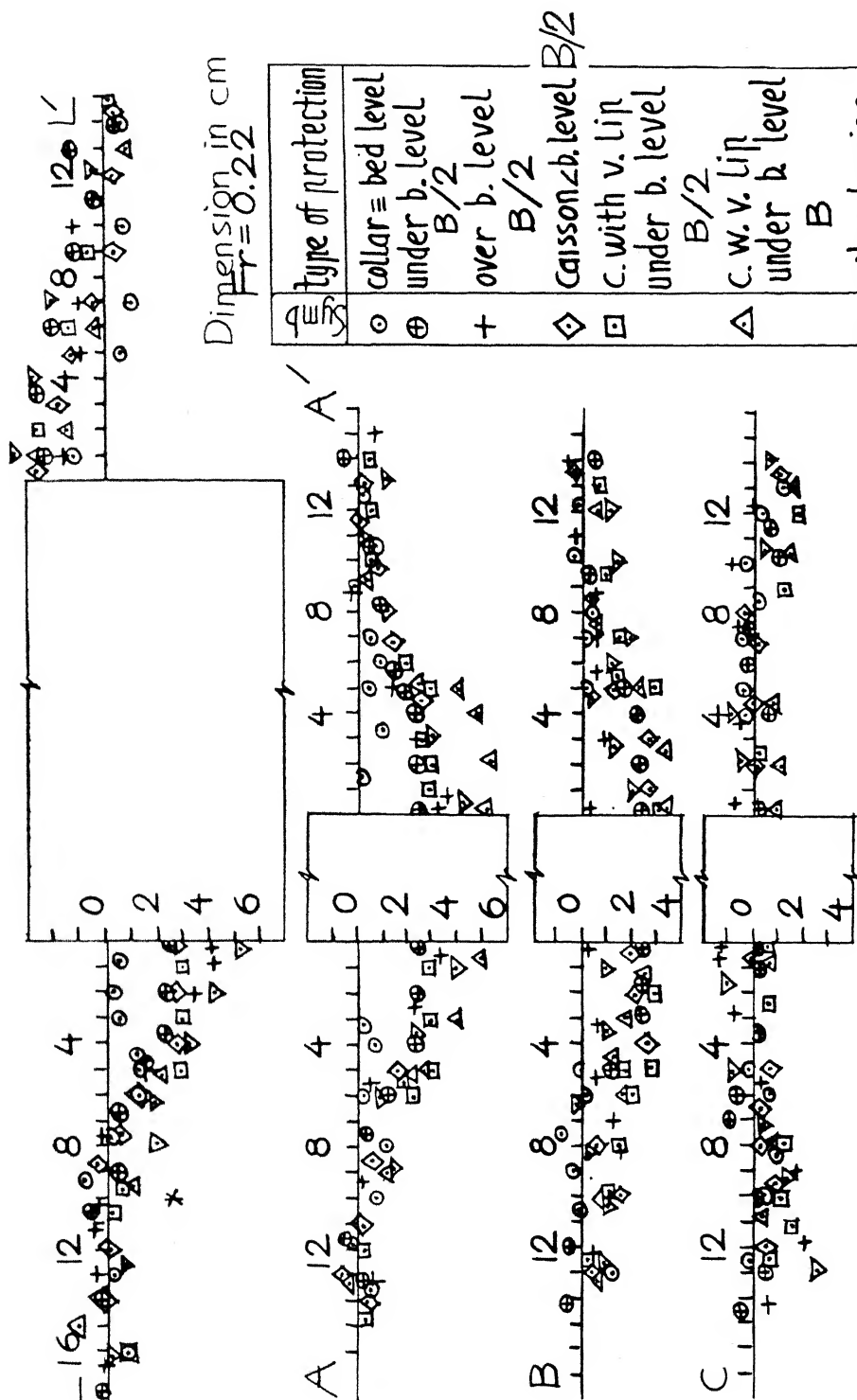


FIG.3.6.b. PROFILES OF SCOUR HOLE WHEN PILES, SCOLLAR, CAISSON AND RIPRAP MAT USED AS PROTECTION DEVICE

depth at the leading nose of the main model pier was found to be 4.98 cm and scour at each pile from left to right was 2.83 cm, 3.03 cm, 2.58 cm, 2.78 cm and 2.48 cm respectively. Perhaps this test does not yield significant reduction in scour because the spacing and flow-alignment of piles are not perfect.

From the above results one can say that reduction of maximum scour depth is evident when some types of protection were inserted around the model pier. Axial collar with its width equal to the model pier width and 'riprap mat' with boulder diameter equal to 1.2 cm to 1.45 cm give no scour. The above data for tests with types 1 to 4 are a good reference for comparison with delta-wing-like passive device and its combination with flat plate in this investigation.

### 3.7 Combination of Passive Devices at Different Height of the Pier Under Different Flow Conditions

From curve no. 2 in Fig. 3.5b it is evident that model No. 40 (dimensions mentioned in section 3.4) gives remarkable reduction of scour depth in a range of 83.72 to 92.1 percent under steady flow condition with average Froude number  $F_r$  equal to 0.22. To know the effectiveness of this model in other flow condition, some tests have been subsequently conducted with device. Probably if the model no. 40 is placed below the bed level, nearest the lowest level of valley of the ripple, the scour may be prevented completely.

With this in view, a combination of model no. 40, with flat plate are tried as model 51 in the next phase of experiments. Model 51 consists of combines passive device fixed on the sand bed level, and a flat plate placed distance  $B/2$  under bed level. Other Model as model 52 formed by two combined passive device, one fixed on the flat sand bed level, and other fixed distance  $B/2$  under bed level respectively, (see Fig. 3.7d). These models gave reduction of maximum scour depth upto 62.9 percent under Froude  $F_r = 0.374$ .

From results of  $M_{40}$ ,  $M_{51}$ ,  $M_{52}$  some observation can be made. Figure 3.7a shows variation of scour depth as function of time when pier is fitted with model device  $M_{40}$  under flow condition  $F_r = 0.30$ . Fig. 3.7b illustrates profiles of local scour hole at section LL', AA', BB', CC' recorded at the end of steady run lasting 185 minutes and after water was drained overnight. Though the reduction of maximum scour depth is only 19.5 percent, however, there is greater reduction in scour depth along downstream half of the pier, high deposit of sand in the near wake region, and maximum scour depth line is diverted far away from pier surface in a range of  $1.5B$  to  $2B$  in that region. Performance model  $M_{40}$  at higher Froude numbers, with respect to scour reduction is very poor, particularly at nose of the pier. From Fig. 3.7a, scour depths increase gradually upto period of 75 minutes, increases rapidly with fluctuations after 75 minutes. It was observed that the incoming ripples height, i.e. the

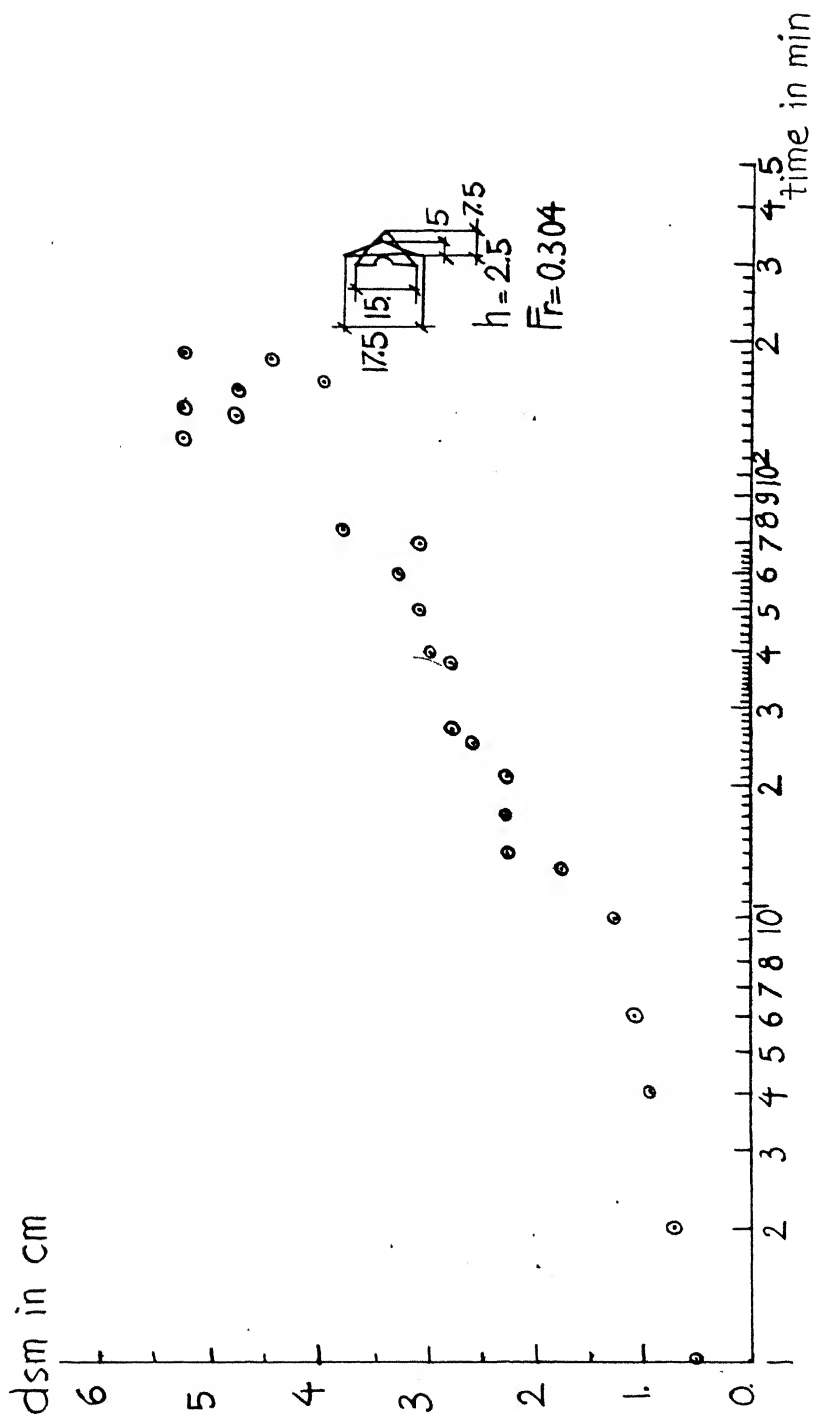


FIG.3.7. a. VARIATION OF SCOUR DEPTH VS TIME WHEN PIER FITTED WITH COMBINED DEVICE AND  $Fr = 0.304$

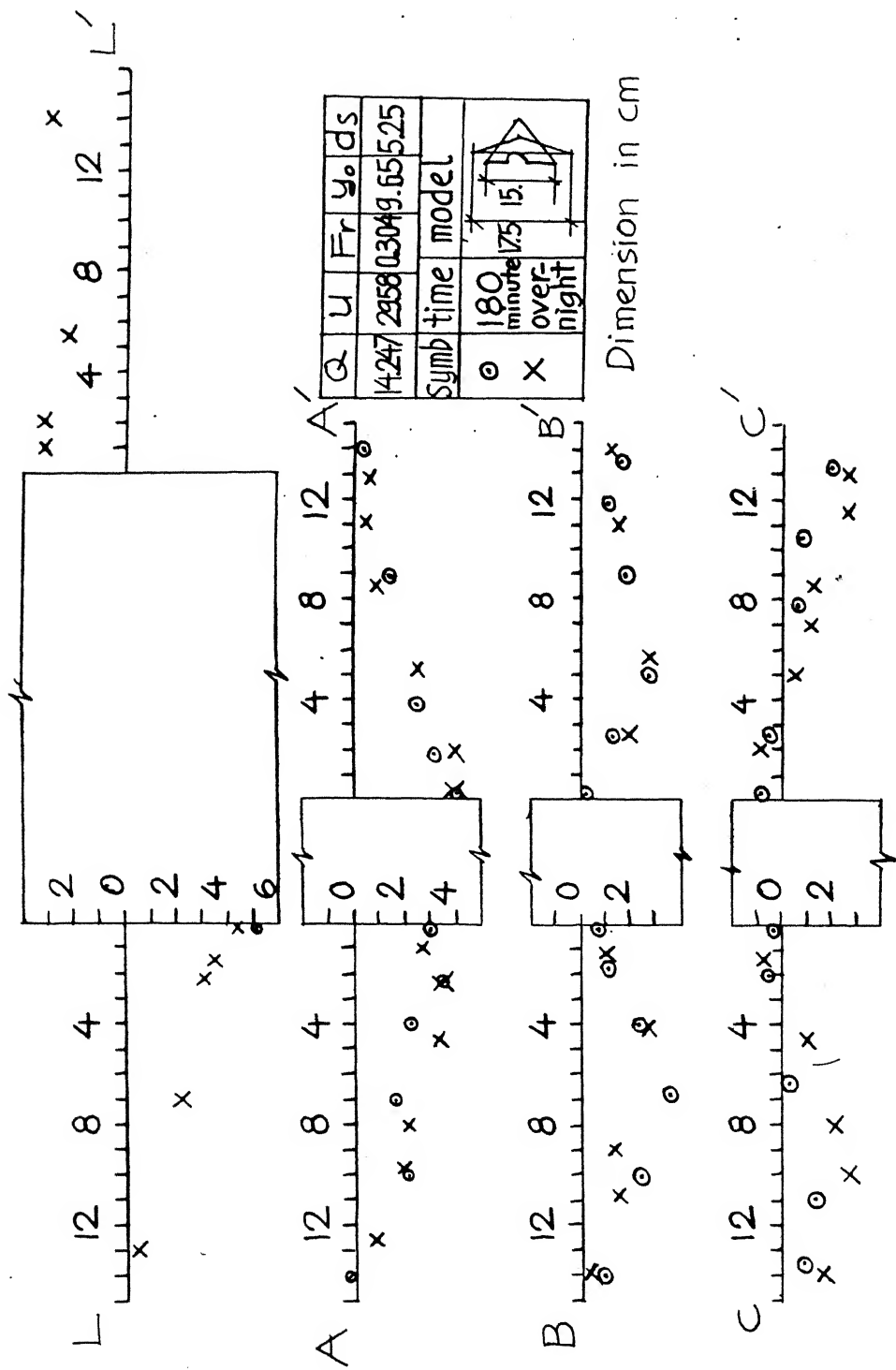


FIG.3.7 b. PROFILES OF SCOUR HOLE WHEN  
PIER FITTED WITH M40 AND  $Fr=0.304$

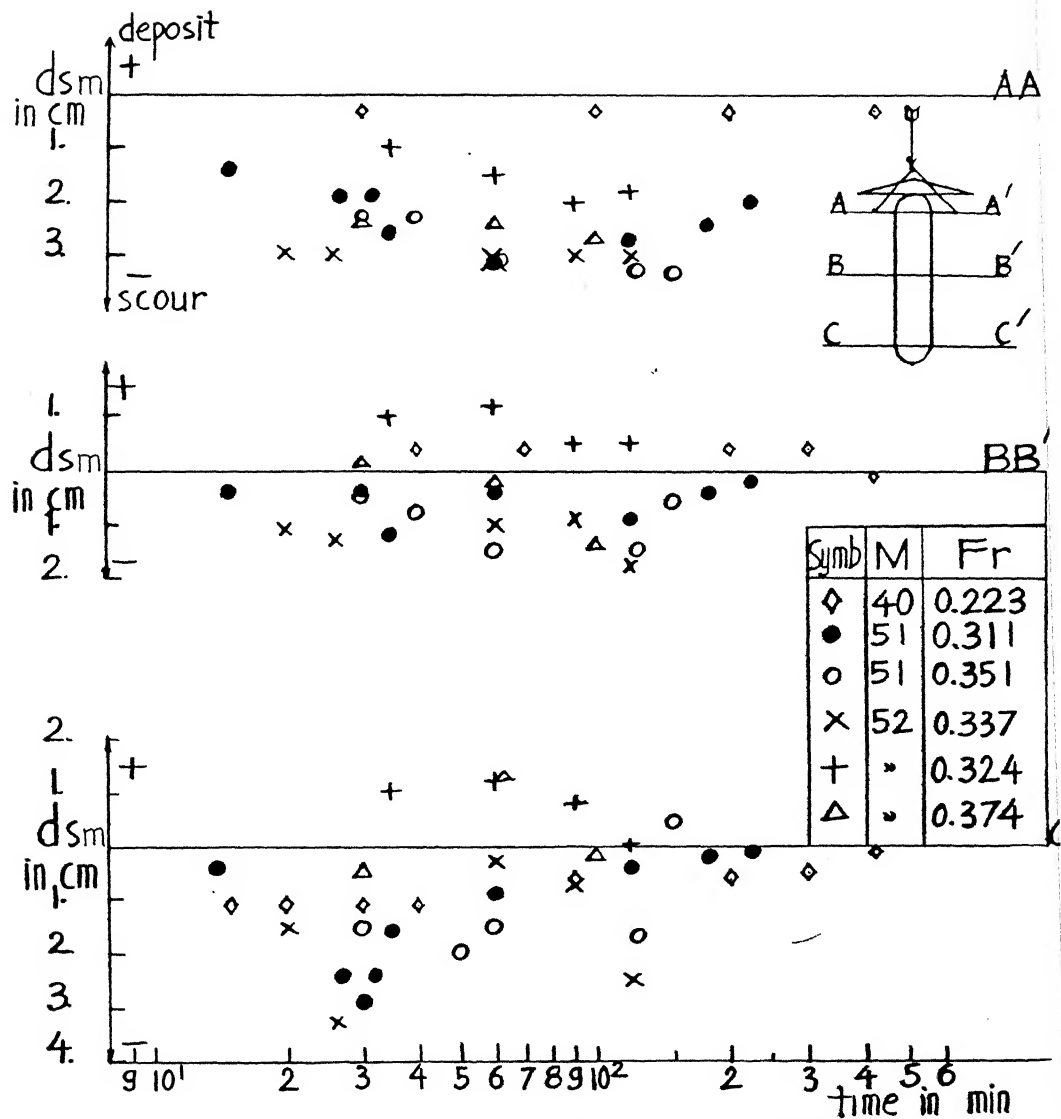


FIG. 3.7.c . VARIATION OF SCOUR VS TIME WITH DIFFERENT MODEL DEVICE UNDER DIFFERENT Fr

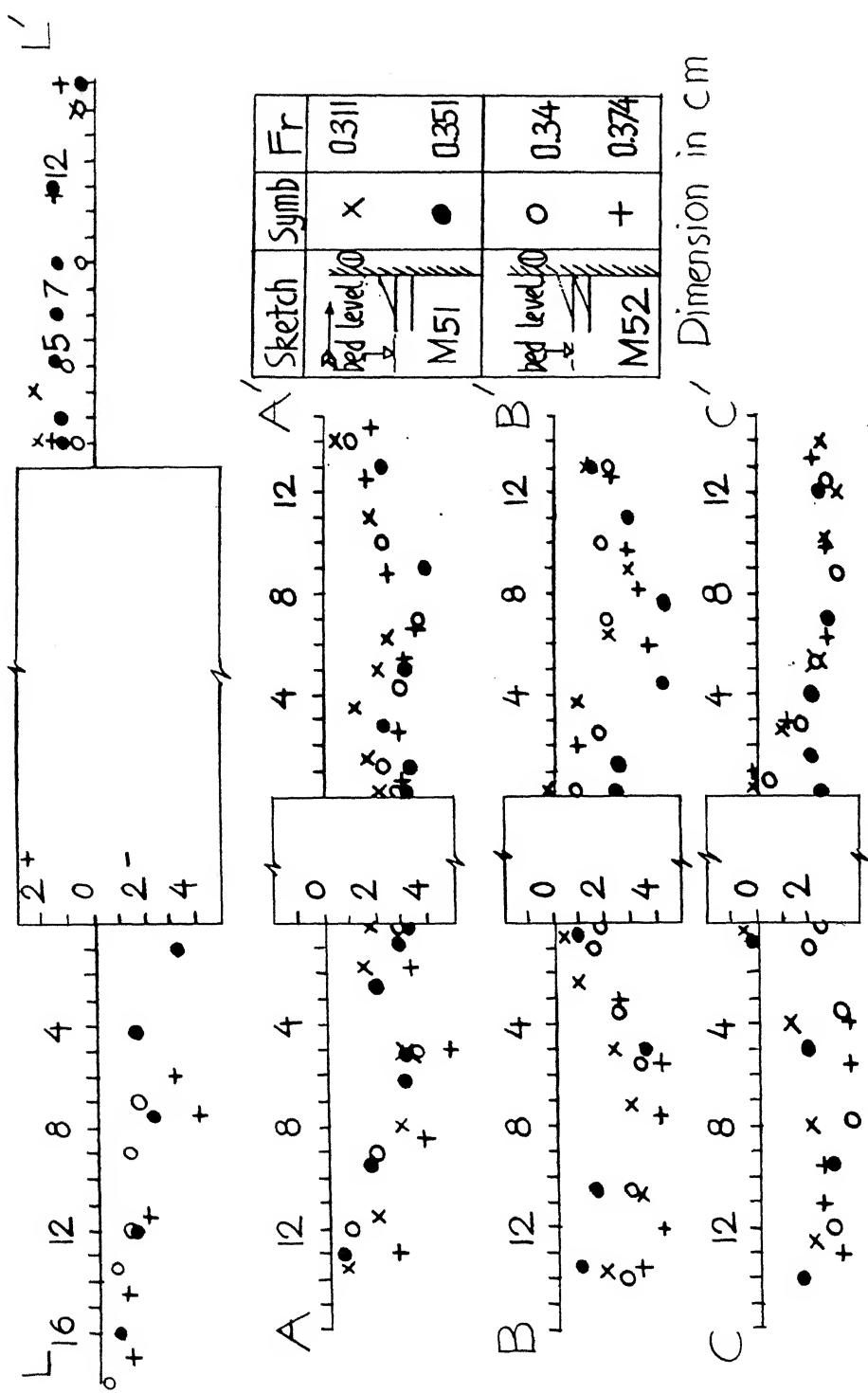


FIG. 3.7.d. PROFILES OF SCOUR HOLE WITH AND WITHOUT DIFFERENT MODEL DEVICE UNDER DIFFERENT Fr NUMBER

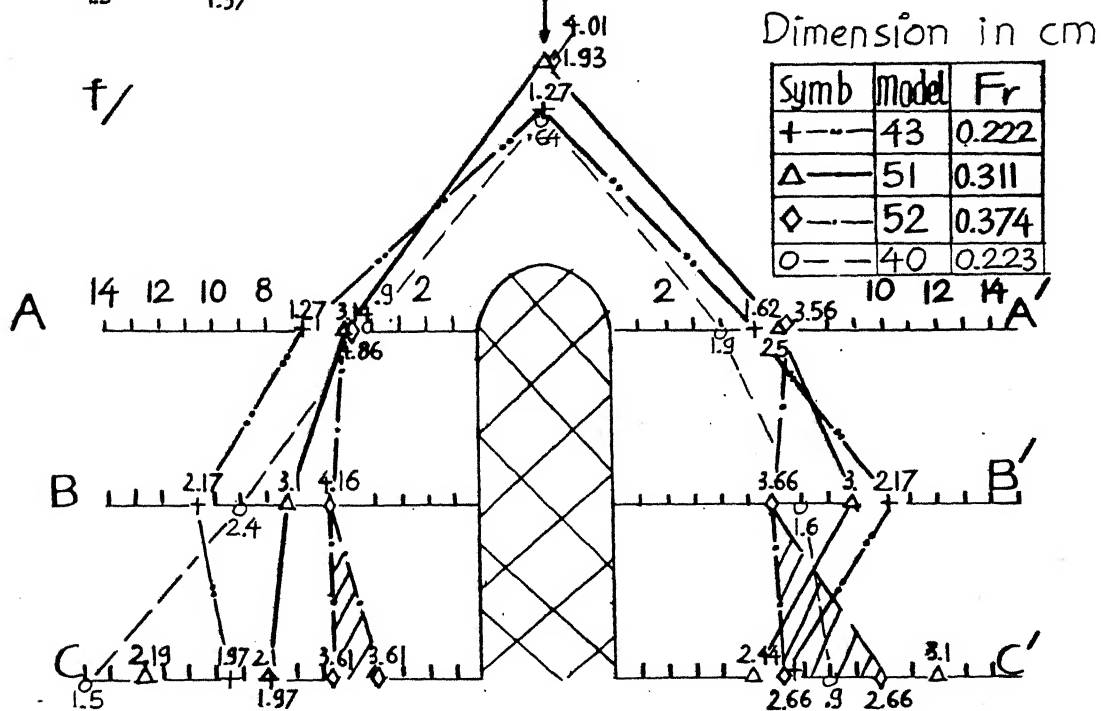
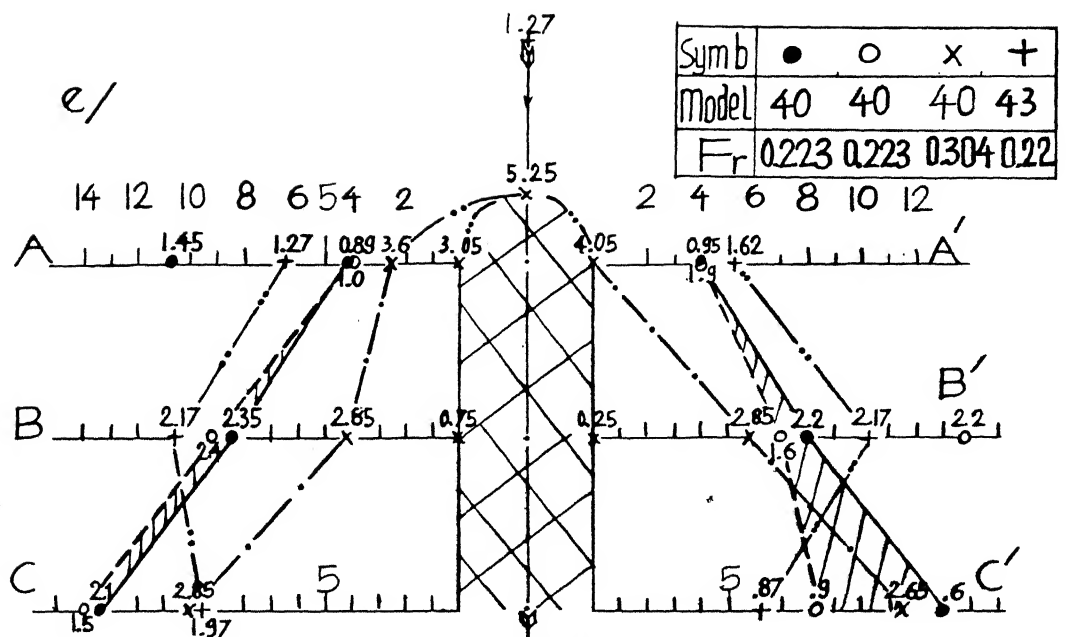


FIG. 37. MAX. SCOUR DEPTH LINES AROUND PIER WITH AND WITHOUT MODEL DEVICES UNDER DIFFERENT  $Fr$  No.

difference between crest to valley is of the order 3.3 cm . When the valley of the ripple reaches near the pier nose the flow may penetrate below the  $M_{40}$  device, leading a phenomena of scour.

Fig. 3.7 c shows the development of maximum scour depth with time for model No. 51 and 52. The scour profiles under equilibrium conditions for these model are shown in Fig. 3.7d. It may be observed that model combination No.52 gives much reduction in maximum scour depth, namely 2 cm for  $F_r = 0.32$  and 2.66 cm for  $F_r = 0.37$  occurring at cross-section AA'. It was observed that scour took place in the front nose of device. The maximum scour reduction for  $F_r = 0.37$  is 62.9 percent of the scour without any device. The maximum scour depth lines are away far from the pier surface at distance of B to 1.5B. The downstream section along L' have depositions of sediment. The position of maximum scour depth lines for models tests  $M_{40}$ ,  $M_{43}$ ,  $M_{51}$  and  $M_{52}$  are shown in Figs. 3.7e and 3.7f. It is observed that the maximum scour depths lines for  $M_{40}$  when  $F_r = 0.3$  as shown in Fig. 3.7e is near the pier nose at AA' and diverges from the pier surface at sections BB' and CC'. For combined model device  $M_{51}$  and  $M_{52}$  the maximum scour depth line is always atleast a distance 0.8 B (see symbol  $\diamond$  in section CC' in Fig. 3.7f) from pier surface. This happens even at a distance 1 B at section AA'. All the combined device results indicate passive device located at bed level and below at distance B/2 gives scour reduction over an order 60 percent.

### 3.8 Comparison with Standard Passive Device as Suggested by Gupta (1987).

A.K. Gupta (1987) suggested delta-wing-like passive device for scour reduction. This model is considered as standard. Standard configuration of passive device has the following geometry. If  $B$ , the width of the pier is taken as characteristic length, the dimensions of the passive device are as follows:

Width equals to  $1.5 B$

Length equals to  $2 B$

Height equal to  $0.5 B$

Under the first phase of test flow condition ( $F_r = 0.22$ ) this standard configuration gives maximum scour depth reduction at the leading nose of the pier in a range of 4.15 cm to 4.5 cm, the corresponding reduction is 29.3 percent to 34.6 percent.

From the present investigation the combined passive device has the following dimensions:

$$\begin{array}{lll} b_u/B = 3.5 & l_u/B = 1 & h/B = 0.5 \\ b_b/B = 3 & l_b/B = 2 & \end{array}$$

in which flat bottom plate envelops round leading nose of the pier. Passive device above dimensions one to be placed at bed level and an other at  $B/2$  below bed level. This combination for high Froude Number = 0.37 can reach maximum scour depth reduction over 60 percent.

### 3.9 Flow Visualization by Paint Impression

#### 1) General

This section deals with the analysis of results, such as flow visualization to obtain influence of the passive device width on modification of the horseshoe vortex formation at the leading nose of the model pier. The results of flow visualization study are described in which the efficiency of passive device width in modifying the horseshoe vortex flow structure around the model pier foot at junction with rigid bed illustrated. In all 21 tests, for model pier alone and model pier with model device, were conducted under three different flow conditions as Froude number equal to 0.22, 0.555 and 0.7. The water depth of 9.7 cm at the same location of pier situated in mobile bed was maintained for all 21 tests. The device with its width varied from  $1B$  to  $3.5 B$  for a height equal to  $B/2$  and its length along flow direction equal to  $1.0 B$  has been attached to the leading nose of the pier. Flat plate of dimension 60 cm long and 48 cm width, was used as flat bed at the test section. The pier with model was attached to the bed.

#### 2) Flow visualization

Flow patterns near the bed and pier by paint impression method are obtained. Firstly, steady flow for each flow condition as required is setup. Then model pier alone and model pier with model device painted is tested subsequently. Original flow pattern obtained by paint impression technique

$$y_0/B = 1.94, Fr = 0.226, Re_p = 12.792 \times 10^3$$

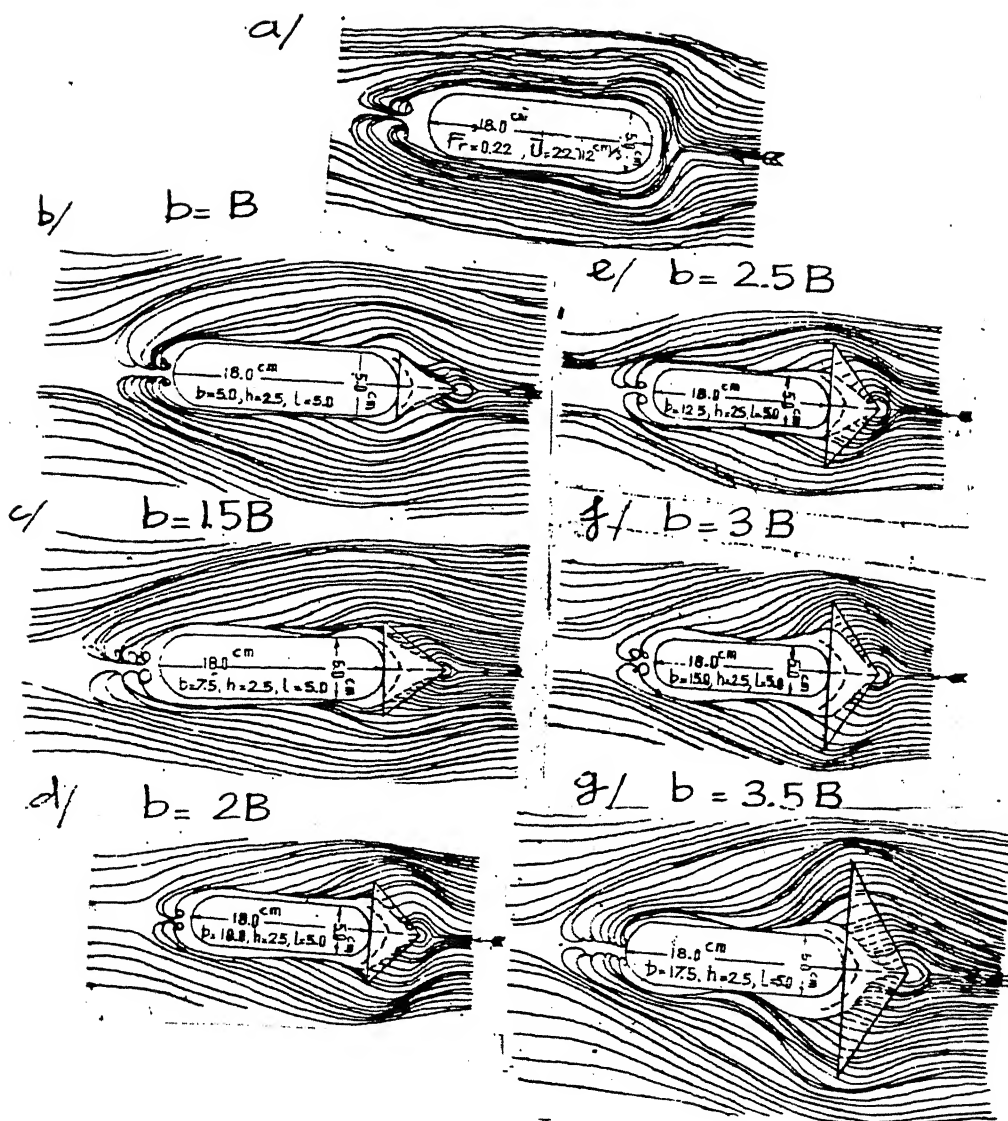
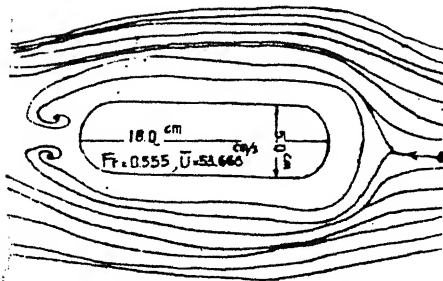


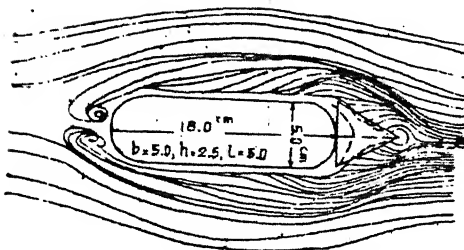
FIG. 3.9.1 PAINT IMPRESSIONS OF FLOW PATTERN ON THE PLATE FOR PIER ALONE AND FITTED WITH DEVICE

$$y_0/B = 1.94, \quad Fr = 0.555, \quad Re_p = 31.045 \times 10^3$$

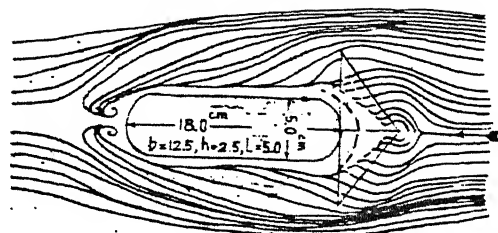
a/



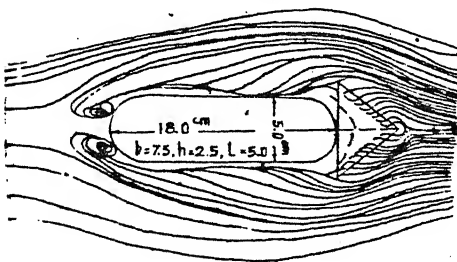
b/  $b = B$



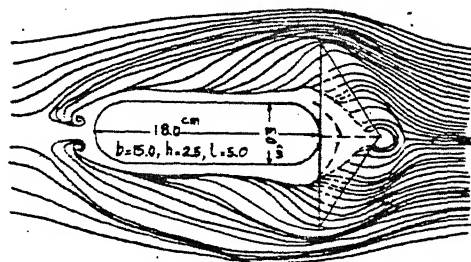
e/  $b = 2.5 B$



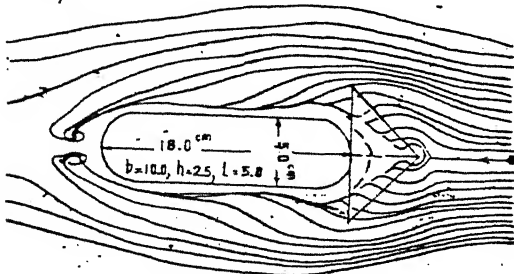
c/  $b = 1.5 B$



f/  $b = 3 B$



d/  $b = 2 B$



g/  $b = 3.5 B$

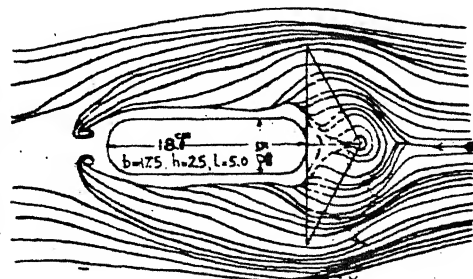


FIG. 3.9.2 PAINT IMPRESSIONS OF FLOW PATTERN ON THE PLATE FOR PIER ALONE AND FITTED WITH DEVICE

$$y_0/B = 1.94, Fr = 0.7, Re_p = 39.257 \times 10^3$$

a/

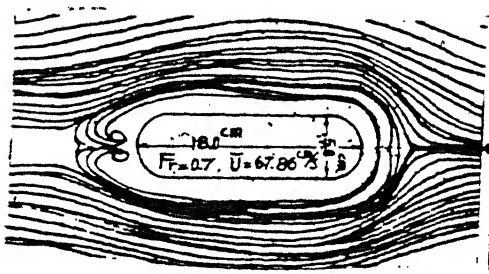
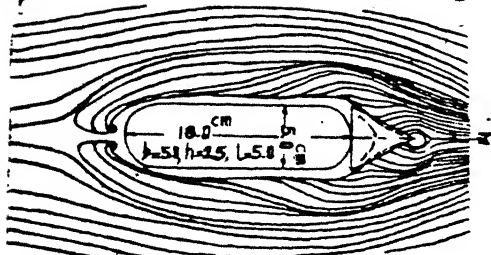
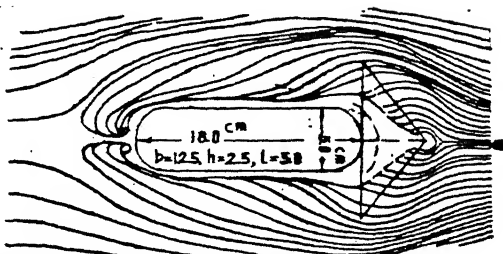
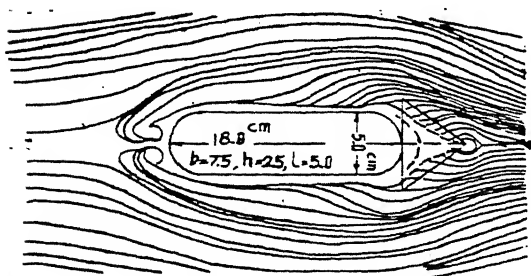
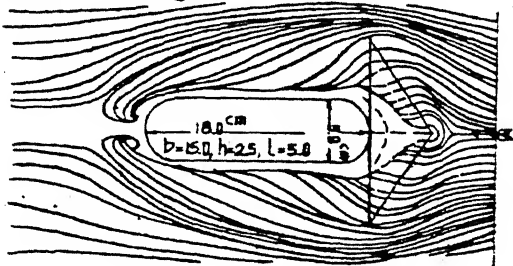
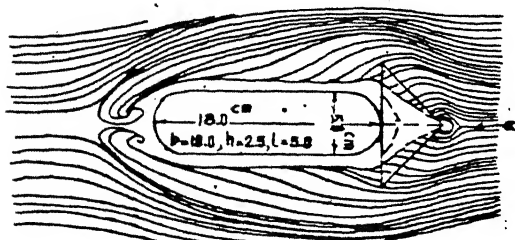
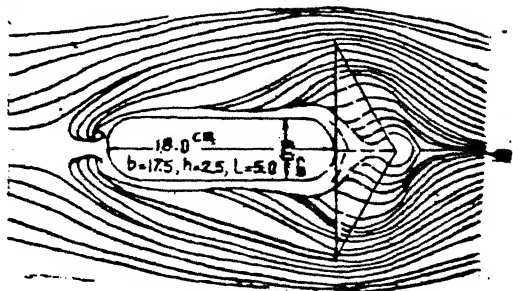
b/  $b=B$ e/  $b=2.5B$ c/  $b=1.5B$ f/  $b=3B$ d/  $b=2B$ g/  $b=3.5B$ 

FIG.3.9.3 PAINT IMPRESSIONS OF FLOW PATTERN ON THE PLATE FOR PIER ALONE AND FITTED WITH DEVICE.

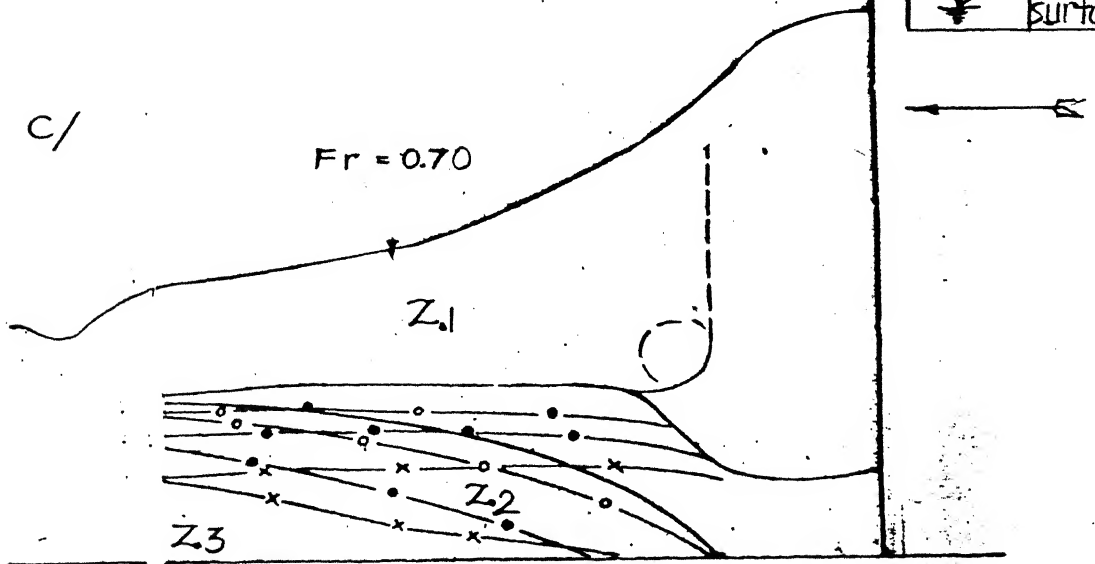
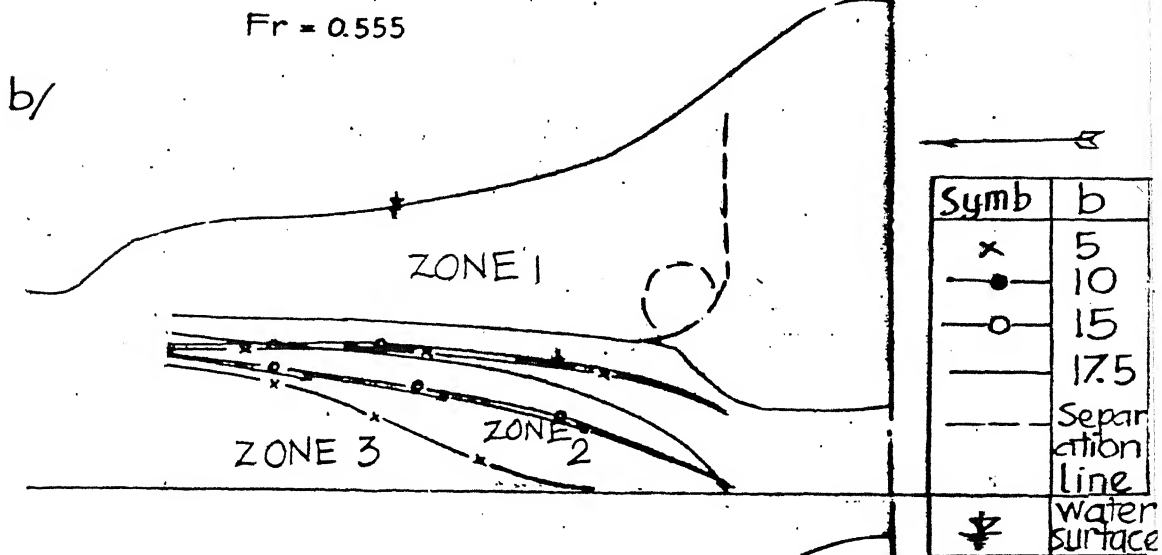
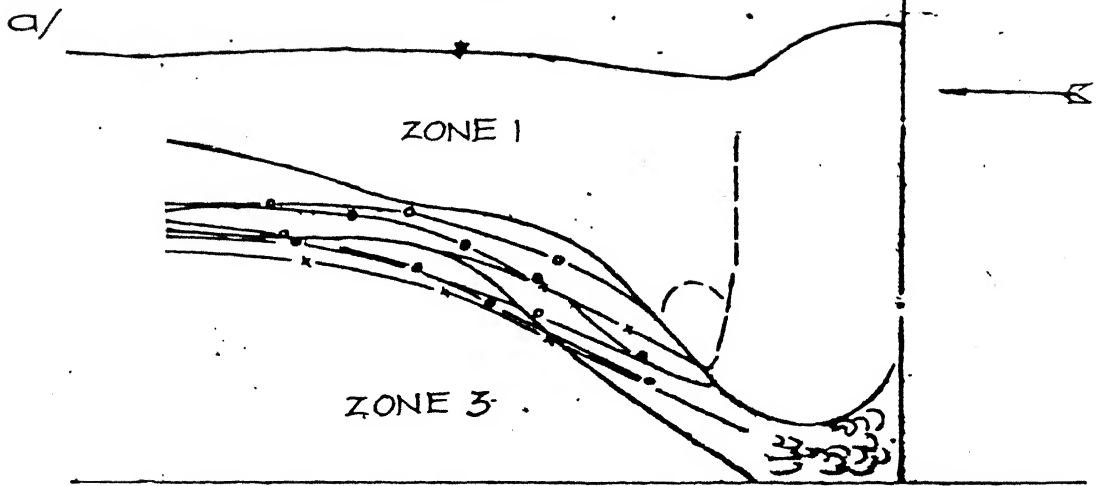


FIG. 3.9.4 PAINT IMPRESSIONS OF FLOW PATTERN ON THE SURFACE OF PIER

has been traced and reduced in size as shown in Figs. 3.9.1, 3.9.2 , 3.9.3 and 3.9.4 respectively. The typical photo view of the flow patterns are shown in Fig. 3.9.6. The typical photo view of horseshoe vortex form at the leading nose of the pier is shown in Fig. 3.9.5.

## 2.1 Flow Pattern on the plate

Regular streak lines of paints are observed on the plate for pier alone and pier with model device width varied under different flow conditions.

### a) For the case of pier alone

- The streak-lines clearly indicate the zone of front stagnation, stagnation point and zone of separation occurring on the plate due to model pier mounted on it. A number of lines indicating the number of vortices inside the separating region are also seen in Figs. 3.9.1, 3.9.2 and 3.9.3. In these cases at least four vortices, (horseshoe vortex) form. In the wake region the streaklines close systematically in the downstream of the pier. The vortices wrap the pier on the plate, and form large vortices behind the pier. Two large vortices penetrate each other as shifting downstream to form a vortex sheet behind the pier along flow direction.

### b) For the case of model pier fitted with model device

The streaklines obviously show separation point upstream of the vortex of passive device. The line of separation ahead and beneath the passive device moves down the pier and

wraps the pier. For these test flow conditions and this model pier fitted with device it seems that separation point ahead of the device vortex does not vary in a large range for various flow conditions. Separation point at angle  $\theta = \pm 45^\circ$  on separation line for all tests form curve line. The oncoming flow separates ahead of passive device, curves beneath passive device coming towards the leading part of the pier on either side of the spinal rib and pier. Streak-lines are curved more or less depending upon passive device width. Separation region around pier is less compared to pier alone, representing the modification of the original horseshoe vortex.

As the width of the passive device increases, the separating region in front of the pier nose reduces. The streak lines penetrate deep inside the passive device also they move very close the pier surface on the lateral side of the pier. The wake region in downstream is reduced in size. Thus, from these flow patterns it can be inferred that the reduction in horseshoe vortex near front nose of the pier is due to influence of passive device.

## 2.2 Flow Pattern on the Surface of the Pier

### a) Clear pier

Figure 3.9.4 show the point impressions of the flow pattern on the surface of the pier. For the case a pier alone the separation line starts just above the plate and continues upto the free surface. The stagnation line starting at some

distance above the plate at  $\theta = 0^\circ$  is observed, in all cases. The flow along the pier seems to be divided into two parts, upflow and downflow. Upflow is similar flow past a pier held in uniform flow with free surface on the upstream of the pier. Downflow is affected by horseshoe vortex formed at the leading nose of the pier, near junction with plate. For  $F_r = 0.555$  and  $0.70$  this is quite obvious. Vertical separation line on the pier surface in section AA' is also observed.

b) For pier fitted with device

Separation point is just above plate 2.5 cm on either pier side in section AA' for all cases. It is clear that this point depends on model device height. Depending upon model device width flow on both sides of the pier is divided into three or four zones along pier height. When model device width is larger than  $2B$  on either pier side there are three flow zones from water surface to the bottom. Zone 1 is affected by upflow over the top of model device. Zone 2 is affected by counter-rotating vortex initiated by model device and Zone 3 belongs to wake region.

## CHAPTER IV

### CONCLUSIONS AND SUGGESTIONS

#### 4.1 Conclusions

Based on results of the present investigation some conclusions are as follows:

##### a) Passive device dimensions

- (i) It is observed that the length of the passive device has negligible influence on the scour depth reduction for its length larger than pier width.
- (ii) The width of the device equal  $2B$  give max scour depth reduction 36.8 percent for  $F_r = 0.22$ .
- (iii) The height of the device equal  $B/2$  give the same max. scour depth reduction as 36.8 percent for  $F_r = 0.22$ . Further it is observed that when the height of device is zero, device acts as flat plate and give the reduction in scour depth upto 55.6 percent for  $F_r = 0.22$  for a given width equal to  $2B$ .

##### b) Flat Plate

With the above study, the experiments were conducted to find optimum dimensions of the flat plate for maximum-scour depth reduction. It is observed that the triangular plate with inner diameter  $B$  for enveloping the leading nose of the pier with its width equal to  $3B$  and its lengths equal to  $2B$  gives maximum scour depth reduction about 73.2 percent

for  $F_r = 0.22$ .

c) Combination of passive device with flat plate

From the about two separate studies it is felt that the combination of passive device and flat plate enveloping semicircular nose of the pier may be tested. From series of experiments it is observed that the combination of the device with following dimensions gives the scour reduction upto 83.7 percent for  $F_r = 0.22$ .

$$\begin{array}{llll} b_u/B & = 3.5 & l_u/B & = 1 \\ b_b/B & = 3.0 & l_b/B & = 2 \end{array} \quad h/B = 0.5$$

This combined device even give more reduction in maximum scour depth than flat plate alone.

d) Testing of the combined device for highest Froude Number

It is observed that the combined device placed at bed level for high flow condition did not perform well. When the system of combined device placed on and at distance equal  $B/2$  under bed level gives a very promising scour reduction. The scour reduction is 62.9 percent for  $F_r = 0.37$ .

e) Comparison with device

It seems that passive device gives more effective reduction in scour depth than piles placed ahead of main pier. Combined device is more effective than passive device and flat plate.

#### g) Flow pattern

From flow visualization study, it is observed that the influence of width of the passive device leading to the penetration of streaklines below the device and also towards the pier surface becomes more with increase in width of the passive device. The separating region due to horseshoe vortex formed in front of the leading nose of the pier beneath the passive device decreases with increase in device width.

#### 4.2 Recommendations for Further Study

- (i) For further study, it is suggested to investigate the flow characteristics past the cylinder model with combined device.
- (ii) Study influence of combined device with its dimensions mentioned above on scour depth for some other pier shapes and an other sand grain coarser than sand in this investigation is needed
- (iii) Combined device model having flexible plate should be tested.
- (iv). It will be very interesting to investigate the distribution of pressure and vortices in vicinity of combined device so that flow condition for applying this device will be clear.

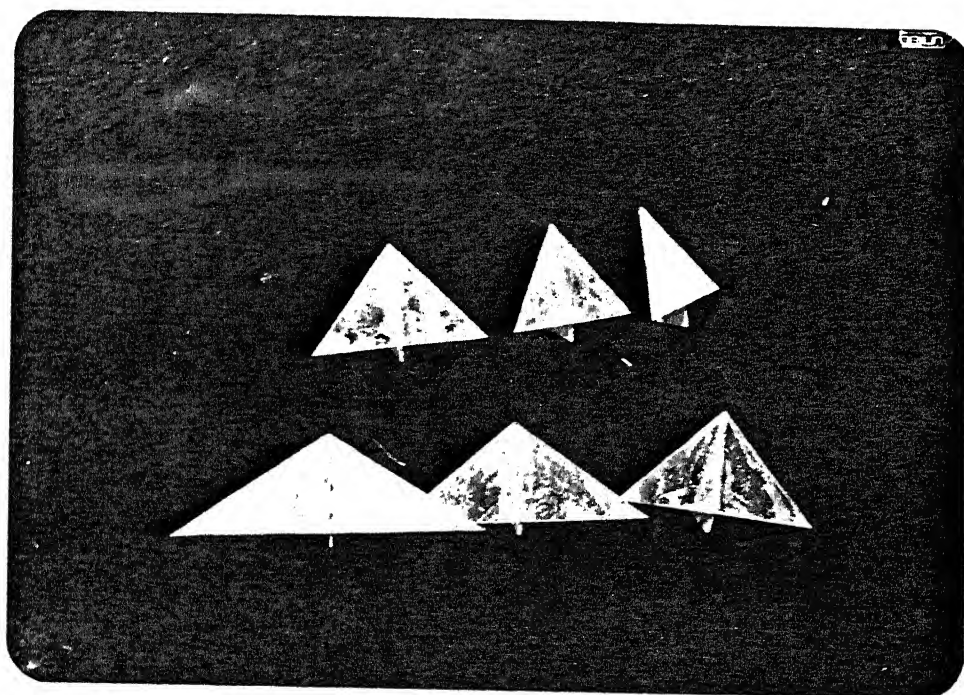
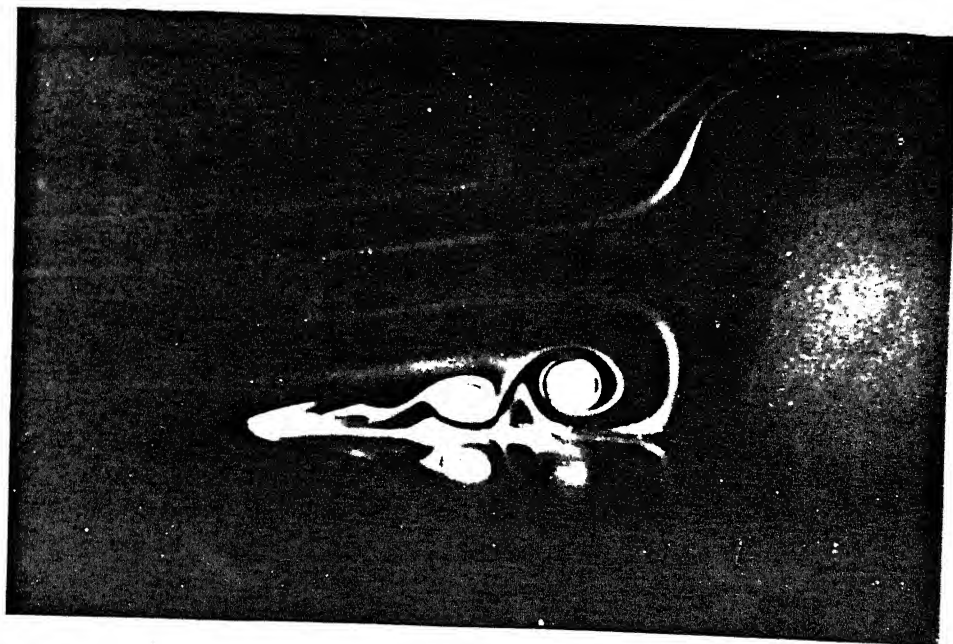


Fig. 3.9.5 : The Typical Photo View of Horseshoe Vortex

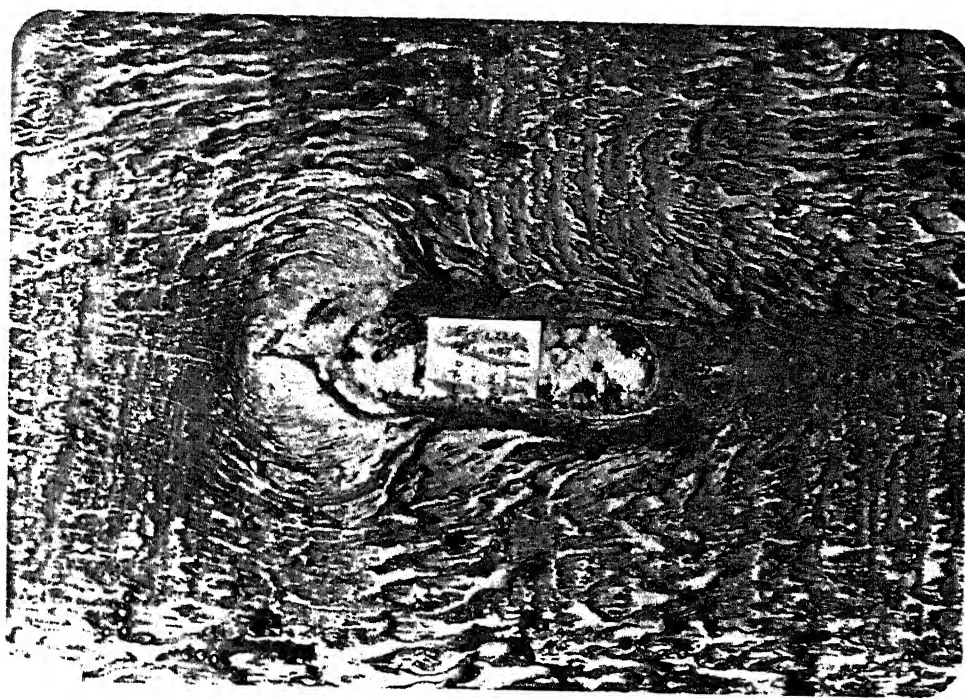
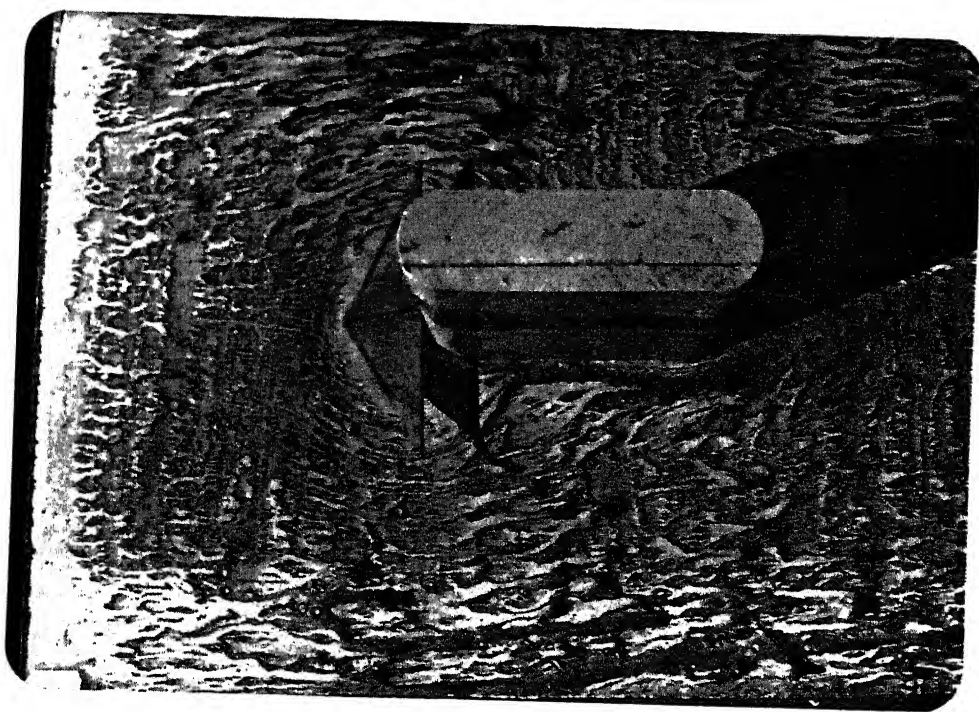


Fig. (a):  $F_r = 0.22$  ,  $b = 17.5$  cm,  $B = 5$  cm

Fig. 3.9.6 : The Typical Photo View of Flow Pattern

Contd...

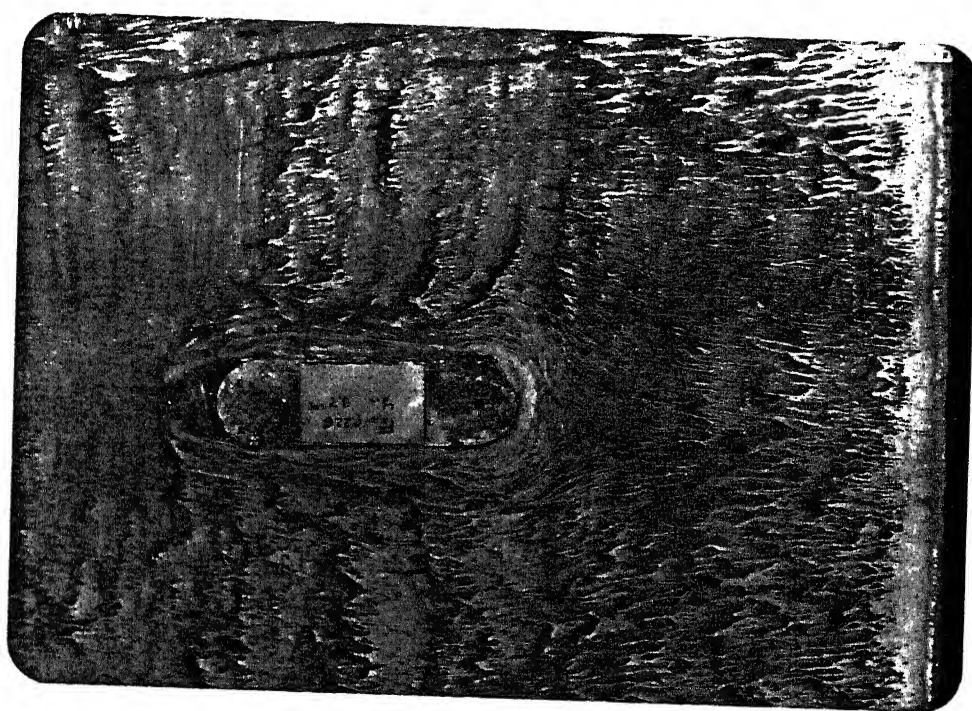
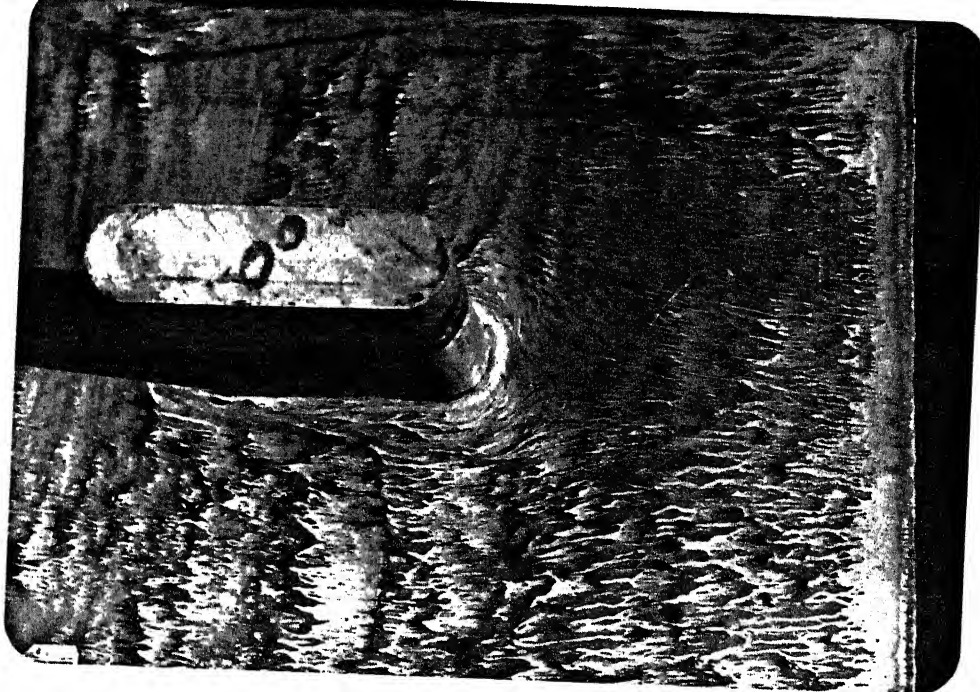


Fig. 3.9.6 (b) :  $F_r = 0.22$ ,  $B = 5$  cm

Fig. 3.9.6 contd...

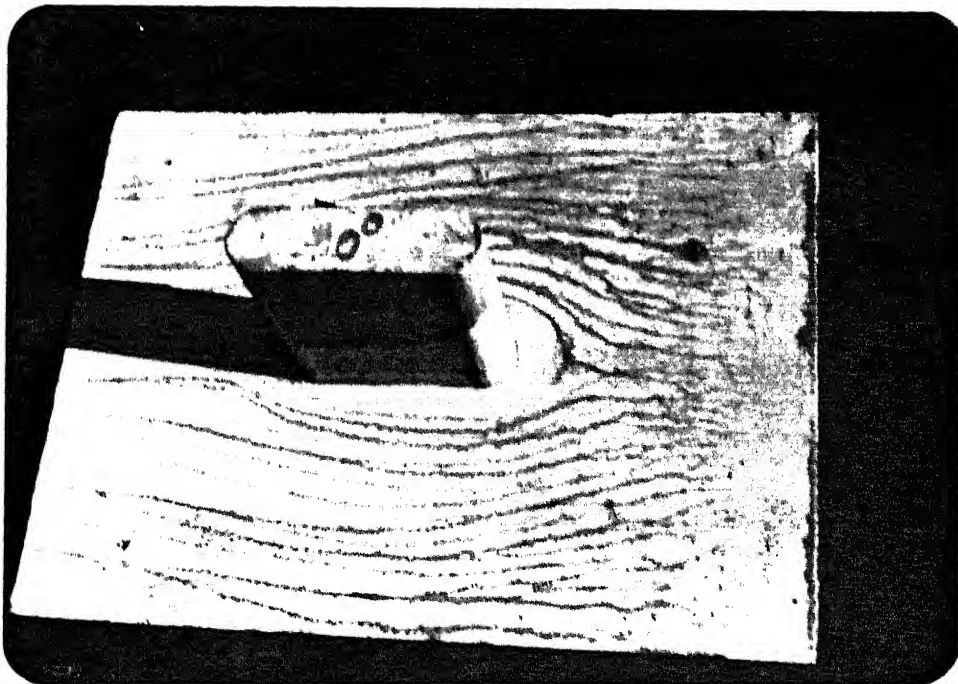


Fig. 3.9.6(c):  $F_r = 0.55$  ,  $B = 5$  cm

Fig. 3.9.6 contd...

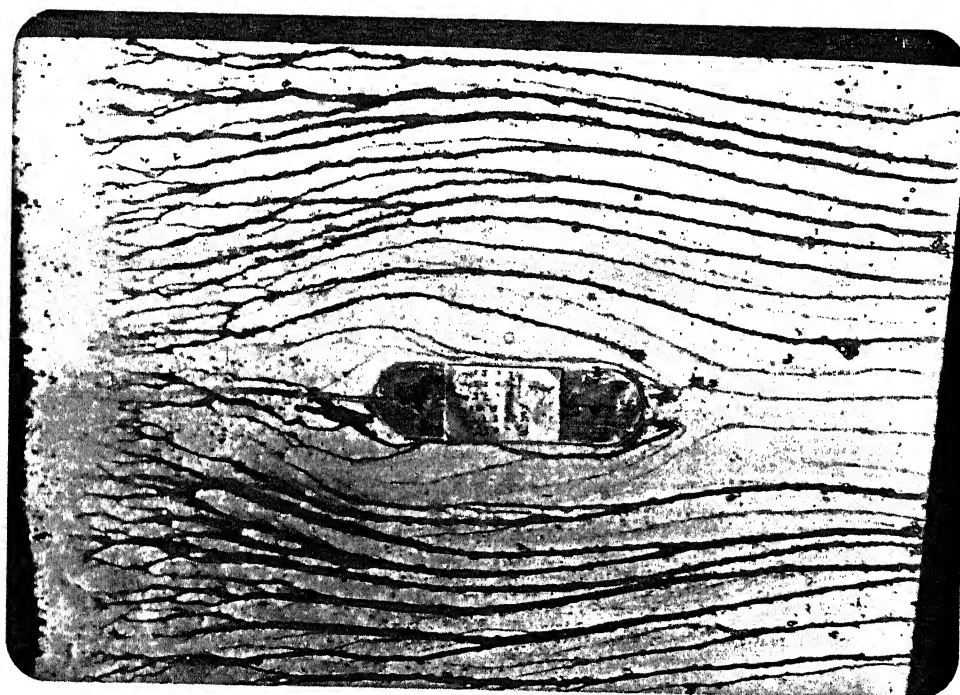
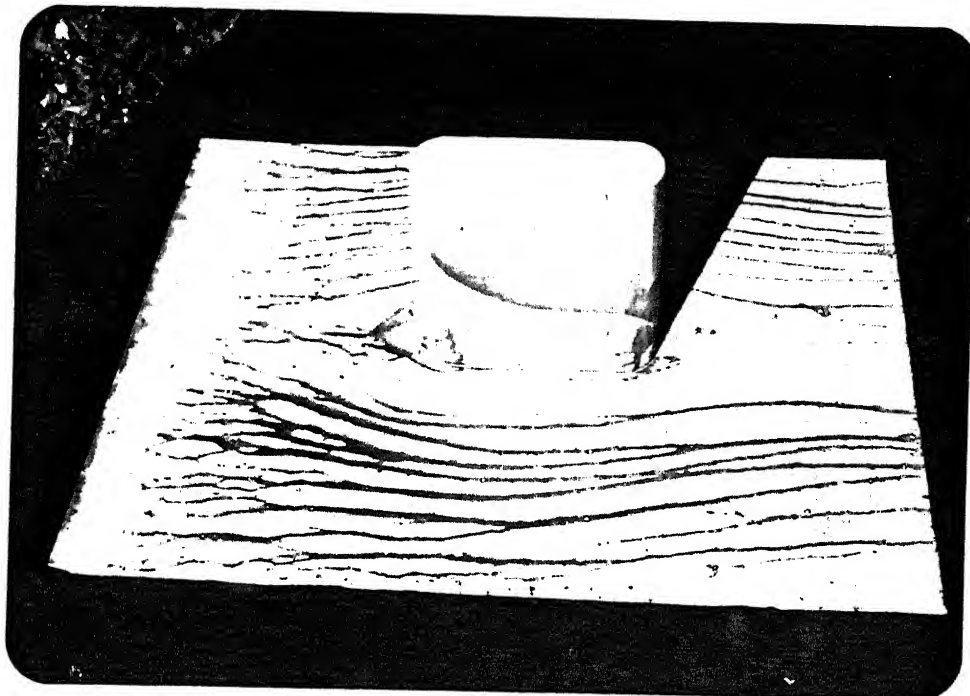


Fig. 3.9.6(d):  $F_r = 0.55$  ,  $b = 7.5$  cm ,  $B = 5$  cm

Fig. 3.9.6 contd...

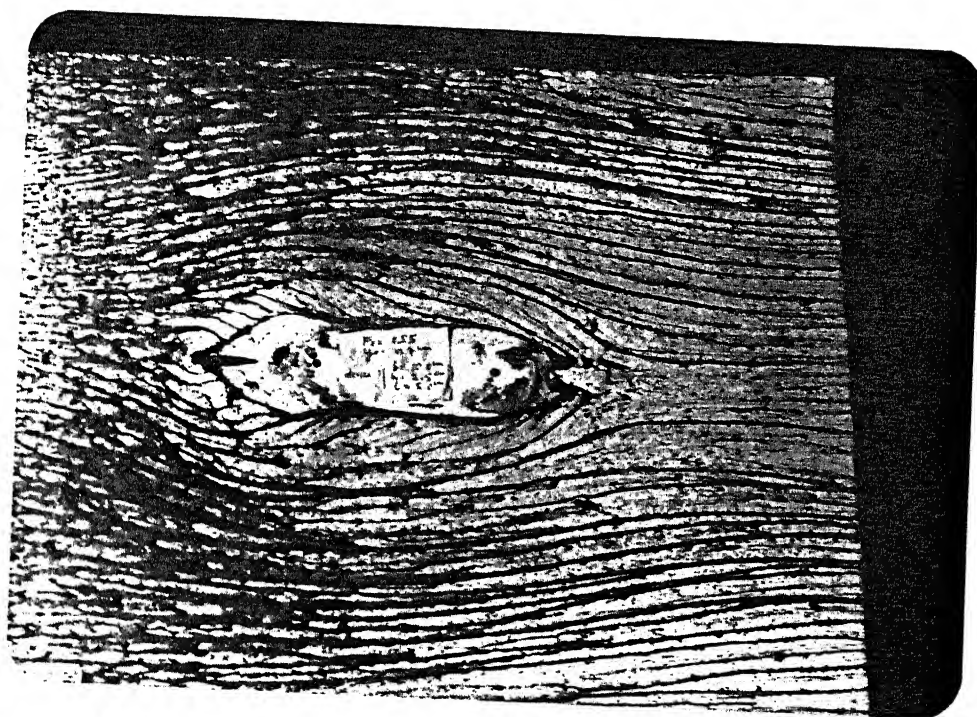
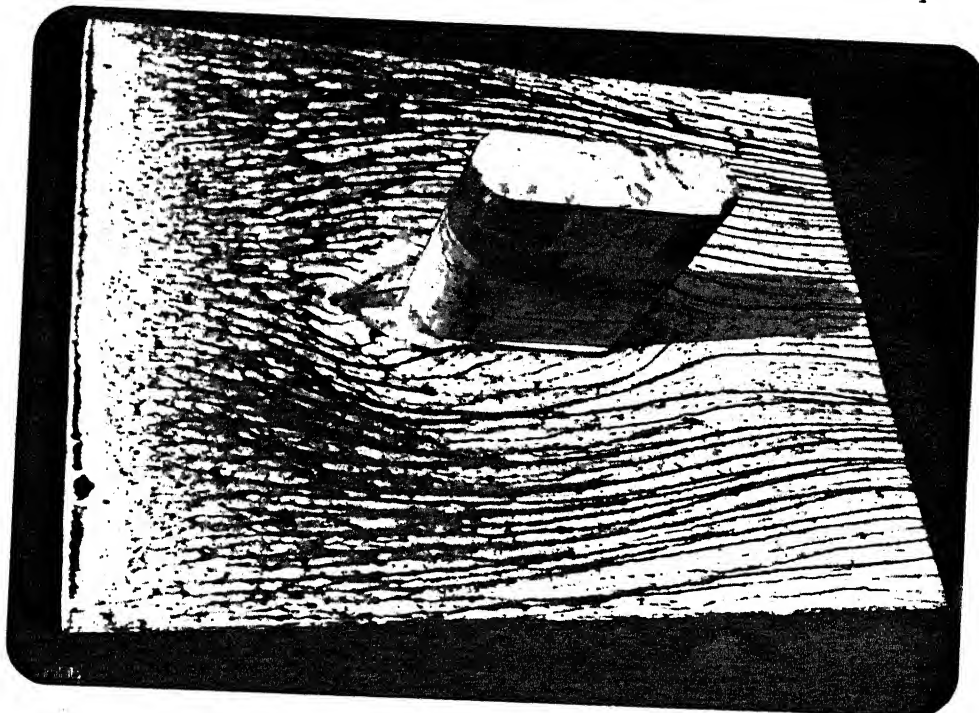


Fig. 3.9.6(e) :  $F_r = 0.55$  ,  $b = 10$  cm,  $B = 5$  cm

Fig. 3.9.6 contd...

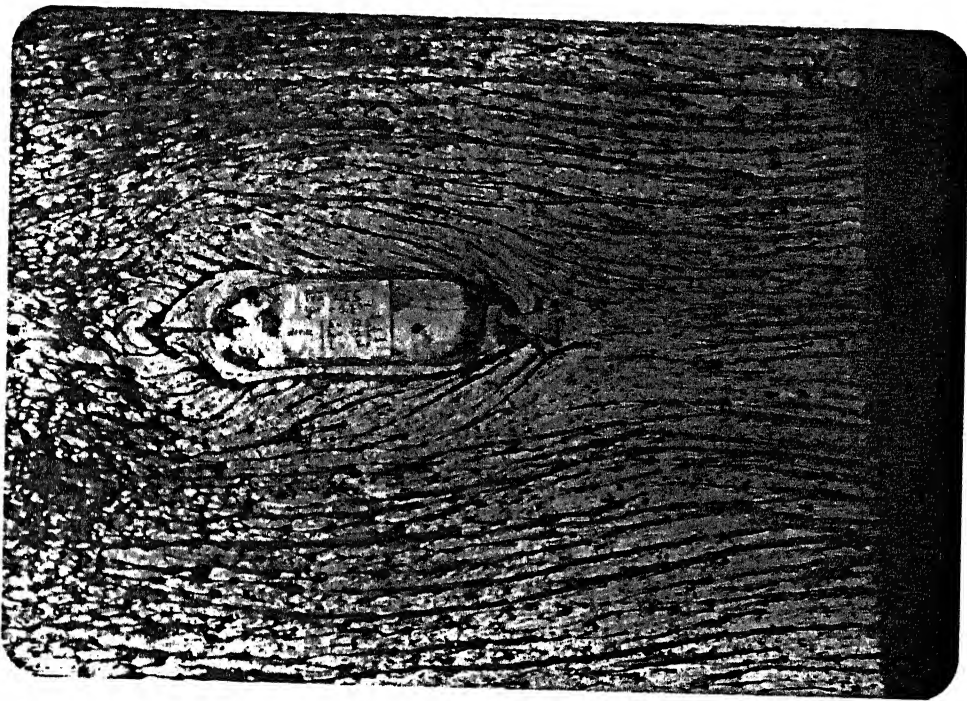
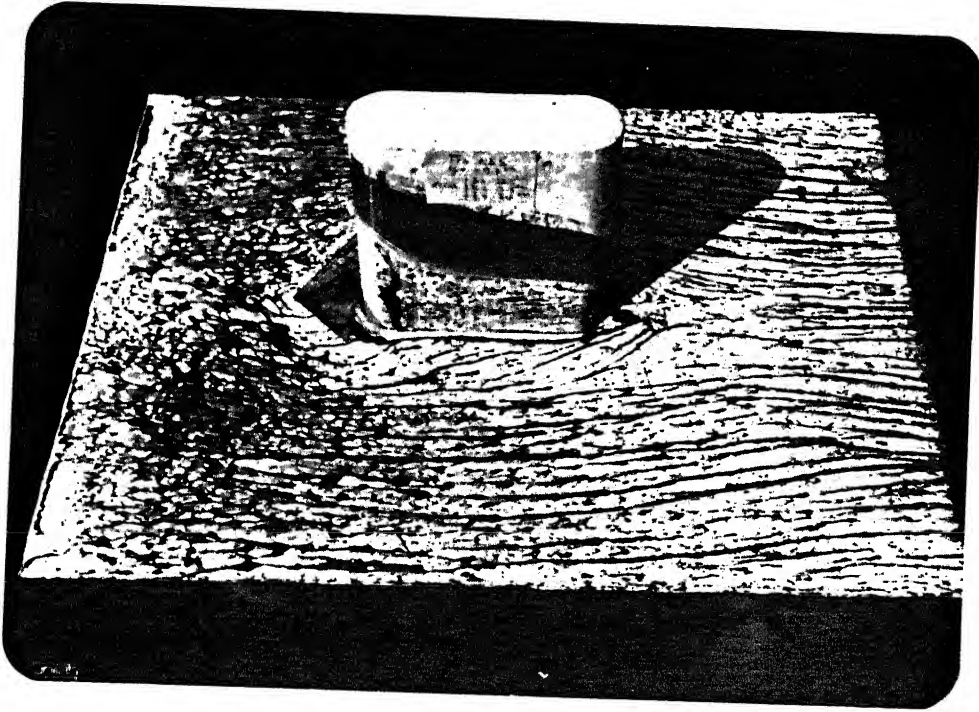


Fig. 3.9.6(f) :  $F_r = 0.55$ ,  $b = 12.5$  cm,  $B = 5$  cm

Fig. 3.9.6 contd...

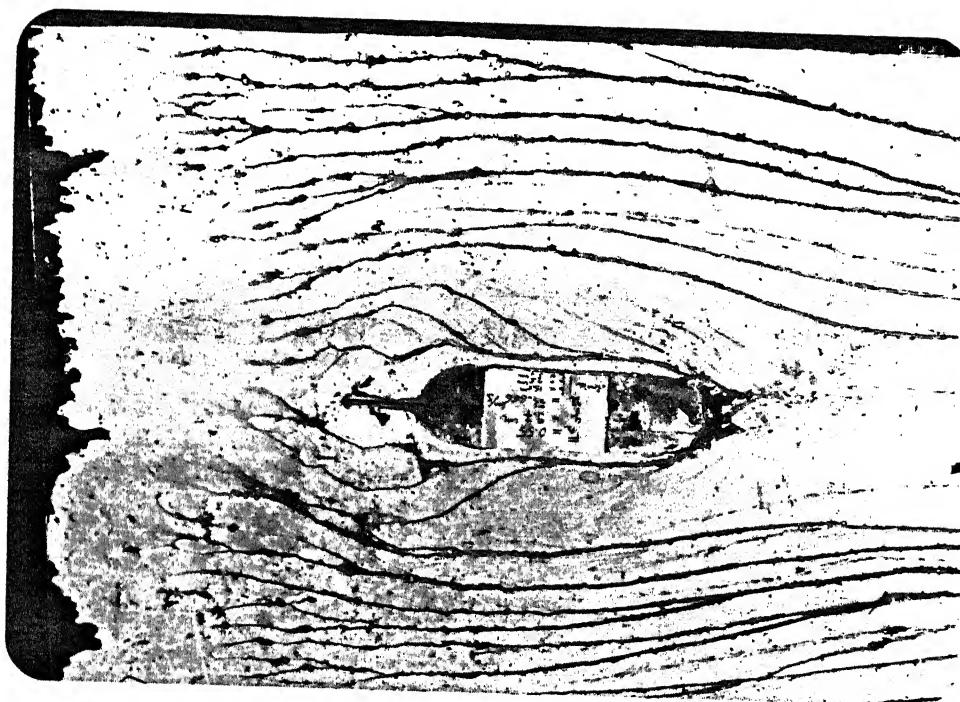
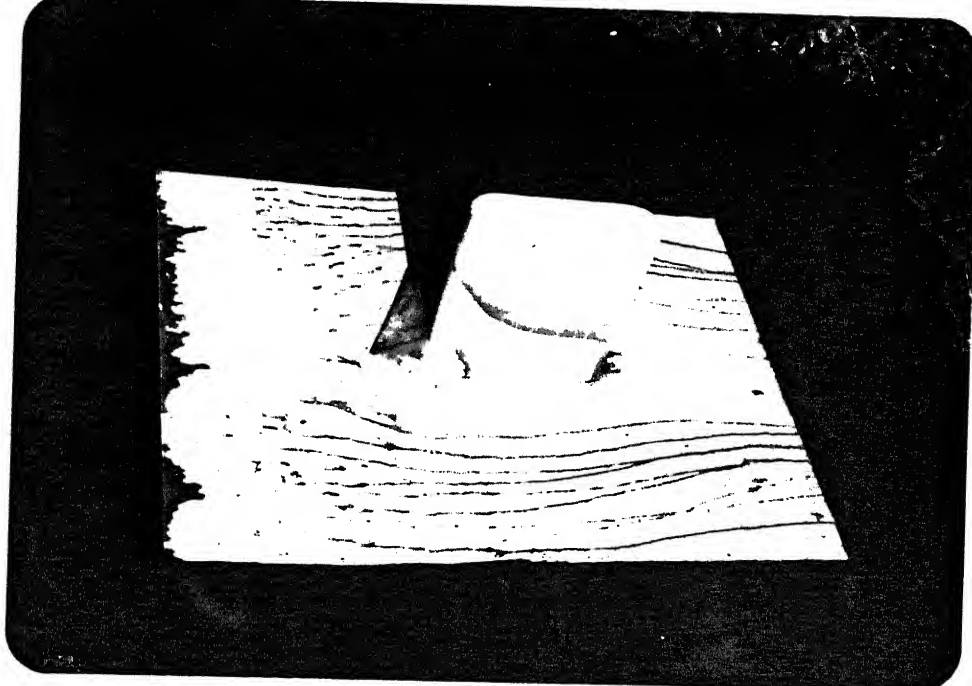


Fig. 3.9.6(g) :  $F_r = 0.55$  ,  $b = 15$  cm,  $B = 5$  cm

Fig. 3.9.6 contd...

TABLE 2.1 : SEDIMENT CHARACTERISTICS USED FOR THIS STUDY

Model Number	Arithmetic mean size in millimeters $\bar{D}$	Median size in mm $D_{50}$	Geometric mean size in mm $D_g$	Standard deviation $\sigma \times 10^{-2}$	Geometric standard deviation $\sigma_g$
1	2	3	4	5	6
1	0.156	0.16	0.160	4.7	1.217
2	0.150	0.15	0.156	4.895	1.155
2	0.157	0.16	0.160	4.892	1.270
3	0.158	0.16	0.160	5.184	1.270
3	0.155	0.155	0.161	5.082	1.240
4	0.164	0.155	0.161	5.234	1.240
4	0.155	0.160	0.161	5.047	1.240
5	0.153	0.155	0.161	4.720	1.240
5	0.159	0.155	0.161	5.413	1.240
6	0.153	0.155	0.161	4.860	1.240
7	0.152	0.155	0.161	4.776	1.240
7	0.154	0.156	0.161	4.940	1.240
7	0.150	0.156	0.157	4.693	1.209
8	0.150	0.156	0.157	4.613	1.209
9	0.150	0.156	0.157	4.682	1.209
10	0.152	0.156	0.157	4.813	1.209
10	0.154	0.155	0.161	4.857	1.240
10	0.152	0.150	0.157	4.790	1.210
11	0.150	0.155	0.164	4.872	1.217
12	0.150	0.155	0.154	4.756	1.210

Contd...

TABLE 2.1 : SEDIMENT CHARACTERISTICS USED FOR THIS STUDY

Model Number	Arithmetic mean size in millimeters $\bar{D}$	Median size in mm $D_{50}$	Geometric mean size in mm $D_g$	Standard deviation $\sigma \times 10^{-2}$	Geometric standard deviation $\sigma_g$
1	2	3	4	5	6
1	0.156	0.16	0.160	4.7	1.217
2	0.150	0.15	0.156	4.895	1.155
2	0.157	0.16	0.160	4.892	1.270
3	0.158	0.16	0.160	5.184	1.270
3	0.155	0.155	0.161	5.082	1.240
4	0.164	0.155	0.161	5.234	1.240
4	0.155	0.160	0.161	5.047	1.240
5	0.153	0.155	0.161	4.720	1.240
5	0.159	0.155	0.161	5.413	1.240
6	0.153	0.155	0.161	4.860	1.240
7	0.152	0.155	0.161	4.776	1.240
7	0.154	0.156	0.161	4.940	1.240
7	0.150	0.156	0.157	4.693	1.209
8	0.150	0.156	0.157	4.613	1.209
9	0.150	0.156	0.157	4.682	1.209
10	0.152	0.156	0.157	4.813	1.209
10	0.154	0.155	0.161	4.857	1.240
10	0.152	0.150	0.157	4.790	1.210
11	0.150	0.155	0.164	4.872	1.217
12	0.150	0.155	0.154	4.756	1.210

Contd.....

1	2	3	4	5	6
13	0.150	0.155	0.157	4.686	1.210
13	0.150	0.155	0.157	4.653	1.210
14	0.150	0.150	0.159	4.828	1.195
15	0.152	0.150	0.159	4.907	1.195
15	0.151	0.150	0.159	5.022	1.195
16	0.150	0.150	0.159	4.949	1.191
17	0.151	0.150	0.159	4.765	1.191
18	0.154	0.154	0.164	4.917	1.223
19	0.151	0.150	0.164	4.899	1.217
20	0.155	0.156	0.164	4.932	1.217
21	0.154	0.156	0.164	4.920	1.217
22	0.152	0.150	0.164	4.896	1.217
23	0.155	0.156	0.164	5.266	1.217
24	0.153	0.156	0.164	4.835	1.217
25	0.151	0.156	0.164	4.870	1.217
26	0.158	0.160	0.168	5.528	1.247
28	0.155	0.156	0.168	5.146	1.247
29	0.157	0.156	0.168	5.216	1.247
36	0.150	0.150	0.160	4.930	1.186
38	0.155	0.150	0.164	5.367	1.217
39	0.151	0.150	0.162	5.115	1.200
40	0.152	0.150	0.164	5.246	1.217
44a	0.152	0.150	0.160	4.857	1.186
45	0.150	0.150	0.160	4.729	1.180

Contd.....

Table 2.1 contd.....

Test	$F_r$	2	3	4	5	6
30	0.224	0.146	0.155	0.164	5.146	1.217
31	0.224	0.147	0.150	0.160	4.605	1.217
90	0.304	0.151	0.155	0.164	4.790	1.217
92	0.351	0.154	0.155	0.164	5.040	1.217
95	0.324	0.156	0.156	0.164	5.097	1.217
96	0.374	0.155	0.150	0.164	5.367	1.217
99	0.336	0.152	0.160	0.157	4.703	1.209
101	0.363	0.157	0.160	0.161	5.054	1.240

TABLE 3.1 : MAXIMUM SCOUR DEPTH FOR PIER WITHOUT PROTECTION  
FOR DIFFERENT FLOW CONDITIONS

Run	$y_o$ (cm)	U (cm/sec)	Q (l/sec)	$F_r$	$d_{smo}$ (cm)
10	10.62	20.196	10.724	0.198	4.73
30	9.823	22.042	10.826	0.224	5.37
31	9.780	21.930	10.724	0.224	6.35
97	10.000	37.400	18.700	0.378	7.17
98	10.420	35.990	18.750	0.356	6.78
99	9.613	32.660	15.700	0.336	6.74
100	9.530	29.910	14.250	0.310	6.52
101	10.27	36.460	18.720	0.363	6.88

TABLE 3.2 : MAXIMUM SCOUR DEPTH FOR DIFFERENT DEVICE LENGTHS WHEN OTHER GEOMETRIES FIX  
 $h = 0.5B$ ,  $b = 1.5 B$ .

Model (M)	1 (cm)	$d_{sm}$ (cm)	$y_o$ (cm)	U (cm/sec)	Q (l/sec.)	$F_r$	L/B	$\frac{d_{sm}}{d_{smo}}$	$\frac{d_{smo}-d_{sm}}{d_{smo}}$ (percent)
1	2	3	4	5	6	7	8	9	10
1	15.0	4.23	9.80	21.89	10.73	0.223	3.00	0.67	33.4
2	12.5	4.58	9.48	22.62	10.72	0.234	2.50	0.72	27.9
2	12.5	4.04	10.00	21.45	10.72	0.227	2.50	0.64	36.4
3	10.0	4.15	9.89	21.69	10.72	0.220	2.06	0.65	34.6
3	10.0	4.49	9.78	21.93	10.72	0.220	2.06	0.71	29.3
4	7.5	4.08	9.65	22.10	10.65	0.220	1.52	0.64	35.7
4	7.5	4.52	9.85	21.99	10.82	0.220	1.52	0.71	28.8
5	5.5	4.70	9.80	22.04	10.80	0.220	1.12	0.74	26.0
5	5.5	4.10	10.06	21.50	10.79	0.210	1.12	0.65	35.4

TABLE 3.3 : MAXIMUM SCOUR DEPTH FOR DIFFERENT DEVICE WIDTHS AND OTHER GEOMETRIES

FIXED:  $h = 0.5B$ ,  $l = 2.5B$

Model (M)	b (cm)	$d_{sm}$ (cm)	$y_o$ (cm)	U (cm/sec)	Q (l/sec)	Fr	b/B	$\frac{d_{sm}}{d_{smo}}$	$\frac{d_{smo}-d_{sm}}{d_{smo}} \%$
1	2	3	4	5	6	7	8	9	10
6	5.0	4.73	10.21	21.07	10.72	0.21	1.0	0.74	25.5
2	7.5	4.58	9.48	22.62	10.72	0.23	1.5	0.72	27.9
2	7.5	4.04	10.00	21.45	10.72	0.22	1.5	0.64	36.4
7	10.0	3.62	9.84	21.80	10.72	0.22	2.0	0.57	42.8
7	10.0	3.90	9.98	21.70	10.82	0.22	2.0	0.62	38.6
7	10.0	3.67	10.04	21.36	10.72	0.22	2.0	0.58	42.2
8	12.5	4.21	9.91	21.62	10.72	0.22	2.52	0.66	33.7
9	15.0	3.99	9.73	22.03	10.72	0.22	2.96	0.63	37.2

TABLE 3.4 : MAXIMUM SCOUR DEPTH FOR DIFFERENT MODEL HEIGHTS WHEN OTHER GEOMETRIES  
FIXED:  $b = 2B$ ,  $l = 2.5B$ .

Model (M)	h (cm)	$d_s$ (cm)	$y_o$ (cm)	U (cm/sec)	Q (l/sec)	$F_r$	h/B	$\frac{d_{sm}}{d_{smo}}$	$\frac{d_{smo} - d_{sm}}{d_{smo}}$ (percent)
1	2	3	4	5	6	7	8	9	10
10	0.00	2.3	10.08	21.28	10.72	0.22	0.00	0.36	63.78
10	0.00	2.5	9.89	21.70	10.72	0.22	0.00	0.39	60.73
10	0.00	2.82	9.95	21.56	10.72	0.22	0.00	0.44	55.62
11	1.025	3.97	9.97	21.51	10.72	0.22	0.20	0.63	37.48
12	1.60	4.14	9.89	21.70	10.72	0.22	0.32	0.65	34.80
13	2.00	4.02	9.86	22.43	11.06	0.22	0.41	0.70	29.87
13	2.00	4.45	9.74	22.03	10.72	0.22	0.41	0.63	36.69
7	2.50	3.625	9.84	21.80	10.72	0.22	0.52	0.57	42.91
7	2.50	3.90	9.98	21.70	10.82	0.22	0.52	0.61	38.58
7	2.50	3.67	10.04	21.36	10.72	0.22	0.52	0.58	42.21
14	3.10	4.74	9.78	21.93	10.72	0.22	0.62	0.75	25.31
15	3.75	4.38	9.83	21.82	10.72	0.22	0.75	0.69	31.02
15	3.75	4.75	9.69	22.14	10.72	0.22	0.75	0.75	25.20
16	4.82	4.84	9.82	21.84	10.72	0.22	0.96	0.76	23.78
17	6.40	4.42	10.04	21.56	10.82	0.22	1.28	0.70	30.39
18	7.50	4.95	9.88	21.71	10.72	0.22	1.50	0.78	22.05

TABLE 3.5a: MAXIMUM SCOUR DEPTH FOR DIFFERENT FLAT PLATE WIDTHS ENVELOPING PIER NOSE

Model	Varied dimension (cm)	$d_{sm}$ (cm)	$y_o$ (cm)	U (cm/s)	Q	$F_r$	Varied geometry over B	$\frac{d_{sm}}{d_{smo}}$	$\frac{d_{sm}-d_{smo}}{d_{smo}}$ (percent)	Remarks
1	2	3	4	5	6	7	8	9	10	
19	R = 5.0	4.42	9.83	21.83	10.724	0.222	2R/B = 2	0.7	30.4	Semi-circular plate
20	7.5	1.95	9.95	21.56	10.724	0.218	3	0.307	69.2	
20	7.5	2.45	10.07	21.29	10.724	0.214	3	0.386	61.4	
22	$b_b=10.0$	2.30	9.90	21.66	10.724	0.220	$b_b/B = 2$	0.36	64.0	Triangular plate
24	12.5	1.90	10.01	21.42	10.724	0.216	2.5	0.30	70.1	
25	15.0	1.70	9.82	21.48	10.724	0.217	3.0	0.267	73.2	
21	$l_b=5.0$	2.37	9.97	21.51	10.724	0.218	$l_b/B = 1.0$	0.37	62.6	Semi-circular plate
23	10.0	2.30	9.77	21.96	10.724	0.224	2.0	0.36	63.8	
23	10.0	2.54	9.83	21.81	10.724	0.222	2.0	0.40	60.1	
22	7.5	2.30	9.90	21.66	10.724	0.222	1.5	0.36	64.0	Triangular plate
10	$l_b=12.5$	2.30	10.08	21.82	10.724	0.214	$l_b/B = 2.5$	0.36	63.8	
10	12.5	2.50	9.89	21.70	10.724	0.220	2.5	0.39	60.6	
10	12.5	2.82	9.95	21.56	10.724	0.218	2.5	0.44	55.6	

TABLE 3.5b: MAXIMUM SCOUR DEPTH FOR DIFFERENT FLAT PLATE WIDTHS NOT ENVELOPING PIER NOSE

TABLE 3.6 a,b , c : MAXIMUM SCOUR DEPTH FOR DIFFERENT COMBINED DEVICES

Model	Varied dimension (cm)	$d_{sm}$ (cm)	$y_0$ (cm)	$U$ (cm/s)	$Q$ (l/s)	$Fr$	Varied geometry over B	$\frac{d_{sm}}{d_{smo}}$	$\frac{d_{smo}-d_{sm}}{d_{smo}}$ (percent)	Remarks	
28	$b_b = 5.0$	4.96	9.93	21.6	10.724	0.22	$b_b/B=1.0$	0.78	21.9	Combined device touches pier nose: Table 3.6a	
28	5.0	4.67	9.75	22.0	10.724	0.225	1.0	0.74	26.5		
26	10.0	3.48	9.77	21.95	10.724	0.224	2.0	0.55	45.2		
26	10.0	3.56	9.88	21.71	10.724	0.22	2.0	0.56	43.9		
26	10.0	2.57	9.88	21.71	10.724	0.22	2.0	0.40	59.5		
44a	15.0	2.42	9.92	21.6	10.724	0.22	3.0	0.38	62.9		
44a	15.0	2.45	9.80	21.9	10.724	0.22	3.0	0.38	61.9		
44	$b_u = 10.0$	2.40	9.92	21.61	10.724	0.219	$b_u =$	0.66	0.378	62.2	Combined device envelops pier nose: Table 3.6b
45	15.0	3.18	10.30	21.38	10.724	0.216	$b_b$	0.83	0.50	49.9	
47	17.5	2.96	9.95	21.56	10.724	0.218		1.17	0.466	53.4	
36	7.5	2.6	9.87	21.73	10.724	0.221		0.5	0.41	59.1	
37	10.0	2.03	9.91	21.64	10.724	0.22		0.67	0.32	60.3	
39	15.0	1.46	9.55	21.56	10.724	0.218		1.00	0.23	78.0	
40	17.5	0.50	9.80	21.89	10.724	0.223		1.17	0.08	92.1	
40	17.5	1.10	9.82	21.84	10.724	0.223		1.17	0.17	83.7	
43	17.5	1.77	9.92	21.62	10.724	0.22		1.17	0.28	72.1	
1	2	3	4	5	6	7	8	9	10	Column no.	

Contd.....

Contd.,...

TABLE 3.6 c

1	2	3	4	5	6	7	8	9	10	11
30	$h = 2.50$	1.527	10.03	21.39	10.724	0.216	$h/B = 0.25$	0.24	75.24	Combined
31	1.25	3.0	9.87	21.73	10.724	0.221	0.5	0.47	52.76	device with height
40	2.5	0.5	9.80	21.89	10.724	0.223	$h/B = 0.5$	0.08	92.10	variation an
40	2.5	1.10	9.82	21.84	10.724	0.223	0.5	0.17	83.70	enveloping
42	3.75	1.54	9.96	21.53	10.724	0.218	0.75	0.243	75.75	pier nose

TABLE 3.7 : MAXIMUM SCOUR DEPTH FOR DIFFERENT MODEL DEVICES

Run	$d_{sm}$ (cm)	$y_o$ (cm)	$U$ (cm/s)	$Q$ (l/s)	$F_r$	$\frac{d_{sm}}{d_{smo}}$	$\frac{d_{smo}-d_{sm}}{d_{smo}}$ (percent)	Remarks
78	4.98	9.73	22.04	10.724	0.226	0.78	21.57	Small pile dia 1 cm(= B/5)
81	0.00	9.95	21.56	10.724	0.218	0.00	0.00	Collar on bed level
82	4.30	9.91	21.64	10.724	0.220	0.676	32.44	Collar over bed level B/2
83	2.50	10.15	21.13	10.724	0.212	0.394	60.63	Collar below bed level B/2
85	2.70	9.93	21.60	10.724	0.219	0.430	57.48	Caisson below bed level B/2
86	5.24	9.86	21.75	10.724	0.220	0.830	17.48	Caisson with V-lip below bed level B
87	2.90	9.73	22.04	10.724	0.226	0.450	54.80	Caisson with V-lip below bed level B/2
88	0.00	9.77	21.95	10.724	0.224	0.000	0.00	-
5	4.15	9.89	21.69	10.724	0.220	0.650	34.60	Standard configura- tion of passive device M <sub>3</sub> : l=2B, b = 1.5B, h=0.5B
28	4.49	9.78	21.93	10.724	0.224	0.710	29.30	Passive device M7 l = 2.5B, b=10, h = 0.5
103	3.625	9.84	21.80	10.724	0.222	0.572	42.91	
29	3.900	9.98	21.70	10.826	0.220	0.614	38.58	
43	3.670	10.04	21.36	10.724	0.215	0.578	42.21	
	0.50	9.80	21.89	10.724	0.223	0.087	92.13	
	1.10	9.81	21.84	10.724	0.223	0.170	83.68	M <sub>40</sub>

TABLE 3.8 : SCOUR REDUCTION BY COMBINED DEVICE AT DIFFERENT FLOW CONDITIONS

Model (M)	U (cm/s)	F <sub>r</sub>	Y <sub>o</sub> (cm)	d <sub>sno</sub> (cm)	d <sub>sm</sub> (cm)	$\frac{d_{sm}}{d_{sno}}$	$\frac{d_{sno}-d_{sm}}{d_{sno}}$ (percent)	Protection device
	21.93	0.22		6.35				None
M <sub>40</sub>	21.89	0.22	9.80		0.5	0.08	92.13	M <sub>40</sub> : combined device
M <sub>40</sub>	21.84	0.22	9.81		1.1	0.17	83.68	None
M <sub>40</sub>	29.91	0.31	9.53	6.52	5.25	0.81	19.50	M <sub>40</sub> : combined device
M <sub>51</sub>	29.58	0.31	9.65		3.09	0.47	52.61	M <sub>51</sub> : combined device
	29.96	0.31	9.51					None
	35.99	0.36	10.42	6.78				M <sub>51</sub> : Combined device
M <sub>51</sub>	33.63	0.35	9.36		3.24	0.48	52.21	None
	32.66	0.34	9.61	6.74				M <sub>51</sub> : combined device
M <sub>51</sub>	32.72	0.34	9.62		3.78	0.56	43.92	None
	37.40	0.38	10.00	7.17				M <sub>52</sub> : combined device
M <sub>52</sub>	37.17	0.37	10.00		2.66	0.37	62.90	None
	31.90	0.32	9.87		2.00	0.31	69.30	M <sub>52</sub> : combined device
	36.46	0.36	10.27	6.88				None

REFERENCES

1. ARMSTRONG, W.D. (1957), 'An experimental investigation of the secondary flow occuring in a compressor cascade', Aeronautical Quarterly, Vol.III, pp.240-254, Aug.1957.
2. ALTINBILEX, H.D. (1971), 'Similarity laws for local scour with special emphasis on vertical circular pile in oscillatory flow', Proceedings Fourteenth Congress of IAHR, Vol.III, pp.339-346, Sept. 1971.
3. BAKER, C.J. (1979), 'Laminar horseshoe vortex', J. Fluid Mechanics, Vol.95, pp. 347-367, 1979.
4. BAKER, C.J. (1980), 'Theoretical approach to prediction of Local scour around Bridge Piers', J. Hydraulic Research, Vol.18, No.1, pp. 1-12, 1980.
5. BAKER, C.J. (1981), 'New design equation for scour around bridge piers', J.H.D., ASCE, Vol.107, pp. 507-511.
6. BREUSERS, H.N.C. (1975), 'Computation of Velocity profiles in scour hole', Proceedings, XVIth Congress of IAHR, Vol.II, pp. 300-306, 1975.
7. BREUSERS, H.N.C. and NICOLLET, G. and SHEN, H.W. (1977), 'Local scour around cylindrical piers', Journal of Hydraulic Research, IAHR, Vol.15, No.3, pp211-252, 1977.
8. BREUSERS, H.N.C., 1970, Discussion on Shen et al.(1969), Proc. ASCE, 96, HY7, pp. 1638-1639.

9. BELIK, L. (1973), 'Secondary flow about circular cylinders mounted normal to a flat plate', Aeronautical Quarterly Vol.24, Feb.1973, part 1, pp.47-54.
10. BRIDGES SCOUR and WATERWAY- Bulletin 242.
11. BRUCE, W. MELVILLE and ARVED J. RAUDKIVI (1971), 'Flow in local characteristics/scour at bridge piers', I.H.R., No.4, pp. 373-380, 1977.
12. CARSTENS, T. and SHARMA, H.R. (1975), 'Local scour around large obstruction', Proc. 16th IAHR Congress, Sao Paulo, 2, pp. 251-262, 1975.
13. CUNHA, L.V. (1975), 'Time evaluation of local scour', Proc. 16th IAHR congress, Sao Paulo, 2, pp. 285-299.
14. COLEMAN, N.L. (1971), 'Analysing laboratory measurements of scour at cylindrical piers in sand beds' Proc. 14th IAHR congress, PARIS, 3, pp.307-313.
15. CHIEW, Y.M. and MELVILLE, B.W. (1987), 'Local scour around bridge piers', J. Hyd. Research IAHR, Vol.25, No.1, pp. 15-26.
16. T. GANGADHARIAH, M. MUZZAMMIN and K. SUBRAMANYA (1985), 'Vortex strength approach for bridge pier scour predictions', (SIWARP) Roorkee, U.P.
17. GARDE, R.J., SUBRAMANYA, K. and NAMUDRIPAD, K.D. (1961), 'Study of scour around Spur-Dikes', Proc. ASCE, JHD, HY6, pp. 23-37.

18. GUPTA, A.K. (1987), 'Hydrodynamic modification of the horseshoe vortex at vertical pier junction with ground', Phys. Fluids 30(4), April, pp.1213-1215, 1987.
19. GUPTA, A.K. (1984), 'Boundary layer flow past a circular cylinder mounted on a flat plate', M.Tech. Thesis, I.I.T. Kanpur, January, 1984.
20. GUPTA, A.K. (1986), 'Characteristics of vortex in the scour hole' M.Tech. Thesis, IIT Kanpur, January, 1986.
21. GALLEX, B., and BUTTE, J.N. (1971), 'Regime non-stationnaire Auto-exite et afforillement des piles', Proc. 14th IAHR congress, PARIS, 3, pp. 291-298.
22. HAWTHORNE, W.R. (1954), 'The secondary flow about struts and airfoils', J. of Aeronautical sciences, Vol.21, Sept., pp. 388-609.
23. HANCU, S. (1971), 'Sur le calcul affouillements locaux dans la zone des piles du pont', Proc. 14th Congress, Vol.3, PARIS, 1971, pp. 299-305.
24. JAIN, S.C. (1981), 'Maximum clear-water scour around circular piers', ASCE, JHD, pp. 611-625, May, 1981.
25. KNIGHT, D.W. (1975), 'A laboratory study of local scour at bridge piers', Proc. 16th congress, S. Paulo, IAHR, pp. 243-250.
26. LECLERC, J.P. (1971), 'Recherche des lois regissant les phenomenes d'affouillement au pied des piles de pont , premiers resultats', Proc. 14th congress, Vol.3, Paris, pp. 323-330.

27. LAIRD, A.D.K. (1971), 'Eddy formation behind circular cylinder', J.H.D., ASCE, June 1971, pp. 763-775.
28. MUZZAMMIL, M. (1985), 'Open channel flow past a circular cylinder mounted on a rigid bed and on a mobile bed', M.Tech. Thesis, I.I.T. Kanpur, March, 1985.
29. MEULEN, T. VAN DER and VINJE, J.J.(1975), 'Three dimensional local scour in non-cohesive sediment', Proc. 16th congress, Vol.2, S. Paulo, IAHR, pp. 263-270, 1975.
30. MEHROTRA, S.C. (1975), 'Scale effects in model tests of rock-protected structures', Proc. 16th congress, vol.2, S. Paulo, IAHR, pp. 453-461, 1975.
31. MELVILLE, B.W. and RAVDKIVI, A.J. (1977), 'Flow characteristic in local scour at bridge piers', J.Hyd. Research 15(1977), No.4, pp. 373-380.
32. MUKHAMEDOV, A.M., ABDURAUPOV, R.R. and IRMUKHAMEDOV, K H.A.
33. KAYAMOV, O.A. and URKINBAEV, R. (1971), 'Study of local scour and kinematic structure of flow around solid and through spur-dikes', Proc. 14th congress, IAHR, Vol.3, pp. 389-396, 1971.
34. MODI, P.N. and JAIN, B.P. (1986), 'Comparative study of various formulae on scour around bridge piers', Journal -CI, Vol.67, pp. 149-159, Nov. 1986.

35. NICOLLET, G, and RAMETTE, M. (1971), 'Affouillements an voisinage de pipples de pont cylindriques circularies', Proc. 14th congress, Vol.3, IAHR, pp.315-322, PARIS, 1979.
36. NICOLLET, G. (1975), 'Affouillements au pied des piles de pont en milieu cohesif', Proc. 16th congress, Vol.2, IAHR, pp. 478-484, S. Paulo, 1975.
37. NAKAGAWA, HIROJI and SUZUKI, KOICHI (1975), ' An application of stochastic model of sediment motion to local scour around a bridge pier', Proc. 16th congress, vol.2, IAHR, pp. 228-235, S. Paulo, 1975.
38. POSEY, C.J. (1949), 'Why bridge fails in the floods', Civil Engg., Vol.19, Feb., pp. 42,90 , 1949.
39. POSEY, C.J. and APPEL, D.W. (1951), 'Investigation of Flexible mats to reduce scour around bridge piers', Highway research Board, Research report No. 13-B, 1951, Washington, D.C.
40. PEDER HJORTH (1975), 'Study on the nature of local scour', Bulletin series A, No. 46, Lund, 1975.
41. QADAR, A. (1981), 'The vortex scour mechanism at bridge piers', Proc. Inst. Civil Engrs., Part 2, 1981, 71, Sept. 739-757.
42. RAUDKIVI, A.J. and ETTEMA, R. (1983), 'Clear-water scour at cylindrical piers', Proc. ASCE, J.H.D., Vol.109, No.3, March, 1983.

43. RAUDKIVI, A.J. and ETTEMA, R. (1977), 'Effect of Sediment gradation on clear water scour', J.H.D., ASCE, Vol.103, pp. 1209-1213, Oct. 1977.
44. ROPER, ALANT; VERNE, R. SCHNEIDER and H.W. SHEN (1967), 'Analytical approach to local scour.....', Proc. IAHR, Vol.3, pp.151-162, Sept. 1967.
45. ANSARI, S.A. (1986), 'A study of local scour', M.S. in Engg. (Civil), Z.H.College of Engg. and Technology, Aligarh Muslim University, Aligarh (India), Feb.1986.
46. SHEN, H.W., SCHNEIDER, V.R. and SUSUMU KARAKI (1969), 'Local scour around bridge piers', JHD, ASCE, HY6, pp. 1919-1937, November, 1969.
47. SHARMA, K.V.N. (1969), 'Study on scour phenomenon and its functional form', Ph.D. thesis, Department of Civil Engg., Indian Institute of Science, Bangalore, Sept.1967.
48. SHARMA, K.V.N. and M. KRISHNAMURTHY - Status report on research in scour around bridge piers.
49. TANAKA, S H. and MOTOAKI, Y. (1967), 'Local scour around a circular cylinder', Proc. 12th Congress, Vol.3, pp. 193-202, IAHR, Fort Collins, Colorado, Sept.1967, USA.
50. TEMEZPELAEZ, JOSE RAMON (1975), 'General law about scour at bridge crossings', Proc. 16th Congress, Vol.2, pp. 236-242, S. Paulo, 1975.

51. THOMAS, Z. (1971), 'Time development of the deformation of an alluvial bottom', Proc. 14th Congress, Vol.3, pp. 347-354, Paris, 1971.
52. THOMAS, Z. (1967), 'An interesting hydraulic effect occurring at local scour', 12th Congress, Vol.3, pp. 125-135, IARH, Fort Collins, Colorado, Sept.1967, USA.
53. VINJE, J.J. (1967), 'On the flow-characteristics of vortices in three-dimensional local scour', Proc. 12th Congress, Vol.3, pp. 207-218, IARH, Fort Collins, Colorado, Sept. 1967, U.S.A.